FLUID GEL PRODUCTION AND TRIBOLOGICAL BEHAVIOUR OF ALGINATE AND AGAR

by

ISABEL FERNÁNDEZ FARRÉS

A thesis submitted to

the University of Birmingham

for the degree of

DOCTOR OF ENGINEERING

School of Chemical Engineering
College of Physical and Engineering Sciences
The University of Birmingham
March 2015

Abstract

This thesis aims to develop a better understanding of the formation and properties of fluid gels using the microstructural engineering approach. In general terms, the two main objectives of this research are 1. to advance the knowledge on the structuring processes for fluid gel design; and 2. to develop new models for the structure-function relationship for fluid gels.

With regard to the structural design of fluid gels, there is currently a lack of understanding on the formation of thermo-stable fluid gels due to the absence of processing techniques for their production. In this thesis, two processing techniques were developed to produce thermo-stable fluid gels from alginates. The first technique is a continuous process comprising a pin stirrer device with a Ca^{2+}-injection system. Results on alginate fluid gels produced using this method showed a reduction in particle size with increasing alginate concentration. This arises from the increased viscosity which results in a greater shear stress acting on the initial gel nuclei. Increasing alginate concentration was also shown to increase both the yield stress and G' of the produced fluid gels, due to an increase in both particulate volume and particle stiffness.

The second developed technique involves a rheometer combined with an internal gelation method. By using this technique, the kinetics of fluid gel formation was studied as function of applied shear rate, calcium concentration and alginate molecular weight (M_W). Increasing applied shear rate increased the onset time of gelation, suggesting lower rates of particle growth. When the shear was removed after fluid gel completion, the rate at which particles interacted post-processing was not dependent on applied shear rate but slightly on calcium

concentration. When the shear was removed before fluid gel completion, the rate of particle growth was controlled by both the applied shear rate and calcium concentration.

Fluid gels produced from high M_W alginates yielded increased gelation rates due to a greater length scale affected by the same G/Ca interactions compared to low M_w alginates. This enhanced network formation along with an increasing number of rheologically-effective crosslinks, leading to an increase in both viscosity and G'.

These internally-set alginate fluid gels showed the same value of saturated calcium concentration to that of quiescent gels, indicating a similar network connectivity and equivalent number of egg-box dimmers. This was attributed to the fast dimerization process of alginate leading to kinetically trapped fluid gel structures.

With regard to the structure-function relationship, the lubricating behaviour of agar fluid gels was explored using a new approach which consisted in decoupling the contributions of the continuous phase and the particulate gelled phase. The friction of the continuous phase was higher than that of the fluid gel at all lubrication regimes, indicating that the entrainment of particles takes place at all speeds. The effect of added co-solutes on lubricating properties of agar fluid gels was also explored. The addition of glycerol increased particle size and reduced particle stiffness such that the ability of particles to support the applied load diminished. This increased the surface contact area thereby increasing the friction of the particulate gel phase. As a result, the friction of fluid gels increased. At glycerol concentrations above a critical value, the fluid gel lubrication was no longer driven by the particulates but it was governed by the continuous phase which formed a lubricating layer with a thickness exceeding the particle dimensions. Under these conditions, the

friction of fluid gels decreases with increasing glycerol concentration due to the increase in the continuous phase viscosity.

Acknowledgments

Foremost, I would like to thank my supervisor, Professor Ian Norton, for his support, mentorship and invaluable guidance throughout my EngD. In particular, I thank Ian for the inspiration to do something new and to always work at the frontier of knowledge. By doing this I learned that whether the path follows my impulses is irrelevant and I enjoyed research seeking knowledge from any unexpected result or failed experiment. I am especially grateful to Ian for encouraging me to consider and pursue both my research goals and career ambitions.

I would like to thank Dr. Richard Greenwood for his help and support during the EngD. I also extend my appreciation to the administrative staff within the School of Chemical Engineering, especially Lynn Draper and John Hooper.

I would also like to acknowledge Mondelēz UK for their financial support and permission to publish the results in peer-reviewed scientific journals. Especially, I thank Dr. Tülay Massey and Dr. John Melrose for their interest in the project and support. I also thank the EPSRC for funding.

My gratitude also goes to my colleagues and friends at the University of Birmingham, particularly the food microstructure group for their help, for all the scientific as well as the non-scientific discussions, all the laughs, the squash games and great memories.

Last but not least, I thank my family and friends. This thesis would not have been possible without their unconditional encouragement, patience and love.

Table of Contents

List of Figures

List of Tables

Nomenclature

Rheology

η	Apparent viscosity
η^*	Complex viscosity
η_0	Viscosity at zero shear rate
η_∞	Viscosity at infinite shear rate
C	Time constant related to relaxation time (Cross equation)
m	Dimensionless exponent (Cross equation)
$\dot{\gamma}$	Shear rate
σ	Shear stress
σ_γ	Yield stress
G'	Elastic (storage) modulus
G''	Viscous (loss) modulus
δ	Phase angle
J	Compliance
k	Consistency constant
n	Power law index

Tribology

F_t	Tangential frictional force
μ	Friction coefficient
W	Normal load
U_{disc}	Disc speed
U_{ball}	Ball speed
U_{entr}	Entrainment speed
SRR	Slide to roll ratio
A	Contact area
A_r	Real (interfacial) contact area
A_a	Apparent (geometrical) contact area
τ	Interfacial shear strength
a	Radius of the contact area
E'	Equivalent (effective) elastic modulus
R	Radius
ν	Poissons' ratio
P	Pressure
h	Film thickness
h_m	Minimum film thickness
H	Hersey Number
S_o	Sommerfeld Number
rms	Root mean square

Texture Analysis

σ_E	Engineering stress
σ_E	True stress
ε_E	Engineering strain
ε_H	True (Hencky) strain
H_0	Initial height of specimen
A_0	Initial cross-sectional area of specimen
h	Height of specimen
F	Force applied

Other

ϕ	Volume fraction
c	Polymer concentration
c^*	Critical polymer concentration
E	Young's Elastic modulus
M_w	Molecular weight
K	Boltzmann constant
N_A	Avogadro number
Z	Number of junction zones (Oakenfull equation)
T	Temperature
T_m	Melting temperature
T_g	Gelling temperature

$\Delta_{m,QG}$	Enthalpy of melting a quiescent gel
$\Delta_{m,FG}$	Enthalpy of melting a fluid gel
o/w	Oil-in-water emulsion
$\approx$	Approximately
ρ	Density

Chapter 1 : INTRODUCTION AND BACKGROUND

1.1. Context for the study

Hydrocolloids (polysaccharides and proteins) are commonly used in the manufacturing of food products to impart a range of functional properties such as texture, stability and appearance (Guarda *et al.,* 2004; Inglett *et al.,* 2005; Saha and Bhattacharya*,* 2010). Their role in the food industry has become increasingly important due to the recent rise in health problems associated with obesity and consumer demand for tasty products. The health benefits of hydrocolloids are contingent on the way in which they are incorporated into food products. Polysaccharides can be added to products in order to replace fat thereby allowing the design of lower calorie products without a significant loss in sensory attributes (*e.g.* texture, mouthfeel) (Bullens *et al.*, 1994; Schmidt *et al.*, 1993; Xiong *et al.,* 1999). Furthermore, the addition of indigestible polysaccharides to products would potentially increase the dietary fibre content, leading to additional health benefits. However, this has not been established yet as the definition of dietary fibre has been the subject of a prolonged, continuing debate. Current discussions relate to the role of the plant cell and the extent to which the definition should refer to the chemical structure or the physiological benefits (Phillips, 2013). Thus, it remains to be agreed which hydrocolloids are dietary fibre.

Apart from the potential health benefits, another important factor to be considered when using hydrocolloids (polysaccharides) in food formulation is their fluctuating cost price, often related to climate conditions affecting crop production. Therefore, the capacity to change formulations and alternate between different hydrocolloids without compromising on quality is essential to the food industry. This requires a scientific understanding of the hydrocolloid structure in relation to its functionality. On this basis, the microstructural engineering approach emerged and became a successful tool for bridging the gap between

fundamental science and industrial application. This approach, as schematically presented in Fig. 1.1, uses a scientific understanding of the relationships between the microstructure and both process and ingredients and the relationship between the microstructure and the properties in order to either design products from new ingredients without changing the product microstructure or to develop novel microstructures with desirable functionalities.

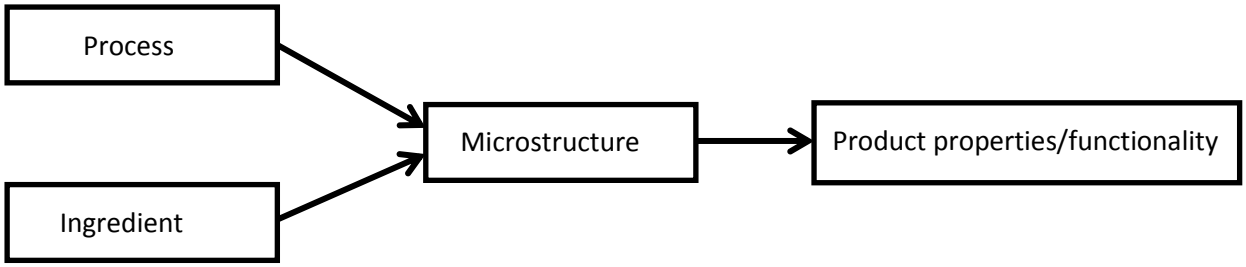

Figure 1.1: Schematic representation of the microstructural engineering approach.

The microstructural engineering approach is widely used in the processing and design of emulsions. Relevant developments in this field include nano-emulsions (Acosta, 2009) and double emulsions (Malone *et al*., 2003) which enable the controlled release of nutrients and flavor, respectively. Another example is Pickering emulsification which, instead of emulsifiers, uses particles adsorbed at the interface to stabilize emulsions and foams (Binks, 2002; Murray, 2007).

With regard to hydrocolloid-based systems, the microstructural approach has given rise to the development of fluid gels (Norton *et al*., 1999) which are suspensions of micro-gel particles with structures that can be designed to meet a wide range of functionalities. As such, fluid gel particles can be designed with structural characteristics resembling those of oil droplets, potentially enabling replacement of fat in emulsion-based products without a loss in product functionality. Fluid gels can be produced from the application of shear during

gelation of most gelling polysaccharides. However, to date, the processing methods developed for fluid gel production are only applicable to hydrocolloids undergoing thermal transitions where the gelation kinetics is controlled by processing conditions (applied cooling rate). These fluid gels are thermo-reversible, that is, they melt when heated to temperatures above their melting temperature. Thus, an exciting challenge that has been attempted in this thesis is the development of processing techniques for the production of thermo-stable fluid gels using hydrocolloids undergoing ionic thermo-irreversible transitions, such as alginates. In order to accomplish this, knowledge of the alginate gelation mechanism and the influence of applied shear on the resulting fluid gel microstructure is required.

Following the microstructural approach to food product design, an understanding of the microstructure-functionality relationship for these new fluid gel systems will have to be developed. This will require studying how changes in the alginate fluid gel structure due to manipulation of both processing conditions and the material influences their functional properties.

Within the context of utilizing fluid gels as structuring agents for food products, it is necessary to study their behavior under thin film conditions as these occur during oral processing. To this end, fluid gel lubrication is investigated by means of tribology. Recent studies have provided an understanding of the tribological properties of fluid gels (Malone *et al*., 2003; Garrec and Norton, 2013) however there is currently no published investigation decoupling the relevant contributions of the continuous phase and the particulate phase to fluid gel lubrication.

When using fluid gels in food systems, understanding the influence of co-solutes on the fluid gel structure is also necessary. So far, only one work has investigated the effect of alcohols and salt (Mills *et al.*, 2013) whilst no published study has addressed the effects of sugars and polyols on fluid gel lubrication.

1.2. Objectives

Considering the current need for thermo-stable fluid gels and the lack of understanding of the previously described areas, the objectives of this thesis are:

- To develop new techniques for alginate fluid gel production using both a pin stirrer and a rheometer.
- To investigate the effects of both the material and processing conditions on a properties of alginate fluid gels.
- To advance the understanding of fluid gel tribology by decoupling the relevant contribution of the continuous phase and the particulate phase to lubrication as well as exploring the effects of both glucose and glycerol on fluid gel lubrication.

In order to achieve the first objective, experiments have been designed to controllably and continuously introduce calcium ions into the pin stirrer device and to gradually release calcium ions in a rheometer. The properties of the produced alginate fluid gels have then been measured using rheology, tribology and optical microscopy. The obtained results are discussed in terms of the fluid gel structure, aiming to describe the mechanism of alginate fluid gel formation.

The formation kinetics and the rheological behavior of internally-set alginate fluid gels have been investigated as function of applied shear rate, calcium concentration and alginate

molecular weight. The aim of this investigation was to further elucidate the relationship between the microstructure and the two parameters: processing conditions and the materials.

The influence of glucose and glycerol on both the microstructure and properties of fluid gels has been explored, with focus on the lubricating behavior. After centrifuging the fluid gels, the tribological properties of both the sediment (gelled particulate phase) and the supernatant (continuous phase) have been separately investigated. The aim of this study is to establish the role of both the particulate phase and the continuous phase on the tribological properties of fluid gels while bringing a further insight into their lubrication mechanism.

1.3. Relevance to Mondelēz

Mondelēz is a multinational conglomerate which manufactures a range of food products such as biscuits, chesses, chocolates, grocery and on-demand beverages (*e.g.* coffee, hot chocolates, teas).

The work presented in this thesis has been conducted in the domain of microstructural engineering because of its industrial relevance. Fluid gels have the potential to be used as structuring agents and for textural enhancement in the food products previously mentioned.

The development of techniques to produce fluid gels that are stable to heat treatments is of great importance to Mondelēz, in particular for their on-demand beverage portfolio as the manufacturing process of these products includes a sterilization step.

The microstructure of fluid gels can be manipulated by controlling both the material and the processing conditions. As such, understanding how these two parameters affect the final microstructure provides the ability to design a range of fluid gel structures with different functional properties. Similarly, understanding the structure-functionality relationship is a key requirement for the correct design of these structured functional products. These two sets of knowledge must be acquired concurrently such that new functionalities can be developed via innovative processing. This combined understanding can then be used to develop healthier, tastier foods and it is of significant interest to Mondelēz.

1.4. Thesis layout

This thesis covers the production and properties of alginates fluid gels and the tribology of agar fluid gels in the presence of sugars.

In the following chapter (Chapter 2), a critical review of the relevant literature in the area of hydrocolloids and tribology is presented. Chapter 2 is divided in two main sections: Section 2.1 - General literature review and Section 2.2 - State of the art review. The General literature review covers following topics: hydrocolloids, fluid gels and tribology. Particular focus is given to the hydrocolloids used in this work and to the current understanding of fluid gel tribology.

The state of the art review, published as 'Designing biopolymer fluid gels: A microstructural approach' (Fernández Farrés *et al*., 2014), summarizes the latest advances on fluid gel research in the context of microstructural engineering applied to the formulation and processing of foods. As such, the state of the art review includes the most relevant results obtained during this study (presented in Chapter 3 and Chapter 4). This section discusses in

great detail the current understanding of both fluid gel formation and fluid gel tribology. These relevant discussions are therefore also included in the general literature review, referenced as the published article: Fernández Farrés *et al*. (2014).

Chapter 3, published as 'Rheology and tribological properties of Ca-alginate fluid gels produced by diffusion-controlled method' (Fernández Farrés *et al*., 2013), presents both the methods and results of the study conducted on alginate fluid gels produced by a diffusion-controlled method in the pin stirrer device. The rheology and particle size of alginate fluid gels are investigated as function of polymer concentration, providing a discussion on the mechanism of fluid gel formation. The tribological behavior as function of polymer concentration is also explored and results are discussed based on the understanding of fluid gel tribology at that time.

Chapter 4, published as 'Formation kinetics and rheology of alginate fluid gels produced by in-situ calcium release' (Fernández Farrés and Norton, 2014), describes the methods and discusses the results of the rheological study on the formation kinetics of alginate fluid gels produced by in-situ calcium release (*i.e.* internal gelation method). The influence of both the processing conditions (applied shear rate) and materials (alginate molecular weight and calcium concentration) on formation kinetics, structure and rheological properties of fluid gels are discussed.

Chapter 5, published as 'The influence of co-solutes on tribology of agar fluid gels' (Fernández Farrés and Norton, 2015), presents both the methods and the results of the tribological investigation carried out on agar fluid gels in the presence of both glucose and glycerol. The discussion centers around the relative role of both the particles and the continuous phase on fluid gel lubrication.

Finally, Chapter 6 provides a summary of the main conclusions obtained from Chapters 3-5 along with ideas for future work.

1.5. Publications in peer-reviewed journals

The results obtained from this thesis have been published as follows:

- Fernández Farrés, I., Douaire, M., & Norton, I. T. (2013). Rheology and tribological properties of Ca-alginate fluid gels produced by diffusion-controlled method. *Food Hydrocolloids, 32*(1), 115-122.

- Fernández Farrés, I., & Norton, I. T. (2014). Formation kinetics and rheology of alginate fluid gels produced by in-situ calcium release. *Food Hydrocolloids, 40*, 76-84.

- Fernández Farrés, I., Moakes, R. J. A., & Norton, I. T. (2014). Designing biopolymer fluid gels: A microstructural approach. *Food Hydrocolloids*, *42*, 362-372.

- Fernández Farrés, I., & Norton, I. T. (2015). The influence of co-solutes on tribology of agar fluid gels. *Food Hydrocolloids, 45,* 186-195.

1.6. References

Acosta, E. (2009). Bioavailability of nanoparticles in nutrient and nutraceutical delivery. *Current Opinion in Colloid & Interface Science, 14*(1), 3-15.

Binks, B. P. (2002). Particles as surfactants—similarities and differences. *Current Opinion in Colloid & Interface Science, 7*(1), 21-41.

Bullens, C., Krawczyk, G. & Geithman, L. (1994). Reduced-fat cheese products using carrageenan and microcrystalline cellulose. *Food Technology, 48*, 79–81.

Inglett, G. E., Peterson, S. C., Carriere, C. J., & Maneepun, S. (2005). Rheological, textural, and sensory properties of Asian noodles containing an oat cereal hydrocolloid. *Food Chemistry, 90*(1), 1-8.

Garrec, D. A., & Norton, I. T. (2013). Kappa carrageenan fluid gel material properties. Part 2: Tribology. *Food Hydrocolloids, 33*(1), 160-167.

Guarda, A., Rosell, C. M., Benedito, C., & Galotto, M. J. (2004). Different hydrocolloids as bread improvers and antistaling agents. *Food Hydrocolloids, 18*(2), 241-247.

Malone, M. E., Appelqvist, I. A. M., & Norton, I. T. (2003). Oral behaviour of food hydrocolloids and emulsions. Part 1. Lubrication and deposition considerations. *Food Hydrocolloids, 17*(6), 763-773.

Mills, T., Koay, A., & Norton, I. T. (2013). Fluid gel lubrication as a function of solvent quality. *Food Hydrocolloids, 32*(1), 172-177.

Murray, B. S. (2007). Stabilization of bubbles and foams. *Current Opinion in Colloid & Interface Science, 12*(4), 232-241.

Phillips, G. O. (2013). Dietary fibre: A chemical category or a health ingredient? *Bioactive Carbohydrates and Dietary Fibre 1*(1). 3-9.

Saha, D., & Bhattacharya, S. (2010). Hydrocolloids as thickening and gelling agents in food: a critical review. *Journal of food science and technology, 47*(6), 587-597.

Schmidt, K., Lundy, A., Reynolds, J., & Yee, L. N. (1993). Carbohydrate or protein based fat mimicker effects on ice milk properties. *Journal of food science, 58*(4), 761-763.

Xiong, Y. L., Noel, D. C., & Moody, W. G. (1999). Textural and Sensory Properties of Low-Fat Beef Sausages with Added Water and Polysaccharides as Affected by pH and Salt. *Journal of Food Science, 64*(3), 550-554.

Chapter 2 : LITERATURE REVIEW

2.1. General literature review

This section provides a critical discussion of the relevant literature, establishing the current background to this thesis.

It is divided in two main sections: 2.1.1 - Food hydrocolloids and 2.1.2 – Tribology.

Section 2.1.1 - Food hydrocolloids describes the physicochemical properties of the hydrocolloids used in this thesis and discusses the current understanding of their gelation mechanisms. This is developed into a critical literature review in the field of fluid gel research, focusing on the production and properties of thermo-reversible fluid gels. This section identifies the absence of techniques for the production of thermo-stable fluid gels thereby providing the rationale for investigating alginate fluid gel production.

Section 2.1.2 – Tribology covers the technique of tribology and evaluates the research carried out in the field of hydrocolloid and fluid gel tribology. The discussion of the existing work outlines the need for this research by establishing as yet unstudied areas of fluid gel tribology.

2.1.1. Food hydrocolloids

The denomination ‘food hydrocolloids’ refers to biopolymers (polysaccharides and proteins) commonly used in food products to provide a range of functions such as structure stability, texture enhancement or controlled flavour release (Dickinson, 2003). This thesis is primarily concerned with polysaccharides and, as such, they will be the main focus of this section.

Polysaccharides are complex carbohydrates derived from plants, seaweeds and microbial sources consisting of repeating units of monosaccharides bounded by glycosidic linkages

(Atkins, 1985; IUPAC–IUB Joint Commission on Biochemical Nomenclature, 1996). Due to their highly hygroscopic character and high molecular weight, polysaccharides bind free water and exhibit thickening properties.

In solution, a significant increase in viscosity is observed at a critical concentration (c^*) which marks the transition from 'dilute region' where the molecules freely move without interacting with other polymer molecules to the 'semi-dilute region' where interpenetration and overlapping of coils takes place. Polysaccharide solutions generally display Newtonian viscosities at concentrations less than c^*(Phillips and Williams, 2009). At concentrations greater than c^*, non-Newtonian behaviour prevails where the viscosity exhibits three distinctive behaviours with increasing shear rate: 1. Initial Newtonian plateau region at low shear rates. 2. Shear-thinning region due to disentanglement of polymer chains occurring above certain shear rates. 3. A minimum Newtonian viscosity plateau is reached as shear rate approaches ∞. A wide range of empirical mathematical equations have been proposed to describe the flow behaviour of polysaccharides in the semi-dilute region. One of the most widely used equations is the Cross equation (Cross, 1965), as follows:

$$\eta = \eta_\infty + \frac{\eta_0 - \eta_\infty}{1 + (C\dot{\gamma})^m}$$

Eq. 2.1

Where η_0 and η_∞ are viscosities at zero shear rate and infinite shear rate, respectively, C is a time constant related to the polymer relaxation time, $\dot{\gamma}$ is the shear rate and m is the dimensionless exponent indicating the level of shear thinning.

The shear rate dependency of viscosity increases with increasing polysaccharide molecular weight (M_w), with the onset of the shear thinning behaviour shifting to lower shear rate.

The viscosity is also influenced by the structure of the polysaccharide. Stiff, linear polysaccharides display greater viscosity values than those of flexible, branched polysaccharides of equivalent M_w due to their greater hydrodynamic volume.

Under favourable thermodynamic conditions, gelling polysaccharides undergo a change in their molecular conformation by pairing of chains into junction zones (*i.e*. gelation). The thermodynamic transition from solution to solid is characterized by the equilibrium between polysaccharide-polysaccharide interactions and polysaccharide-solvent interactions. During gelation, the reduction in conformational transition and hydration energy is balanced by energetically favourable polysaccharide-polysaccharide interactions (Morris and Rees, 1978).

The junction zones involved in natural polysaccharide gels are typically formed via physical interactions such as hydrogen bonding, ion-mediated crosslinking or hydrophobic interaction as opposed to synthetic polysaccharide gels which form covalently crosslinked networks (Stephen and Phillips, 2014).

Gelation of polysaccharides often occurs on cooling the solution below a gelling temperature T_g which is specific for each polysaccharide. Agar, *k*-carrageenan, gellan gum or xanthan are examples of polysaccharides which undergo thermally-reversible transitions. Alginates and high methoxyl (HM) pectin are thermally-irreversible gelling hydrocolloids where the polysaccharide crosslinking occurs in the presence of divalent cations.

Agar and alginate have been used in this work; the structure and gelation mechanism of these two hydrocolloids will now be reviewed.

2.1.1.1. Thermo-reversible gelling hydrocolloid: Agar

Agar is a seaweed hydrocolloid composed of mixtures of neutral agarose and charged agaropectin, in proportions that vary depending on both raw materials and the production process (Araki, 1956; Phillips and Williams, 2009). Agarose provides the greater part of gelling capability of agar and consists in alternating units of 3-linked β-D-galactose and 4-linked 3, 6-anhydro-α-L-galactose (Araki, 1956)(Fig. 2.1).

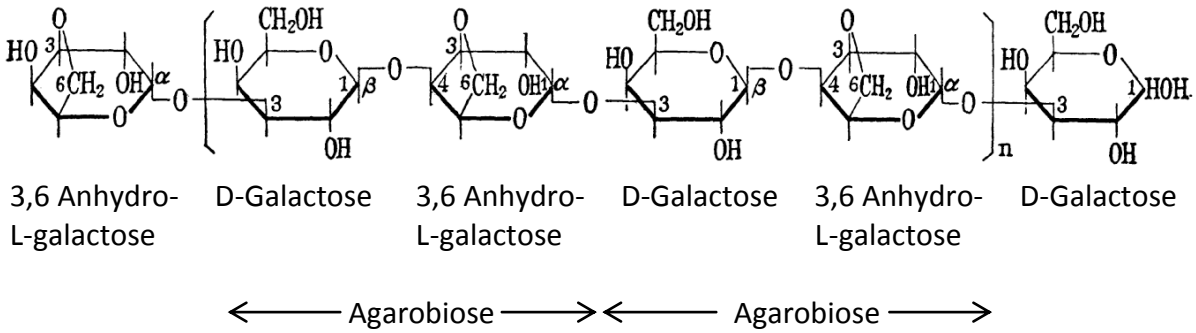

Figure 2.1: Agarose chemical structure (image adapted from Araki (1956)).

When cooling agar solutions and as the transition midpoint temperature is approached, intra-molecular hydrogen bonds start to form between the agarose chains, followed by the formation of inter-molecular hydrogen bonds between polysaccharide chains (Tako and Nakamura, 1988).

The gelation mechanism involves a coil-to-double helix transition and a subsequent aggregation of these helical domains to create a three dimensional structure. These ordered

structures were first characterised by Arnott *et al*. (1974) who, by using optical rotation, X-ray diffraction and computer modelling, reported a left-handed 3-fold double helix structure with a 1.90 nm pitch.

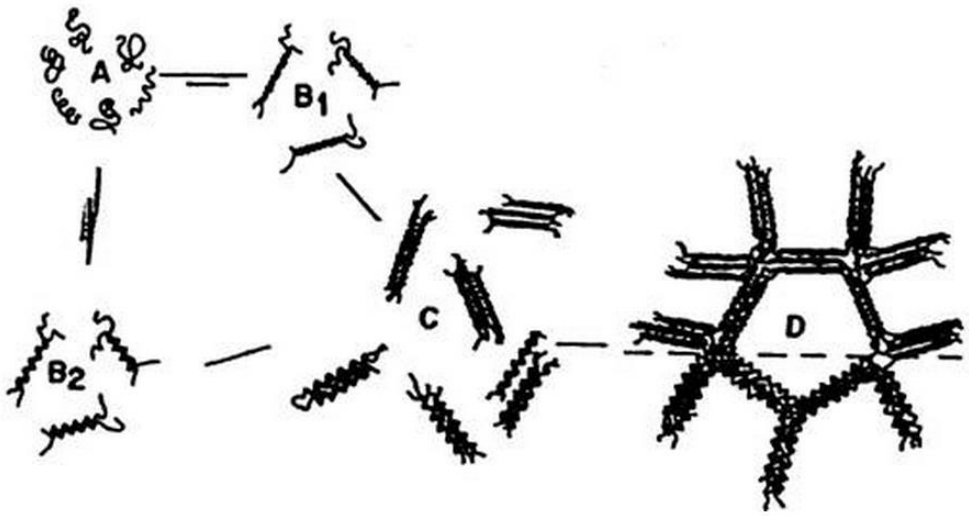

Figure 2.2: Gelation mechanism of agarose (Medin, (1995)).

In solution, random agarose coils are subjected to Brownian motion (A). On cooling, symmetric and antisymmetric double helices (B1, B2) form which subsequently aggregate to give the aggregated structures (C, D) (Fig. 2.2).

This model (random coil $\rightarrow$ ordered domains $\rightarrow$ aggregated domains) was later established by Norton *et al.* (1979) and Morris *et al.* (1980) for the conformational transition and aggregation of gelling carrageenans.

An important characteristic of agar gels is the high difference between the gelling temperature, T_g ($\approx$ 38 °C) and the melting temperature, T_m ($\approx$ 85 °C) compared to most gelling polysaccharides that have on average a temperature difference of $\approx$ 12 °C (Phillips and Williams, 2009). T_g of agar varies depending on the degree of methoxylation of the

agarobioses in the polymer chain which is characteristic of the seaweed species from which the agar has been extracted (Armisen and Galatas, 2000).

2.1.1.2. Thermally-irreversible gelling hydrocolloid: Alginate

Alginates are linear polysaccharides extracted from brown seaweed (Phaeophyceae), consisting of (1-4)-linked blocks of poly-β-D-mannuronic acid (M) and poly-α-L-guluronic acid (G) residues at different proportions and with different sequential occurrence (Draget *et al.*, 2006; Stokke *et al.*, 2000).

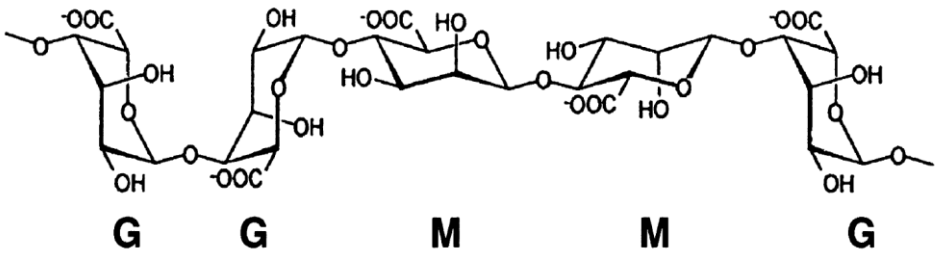

Figure 2.3: Disaccharide repeating units of mannuronan (M) and guluronan (G) (Image from Draget et al. (2005)).

The $^{1}C_{4}$ and $^{4}C_{1}$ conformation of the G and M residues respectively in hompolymeric blocks were first demonstrated by means of X-ray diffraction by Atkins *et al*. (1970) where $^{1}C_{4}$ and $^{4}C_{1}$ refer to the two distinct conformations (Fig. 2.3). In the $^{1}C_{4}$ conformation, C_{1} is located above the plane of the ring and C_{4} is located below. The $^{1}C_{4}$ conformation is the inverse arrangement of $^{4}C_{1}$ conformation. The stability of these conformations is controlled by the energetic benefit of having the voluminous C_{6} group in an equatorial position, where the steric hindrance is minimised.

Several rheological studies had shown that chain stiffness increased following the block series MM < MG < GG. Agreement between this block series and statistical mechanical calculations was found only when the G residues were defined in a $^{1}C_{4}$ conformation (Smidsrød *et al*., 1973). The authors attributed the increased stiffness of the G-blocks to the great, hindered rotation around the diaxial (GG) glycosidic linkage.

The same year and by means of circular dichroism (CD) spectroscopy, Grant *et al.* (1973) described the binding mechanism of Ca^{+2} to the alginate chain in terms of the 'egg-box model' in which inter-chain association takes place through dimerization of chain sequences with Ca^{+2} sandwiched on specific sites. That is, the guluronate residues adopt a 2-fold symmetry giving rise to a buckled structure in which Ca^{+2} are accommodated (Fig. 2.4).

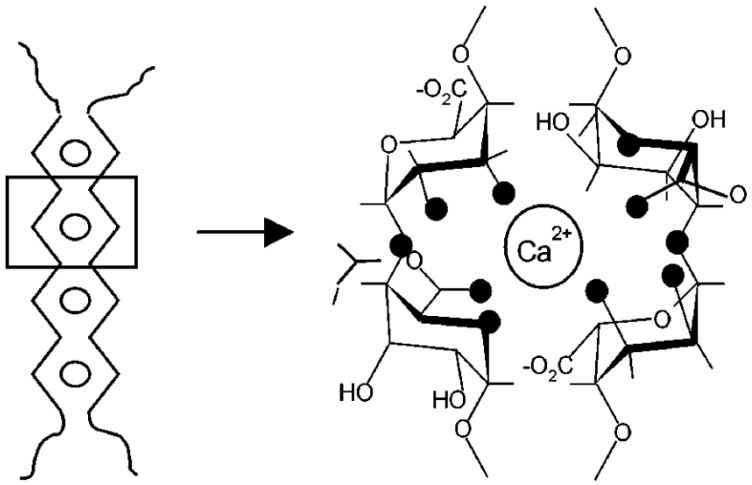

Figure 2.4: Schematic representation of the egg-box model. The black circles symbolize the Oxygen atoms participating in the coordination of Ca^{2+} (Image from Braccini and Pérez (2001)).

More precise models for describing the steric arrangements were later proposed based on X-ray diffraction methods (Mackie *et al*., 1983) and NMR (Steginsky *et al*., 1992). Nonetheless, since the egg-box model correctly describes the main features of the binding

mechanism between Ca^{+2} and alginate, it remains to this date as the definitive model due to its simplicity and intuitiveness. More recently, extensions to the egg-box model have been proposed with regards to the notion of chain dimerization. X-ray scattering measurements have shown that while chain dimerization is the main association mechanism at low fractional Ca^{2+} saturation of G-residues, chain segments associate laterally, beyond dimerization at increased Ca^{2+} concentration and amount of G-residues (Stokke *et al.,* 2000).

The influence of the alginate M/G ratio on the material properties of the resulting gels has been extensively studied, where alginates with high G-residues form strong, brittle gels and alginates rich in M-residues give softer, more elastic gels (Draget *et al*., 1994).

In terms of alginate gel formation, two different methods can be used: Diffusion method and internal method (*i.e.* in-situ calcium release). The former method involves the direct mixing of solutions of Ca^{2+} and Na-alginate, as illustrated in Fig. 2.5.A. As such, the gelation kinetics is controlled by the diffusion of Ca^{2+} through the Na-alginate solution. Due to the fast reaction rate of alginates with Ca^{2+}, the diffusion method is commonly employed to immobilise living cells by entrapping them within the gel beads (Smidsrød, 1974).

In the internal method, the Ca^{2+} is released in a controlled manner from an insoluble calcium salt (*e.g.* $CaCO_3$). By gradually lowering pH, the solubility of $CaCO_3$ increases such that Ca^{2+} are progressively released into the medium (Fig. 2.5.B). The slow hydrolysing glucono-δ-lactone (GDL) is generally used to progressively reduce the pH. Unlike the diffusion method, the gelation kinetics within the internal method is not controlled by the diffusion rate of the Ca^{2+} and hence can be manipulated. Another difference between the two methods is the alginate M_w dependency, which is negligible in diffusion-set alginate

gels with M_w greater than 100 kDa but has a significant influence on internally-set alginate gels (Smidsrød, 1990; Draget *et al*., 1993). This greater M_w dependency in the internal method has been related to the Ca^{+2}-limited environment leading to a greater fraction of loose ends for a given M_w compared to the Ca^{+2}-saturated environment in the diffusion method (Draget *et al*., 1993).

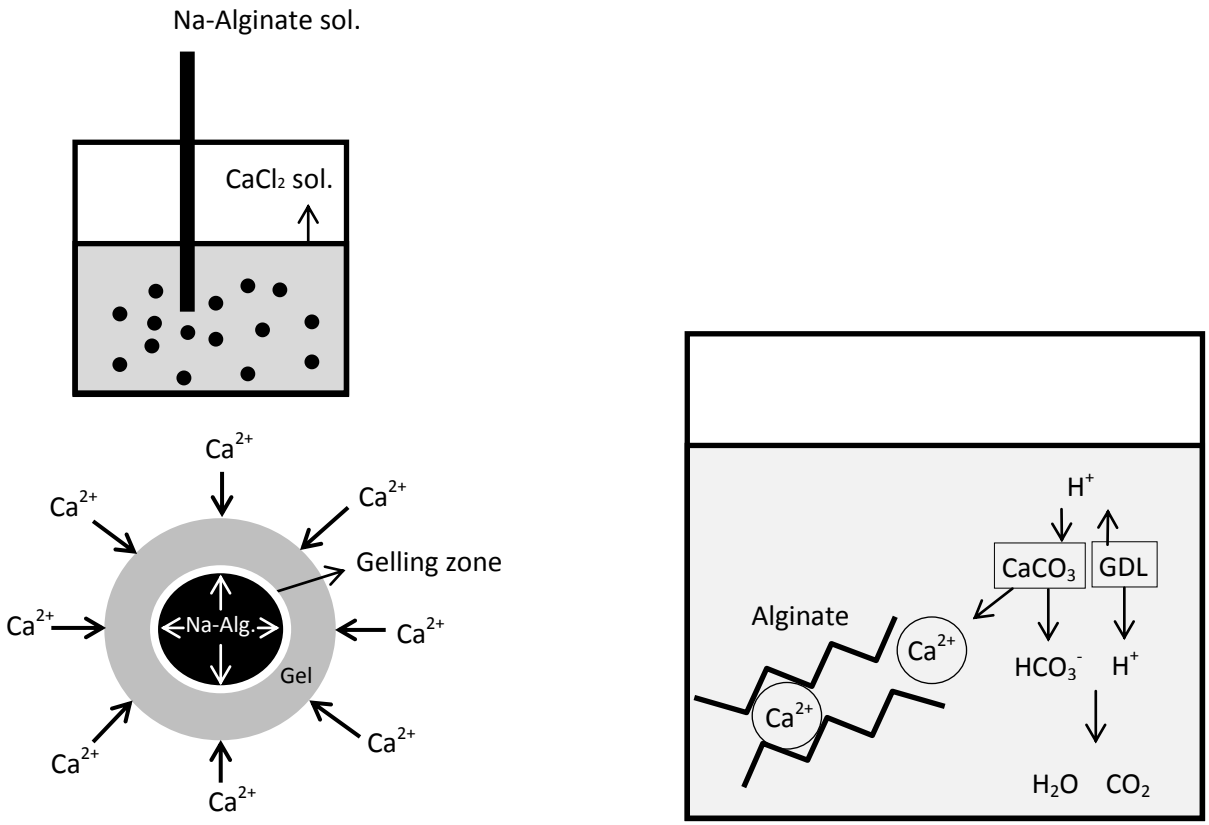

A. DIFFUSION METHOD **B. INTERNAL (IN-SITU) METHOD**

Figure 2.5: Comparison between the diffusion method (a) and internal method (b) using $CaCO_3$/GDL. (Image adapted from Draget et al. (2005)).

2.1.1.3. Fluid gels from thermo-reversible gelling hydrocolloids

Fluid gels are formed by the application of a flow field to a gelling biopolymer solution while undergoing conformational transition and subsequent aggregation. A jacketed pin stirrer has been used to produce fluid gels in a continuous process. Fluid gels can also be formed using a rheometer. The advantage of producing fluid gels in the rheometer is that parameters such as shear rate, viscosity, temperature can be precisely controlled and monitored during fluid gel formation such that the kinetics of that process can be studied. The advantage of using the pin stirrer is that it allows much larger volumes of fluid gel to be produced in a continuous manner.

Hydrocolloids undergoing thermally reversible transition have been typically used to produce fluids gels: agarose (Norton *et al.,* 1999), *k*-carrageenan (Gabrielle *et al.,* 2009), gellan gum (Sworn *et al.*, 1995). For thermo-reversible hydrocolloids, control over the kinetics of the ordering process is achieved by the manipulation of the cooling rate which determines the final particle physical properties. Kinetic competition between the processes of network formation and shear induced break-up that occurs as the midpoint temperature is approached has an effect on the resulting particle structure (size, shape) and the intrinsic particle 'reactivity'. At high cooling rates, the gelation process dominates over the applied shear rate and large irregularly-shaped particles are produced. As the conformational ordering kinetics is more closely matched to the time scale of the applied shear rate (*i.e.* at lower cooling rates) the input from the applied flow field increases, resulting in the formation of small and spherical particles. Consequently, systems exhibit a more fluid-like response (reduced storage modulus) than that of fluid gels produced at higher cooling rates. Under the same applied cooling rate, both particle size and volume

occupancy are strongly influenced by the applied shear field: increasing the magnitude of the shear rate leads to smaller particles and lower volume fractions. Under the same applied cooling rate, both particle size and volume occupancy are strongly influenced by the applied shear field: increasing the magnitude of the shear rate leads to smaller particles and lower volume fractions (Fernández Farrés *et al.,* 2014; work included in this chapter as Section 2.2. - State of the art review). This was demonstrated by Gabriele *et al.* (2009) who showed that big ($\approx$ 110 µm) and irregularly-shaped *k*-carrageenan particles are produced at low shear rates whilst small (> 5 µm) and nearly spherical particles are obtained at high shear rates (Fig. 2.6). In the study by Gabriele *et al.* (2009), fluid gels were produced in the rheometer such that viscosity was monitored during formation. Fluid gels with smaller particles (produced at highest shear rate) displayed lower viscosities than fluid gels with bigger particles. Increased viscosities are expected for suspensions with small particles due to an increased level of inter-particle interactions as the ratio between surface area and total volume increases. Based on that observation, the authors confirmed the suggestion by Norton *et al.* (1999) that the reduced viscosity is the result of a reduction in the volume fraction of the particles.

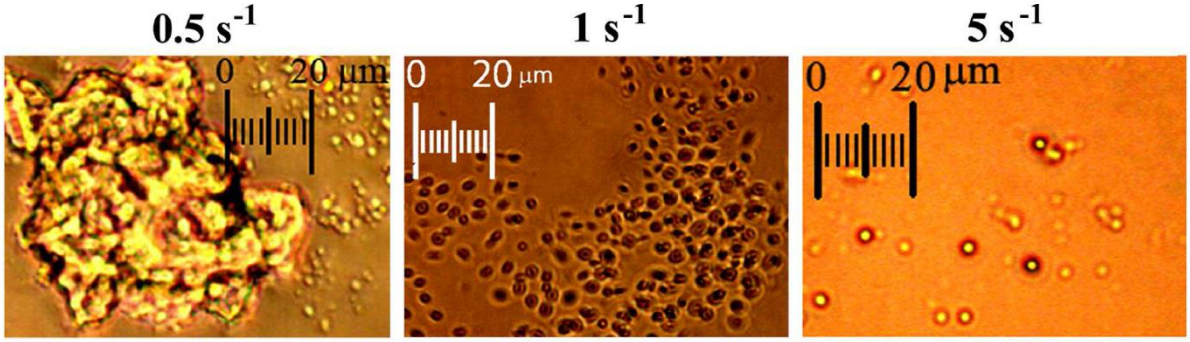

Figure 2.6: Effect of the shear rate on size and morphology of particles for k-carrageenan fluid gels produced at the same cooling rates (Gabriele et al., 2009).

Therefore, a range of microstructures with significantly different physical properties can be produced from minor changes to the processing parameters whilst using the same material. Mechanistically, the formation of fluid gels is a nucleation and growth process (Norton *et al.,* 1999). The applied shear forces ensure the initially formed gel nuclei remain separated from each other which limits the molecular ordering to occur within distinct particles.

The resulting particles have a higher polymer density at the centre which gradually decreases towards the edge due to the weak interfacial tension acting between the gelled and non-gelled phases of the polymer and also that the input from the flow field is higher at the particle surface (Garrec *et al.,* 2013). However, as will be discussed later in this section, the degree to which the applied shear limits molecular ordering depends largely on the nature of the polymer. Both the ordering rate and the cohesive nature of the bonds (*e.g*. weak hydrogen bonds or ionic crosslinking) determine the gelled polymeric network of the individual particles and consequently their stiffness. The polymeric network of thermo-reversible fluid gel particles can be elucidated by comparing the melting profile of a fluid gel with that of the corresponding quiescently cooled gel. The experimental procedure consists of measuring the thermal transitions when the fluid gel is heated above its melting temperature, then cooled and re-heated again. As such, the disordering transition that occurs during the first heating cycle (melting the fluid gel) can be assessed by comparison with that of its corresponding quiescent gel. Results obtained from *k*-carrageenan fluid gels (Fig. 2.7) have shown that the enthalpy of melting for the fluid gel ($\Delta_{m,FG}$ = 0.174 ± 0.003 J/g) is significantly lower than that of the quiescent gel ($\Delta_{m,QG}$ = 0.186 ± 0.002 J/g), indicating fewer number of helical domains in the fluid gel (Garrec and Norton, 2012).

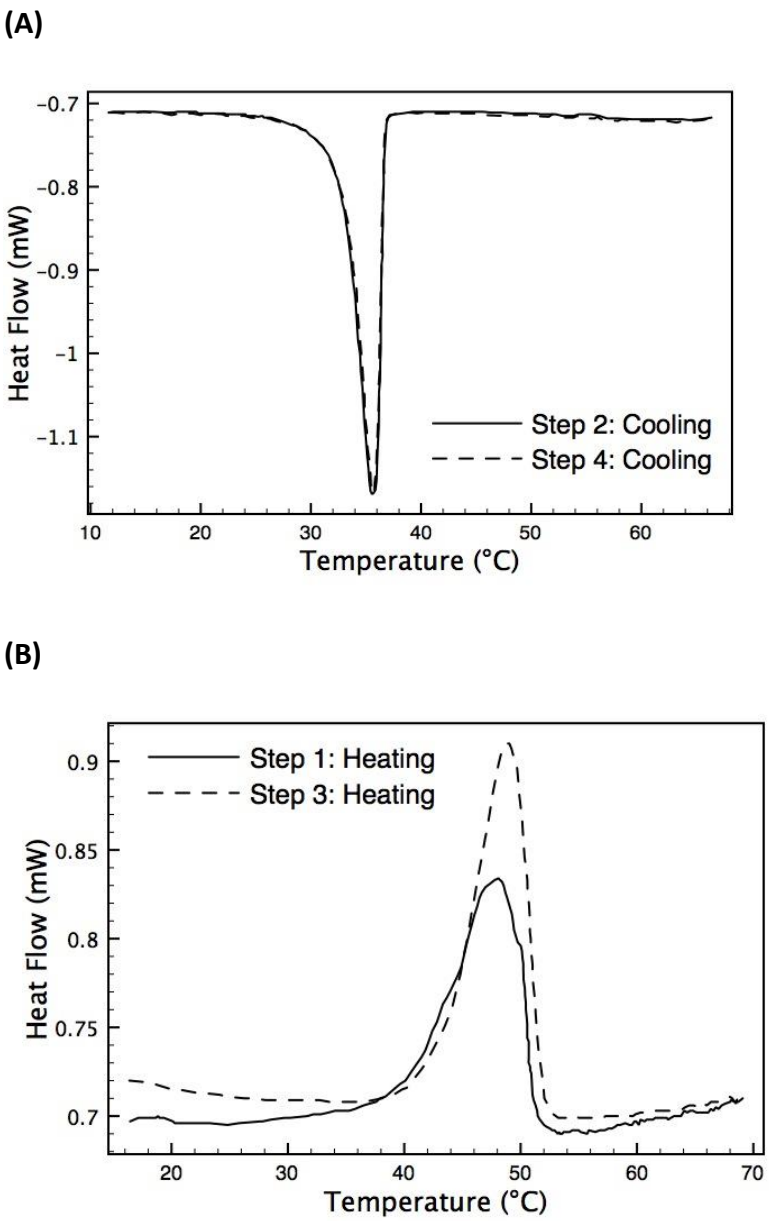

Figure 2.7: *(A) Heating and (B) cooling profiles obtained through DSC for initial k-carrageenan (0.5 wt %, 0.3 wt % KCl) fluid followed by quiescent gel. Step 1 shows melting of a previously prepared fluid gel followed by quiescent gelation (step 2). In situ re-melting and gelling of the quiescent gel is then shown in steps 3 and 4 (Garrec and Norton, 2012).*

As initially suggested by Norton *et al.* 1999, fewer helical domains and thus smaller helical aggregates are formed at the surface of the particles due to the disruption of the coil-helix transition by the applied shear field. Consequently, the density of the gelled network is lower towards the particle surface where the disruption to the aggregation process results

in later ordering of polymer chain, leading to the formation of particles with 'hairs' (*i.e.* partially retained polymer chains). Unlike *k*-carrageenan, fluid gels produced from agarose display similar melting enthalpies and temperature to those of their counterpart quiescent gels (Norton *et al.*, 1999) indicating an equivalent internal structure. This disparity in the calorimetry results for systems produced from *k*-carrageenan compared to those produced from agarose relate to differences in the rate of molecular ordering, being 2-3 orders of magnitude faster for agarose than *k*-carrageenan (Norton *et al*., 1986). The fast ordering transition of agarose kinetically traps the structures into anisotropic shapes and particles typically reach larger dimensions. In contrast to this, fluid gel particles formed from *k*-carrageenan under comparable processing conditions are small (1 μm) and they achieve a thermodynamically favourable spherical shape. Thus, the structural features of the final particles (*e.g.* size, morphology, presence of 'hairs') are strongly dependent on the polysaccharide. These properties have a profound effect on the rheological response of fluid gels, particularly of diluted fluid gels. It is therefore essential to understand the influence of the bulk properties of particles on the degree of dilution, in order to design colloidal structures that will be incorporated into foodstuffs.

The effects of particle shape were addressed in the work of Frith *et al.* (2002) in which the volume fraction dependence of the storage modulus of agarose anisotropic fluid gels was compared with that of model micro-gel suspension of spherical agarose particles. Since both systems were produced from the same hydrocolloid, an equivalent degree of inter-particle interaction was assumed. Spherical particles were achieved by the emulsion route, cooling a water-in-oil emulsion where the gelling polymer is dissolved in the aqueous phase. Initially in this method, a mixture of polymer aqueous solution and oil is sheared while

heating at a temperature above the polymer gelation temperature. This produces droplets with a uniform polymer distribution and a well defined edge at the interface due to the high interfacial tension between the dispersed aqueous phase and the continuous oil phase. Thus, the gelled particles that form upon cooling are spherical particles with homogeneous polymer distribution. Consecutive processes of dilution with water and centrifugation are used to separate the particles from the continuous oil phase. Micro-gel model suspensions are then prepared by dispersing the produced spherical particles in water. As shown in Fig. 2.8, the response to dilution with water of the sheared anisotropic particles is markedly different to that of the uniform spherical particles. The highly irregular and extended morphology of fluid gel particles distribute through the space to a greater degree than the model spherical particles with an equivalent volume. This results in greater inter-particle interaction compared to spherical particles at low volume fractions which leads to the formation of percolated networks although the particles are not aggregated. As such, fluid gels display elastic dominated responses over a broad range of volume fractions (Frith *et al.*, 2002).

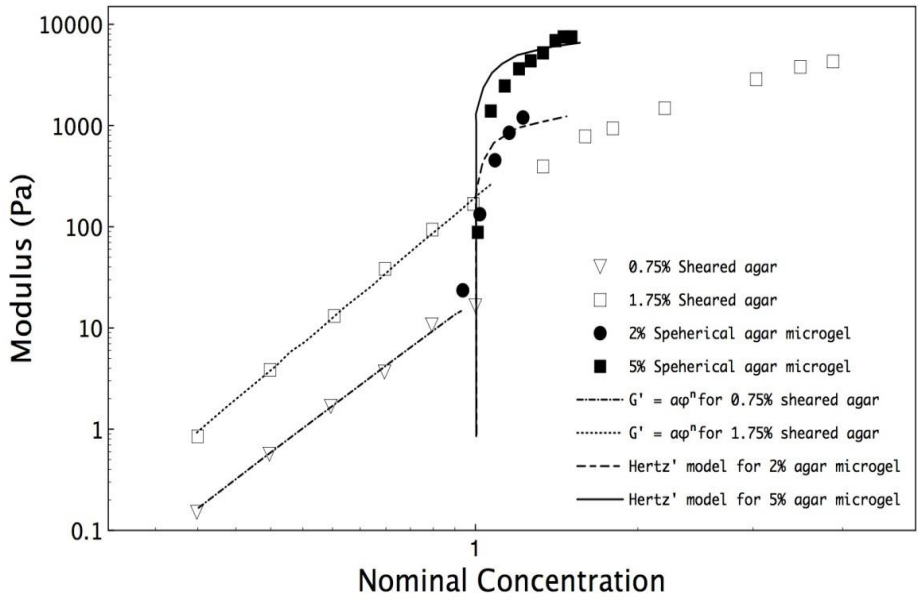

Figure 2.8: Comparative plot for the concentration dependence of the plateau modulus for both sheared and model agar sphere suspensions. Predictions based on the Hertzian interactions between particles have also been illustrated, assuming a particle modulus of 33 KPa (Frith et al., 2002).

In the work of Wolf *et al.* (2001), the influence of particle shape on rheology and the process-morphology relationship was also investigated, where a wider range of microstructures were produced from the sheared gelation of mixtures of polysaccharides (Fig. 2.9). By manipulating the flow conditions during the gelation of one of the polymers, regular spheroidal or cylindrical shaped particles were formed. The use of a rheometer with concentric cylinder geometry allowed the production of uniform and regularly shaped gelled microstructures. Molten mixtures of gellan and *k*-carrageenan were loaded to the rheometer at 60 °C and subjected to a constant stress of 0.05 Pa. Ellipsoidal shapes were achieved by cooling the system below the gelation temperature of the dispersed phase (gellan) whilst applying a constant stress (above 0.05 Pa). Alternatively, cylindrical particles were produced as a result of firstly cooling under small stress (0.05 Pa) and subsequently

increasing the stress up to 0.5 Pa immediately before the gelation of the dispersed phase. Droplets are initially elongated into cylindrical threads which are then trapped via gelation and prior to being broken up. Kinetic trapping of the structure in controlled and defined shapes is achieved by controlling the time scale of the imposed increase in stress such that the process of droplet break up occurs at a lower rate than gelation. If the gelation rate is too slow, spherical particles are formed due to the complete structural relaxation of the droplet phase.

The shear-induced structuring process in mixed systems requires less energy input than is necessary to produce fluid gels from a solution containing a single biopolymer (Norton *et al.,* 2006). The reason for this lies in the fact that the two phases of mixed polymer systems are not pure such that each polymer exists in both gelled and aqueous state. Thus, only the weak interfacial tension has to be overcome by the applied flow field before inducing gelation. Wolf *et al.* (2001) showed a dramatic effect of particle shape on the relative viscosity, specifically at lower shear stresses where increasing the particle aspect ratio results in suspensions with increased viscosities (Fig. 2.9). At high shear stresses, a greater degree of particle orientation occurs upon increasing the particle aspect ratio, resulting in decreased viscosities. These results also showed that particle entanglements form over time after production due to the greater flexibility of cylindrical particles. Arising from this, particle orientation is suppressed. Moreover, once particle entanglement has occurred application of shear does not orient particles and a reduction in viscosity at higher shear rates is not observed (Fernández Farrés *et al.,* 2014; Section 2.2. - State of the art review).

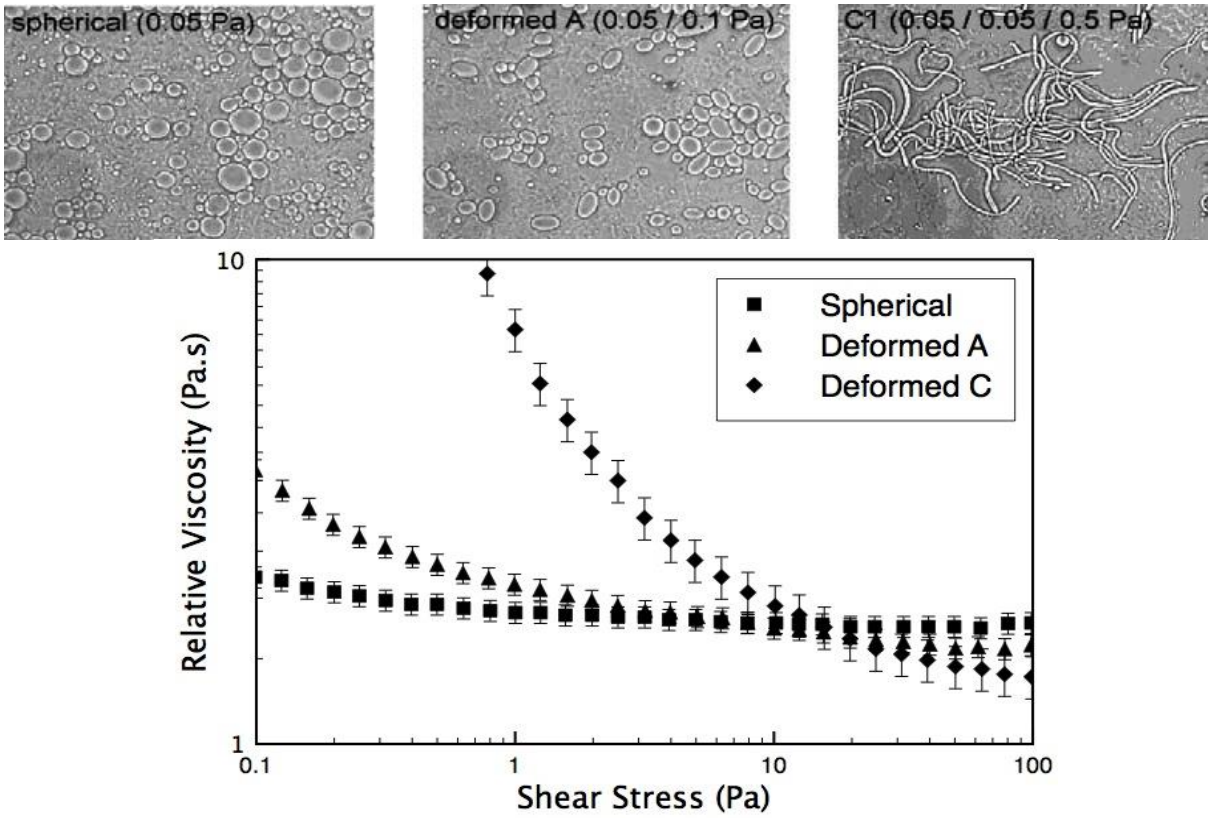

Figure 2.9: Viscosity measurements for particulate asymmetric gel suspensions with varying degrees of aspect ratio. Micrograph inserts depict average particle morphologies for their respective viscometry profile (Wolf et al., 2001).

2.1.2. Tribology

Tribology is the science of interacting surfaces in relative motion and comprises the study of friction, lubrication and wear. The word tribology derives from the *Koine* Greek *τριβω* 'tribos' meaning 'to rub' and *λόγος* 'logos' meaning 'logic' (Pring, 1982) and was first used in England in the 1960's in an effort to consolidate the historically independent research areas of friction, lubrication and wear into a single discipline (Tichy *et al.,* 2000).

Tribological research embraces the understanding of the interactions taking place at the interface of two contacting surfaces and the resulting effects on friction, lubrication and wear. The study of tribology has been historically applied in the design and optimisation of

machinery systems such as bearings and gears so as to minimise friction and wear by the choice of suitable lubricants and surface materials. Tribology as a research technique to study food oral processing first emerged in the 1980's and has been shown to be a promising technique to predict in-mouth sensory perception (Malone *et al.,* 2003).

This section presents the scientific principles of tribology as currently understood, with a focus on the areas that are relevant for this work.

2.1.2.1. Friction

Friction is commonly described as the force resisting motion in a sliding process.

The finding that the friction associated to rolling is lower than that associated to sliding is attributed to Thermistius in 350 BC. The first scientific studies on friction were carried out by Leonardo da Vinci in 1500, found in the *Codex Atlanticus* and in the *Codex Madrid I* and *II*. In his work, da Vinci's mathematically demonstrated that:

- Friction is directly proportional to the applied load.
- Friction is independent on the apparent area contact.

Da Vinci's discoveries had no historical influence as his work was not published for hundreds of years.

By investigating the sliding between dry flat surfaces, Amontons (1699) rediscovered and published the two laws of friction.

These laws were later verified by Charles Augustine Coulomb (1779-1781) who discovered a third law, often referred as Amonton-Coulomb's law:

- Friction is independent of the velocity once motion starts.

The studies from Coulomb were published in a series of papers (Coulomb, 1785) and led to the introduction of the concept of friction coefficient (μ) as previously derived by mathematician Leonard Euler (Euler, 1750):

$$\mu = \frac{F_t}{W}$$

Eq. 2.2

Where F_t is the tangential frictional force and W is the normal load.

Coulomb also showed that surfaces are not ideally smooth but, rather, comprise asperities which he described as a structure with hills and valleys. Coulomb suggested that friction arises from the interlocking asperities. The limitations of this theory become apparent when considering a perfectly sinusoidal interface: when the peak of the first asperity is attained the system starts to slide down without requiring an external force (Bhushan, 2010).

Advances on the fundamental understanding of friction did not occur until the twentieth century when technology allowed measurements of surface roughness and the contact area between surfaces. Based on Coulombs' ideas, Bowden and Tabor (1954 and 1964) proposed an alternative and more accurate theory of friction based on molecular adhesion at the asperity contacts. The basic principle of the adhesion model by Bowden and Tabor is that the contact between the surfaces takes place only between the asperity peaks and consequently, the real (interfacial) contact area A_r is lower than the apparent (geometrical) A_a contact area. During sliding, new contact points are constantly being created whist

others disassociate. On the assumption that A_r remains constant on average and the interfacial shear strength τ is the same for all asperity contacts, the frictional force F_t is given by:

$$F_t = A_r \tau$$

Eq. 2.3

The average stress acting in the contact area is $\sigma = W/A_r$. If σ is independent of W then $A_r \propto W$ such that $\mu = F_t/W = \tau/\sigma$ as per Amontons' law.

A linear relationship between A_r and W was already described by Archard (1957) who attributed the effect to an increasing number of contacts being created upon increasing W .

The W dependency of σ (*i.e.* A_r) was later studied by Greenwood and Williamson (1966) who, by using a probabilistic multi-asperity contact model, referred as the GB model, demonstrated the $A_r \propto W$ thereby confirming Archards' suggestion. Further details on the load dependency of the contact area are provided in Section 2.1.2.2.1. – Asperity contacts in EHL.

More recently, imaging techniques such as atomic force microscopy (AFM) have allowed the investigation of the single asperity contact created between the peak and the lubricant. By using AFM coupled with immunofluorescence microscopy (IFM), studies by Carpick *et al*., (1996) and Carpick and Salmeron (1997) have demonstrated that, in the absence of wear,

the F_t for a single-asperity contact is proportionally related to A_r following the Bowden and Tabor (1954) equation: $F_t = A_r \tau$.

2.1.2.2. Elastohydrodynamic lubrication (EHL)

The friction created between two bodies rubbing against each other is dramatically reduced when an intervening fluid (*i.e.* lubricant) is present between the two contacting surfaces.

Hydrodynamic lubrication is generated in conformal contacts (*e.g.* journals and slider bearings) due to the increased pressure in the contact zone as the fluid is dragged in the converging gap.

Lubricated non-conformal contacts (*e.g.* gears, rolling bearings) operate in Elastohydrodynamic lubrication (EHL) regime where the theory of lubrication (*i.e.* Reynolds equation) describes the fluid flow behaviour as for the conformal contacts. Nevertheless, since the load in non-conformal contact is supported by a small area, the pressure in the contact area is very high which leads to both an elastic deformation of the contacting surfaces and an increase in lubricant viscosity at the contact region. Thus, the formation of a hydrodynamic fluid film in EHL is promoted by these two effects. The mathematical description of the EHL provides a solution for the equations of fluid flow, elastic surface deformation and the lubricant viscosity-pressure relationship. The relevant equations to describe these effects in EHL regime will be discussed in the following sections.

2.1.2.2.1. Asperity contacts in EHL

The deformation of the surface asperities in EHL is initially elastic in the way of Hertz problem between two elastic spheres. Assuming no lubrication at the interface, Hertz (1881)

proposed that for two contacting elastic spheres 1 and 2 of radius R_1 and R_2, the radius of the resultant circular contact area *a* is given by:

$$a = \left[\frac{3W}{2E'\left(\frac{1}{R_1} + \frac{1}{R_2} \right)} \right]^{1/3}$$

Eq. 2.4

where E' is the equivalent (effective) elastic modulus, expressed as:

$$\frac{1}{E'} = \frac{1}{2}\left(\frac{1-\nu_1^2}{E_1} + \frac{1-\nu_2^2}{E_2} \right)$$

Eq. 2.5

where ν_1 and ν_2 are the Poissons' ratio for the contacting surfaces. Note: Johnson (1985) refers to the reduced elastic modulus $E^* = E'/2$ instead of E'. In this thesis, E' is used as it is typically employed in EHL discussion.

The resulting pressure distribution in the contact is hemispherical, given by:

$$P = P_{\max}\left(1 - \frac{x^2}{a^2} - \frac{y^2}{a^2} \right)^{0.5}$$

Eq. 2.6

Where the maximum pressure $P_{\max}$ which occurs on the axis of symmetry is:

$$P_{\max} = \frac{3W}{2\pi a^2}$$

Eq. 2.7

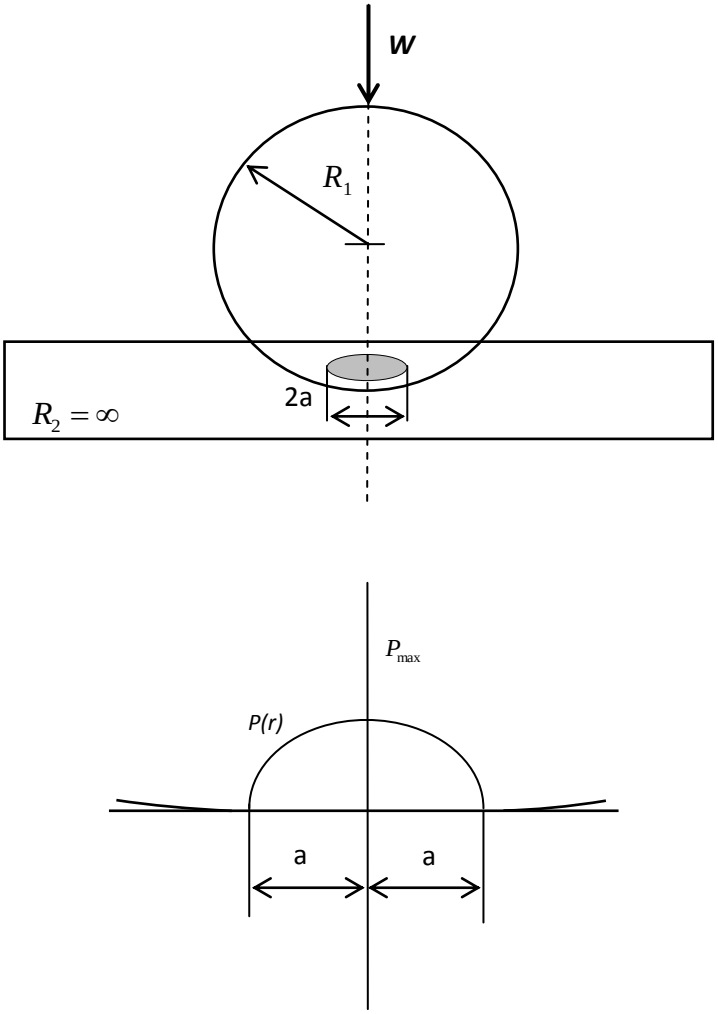

Figure 2.10: Elastic deformation of a ball against a non-deformable surface.

When the above equations are applied to an sphere-plane contact, the radius of the plate is set to ∞. As such, for the tribological contact, as schematically represented in Fig. 2.10., R_1 is the radius of the ball, $R_2 = \infty$ is the radius of the disc and a is the radius of the circular contact area.

The theory of Hertzian contacts assumes that the contact area equals the real (interfacial) contact area, A_r. Thus, for a single asperity contact and according to Eq. 2.4, a is

proportional to $W^{1/3}$. Given that $A_r = \pi a^2$, then $A_r \propto W^{2/3}$ and hence $F_t \propto W^{2/3}$. This dependency has been confirmed experimentally using AFM where single asperity contacts are achieved (Carpick and Salmeron, 1997). Tribological measurements with highly compliant surfaces have also shown this behaviour (Myant *et al*., 2010) where the elastic compliance of the asperities determines the contact area.

For non-compliant surfaces with multiple asperities, $F_t \propto W$ is typically observed even in elastic contacts. A linear relationship $A_r \propto W$ was first predicted by Greenwood and Williamson (1966) while studying the behaviour of asperity populations with exponential and Gaussian height distributions. By applying the Hertz solution to an asperity population with a given height distribution, the Greenwood and Williamson model (GW contact model) successfully describes the load–displacement relation for elastic surfaces in contact. The assumption of the GW contact model is that the deformation of each asperity is not affected by the deformation of the others.

The basic principle underlying the Greenwood and Williamson model is that the number of asperity contacts increases with W provided that the mean size of the contact remains constant. Thus, although elastic deformation is expected for multi-asperity non-compliant surfaces, Amonotons' law of friction $F_t \propto W$ prevails as $A_r \propto W$ due to an increasing number of asperity contacts.

Recent AFM studies have shown a transition from $F_t \propto W$ to $F_t \propto W^{2/3}$ due to the shift from multiple to single asperity contact caused by wear (Reitsma *et al.,* 2006).

2.1.2.2.2. Lubrication and film thickness in EHL

The equations describing the lubrication by fluid films originate from fundamental fluid dynamic equations with geometrical considerations of the fluid film (*i.e.* lateral extent, film thickness).

The theory of hydrodynamic lubrication is based around the Reynolds equation (Reynolds, 1886) which defines the pressure distribution of the lubricant film on a given geometry as follows:

$$\frac{d}{dx}\left(\frac{\rho h^3}{12\eta}\frac{d\rho}{dx}\right)+\frac{d}{dy}\left(\frac{\rho h^3}{12\eta}\frac{d\rho}{dy}\right)=\frac{u_1+u_2}{2}\frac{d(\rho h)}{dx}+\frac{d(\rho h)}{dt}$$

Eq. 2.8

Where η is dynamic viscosity, ρ is density and h is lubricant film thickness. u_1 and u_2 are velocity components in the plane.

The Reynolds equation showed strong agreement between the predictions and the experimental results for conformal contacts in which W is supported by a large area compared to h. After the equation and the hydrodynamic theory were published, attempts were made to expand their application to non-conformal contacts in which W is supported by a small area that increases significantly with increasing W. A representative contribution is the work by Martin (1916) who provided a model for lubrication on gear teeth by an isoviscous fluid. Martin's model predicted a value of minimum film thickness (h_m) lower than the surface roughness, indicating that other effects must be considered. For the next three decades, several independent studies investigated alternative mechanisms that could be responsible for such an increase in fluid film formation. Both the elastic deformation of

the contacting surfaces (Meldahl, 1941; Peppler, 1936) and the viscosity increase in the contact zone due to increased pressure (Block, 1950) were separately shown to increase fluid film formation.

The challenge to resolving the EHL problem was the incorporation of the equations for both terms in the solution. Grubin and Vinogradova (1949) reported the first approximate solution which considered both the elastic surface deformation and the lubricant viscosity-pressure relationship. By integrating a simplified Reynolds equation and curve-fitting the obtained results, an equation was derived for calculating h_m. This work highlighted the relevance of h_m in an EHL contact as an indication of the lubricants' ability to support the load and minimise surface contact.

Grubin's equation demonstrated the basic properties of EHL:

- h is almost constant in the contact area.
- The pressure distribution is similar to Hertzian pressure.

A few years later, Dowson and Higginson (1959) developed an inverse procedure to overcome problems related to iterative calculations thereby allowing the analysis under a broader set of conditions. Using this new procedure, the authors computed the h_m values at a range of loads, materials and speeds conditions (Dowson and Higginson, 1961).

This work, as later published (Dowson and Higginson, 1966), became the basis for smooth surface EHL theory.

2.1.2.3. Lubricated friction: The Stribeck Curve

The first systematic study on the friction of lubricated surfaces as function of velocity was reported by Stribeck (Stribeck, 1902) while experimenting on railway wagon journal bearings. Results showed that the friction decreases with velocity to a minimum value above which friction increases again.

Roughly a decade after Stribeck's publication, Hersey (1914) reported the relationship between the frictions of an oil lubricated bearing and the following dimensionless parameter, known as Hersey number:

$$H = \frac{\eta U}{P}$$

Eq. 2.9

Where η is the viscosity, U is the rotational speed (*e.g.* revolutions per minute of a journal) and P is the pressure.

The Sommerfeld number (Eq. 2.10) was later introduced and is generally used in recent literature to generate Stribeck curves.

$$S_o = \frac{\eta U}{W}$$

Eq. 2.10

The Stribeck curve, as presented in Fig. 2.11, illustrates the three regimes of lubrication. At the lowest S_o, the lubricant is excluded from the contact and the surfaces are in full contact, leading to high μ. In this regime, known as boundary lubrication, μ depends on surface properties since the load is supported by the surface asperities. In the mixed regime,

μ decreases with increasing S_o as the increase in lubricant pressure separates the surfaces resulting in both surface asperities and lubricant film supporting the load. As such, μ in the mixed regime is function of both lubricant and surface properties. With increasing S_o further, μ reaches a minimum value which represents the transition to hydrodynamic regime where the load is only supported by the lubricant and μ is independent of asperity contact. In the hydrodynamic regime, μ increases with S_o due to the increase in the fluid volume being sheared.

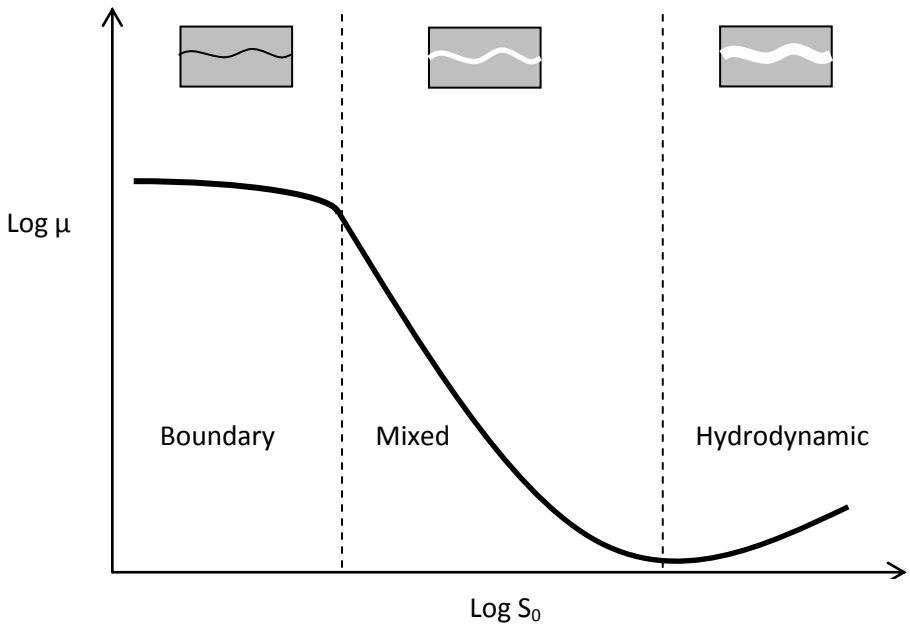

Figure 2.11: Schematic of a Stribeck curve showing the effects of Sommerfeld number $(\eta U/W)$ *on friction coefficient.*

2.1.2.4. Soft-tribometry and its application to food oral research

Tribology is relevant to food oral research as the physical processes involved in eating comprises a range of interacting surfaces (*e.g.* palate-tongue, food-tongue) in relative motion. During eating, the food is mixed with saliva while being squeezed and sheared

between the tongue and the palate which leads to the formation of a thin layer. Together with the chemical stimuli sensed by the taste papillae at the tongue surface, the resistance against moving surfaces plays a crucial role in food sensory perception (Malone *et al.,* 2003; Chen and Stokes, 2012).

Steel-on-steel tribometry gives high pressures ($\approx$ 1 GPa at a W = 10 N, (Cassin *et al.,* 2001)) which are not appropriate for describing the lubricating processes occurring in the mouth. In addition, the surface chemistry of steel differs significantly from that of the oral tissue and, as a result, the wetting and adsorption properties are different from that of the oral cavity.

By using at least one soft surface, a reduced pressure is achieved, resembling the physical parameters such as those occurring during oral processing. Yet, the major challenge in food tribology research remains the selection of an adequate soft surface material to best match oral tissue. The surface of the tongue is hydrophobic and rough due to the presence of conical filiform papillae (Dresselhuis *et al.,* 2008) but can be hydrophilic when covered by the mucus layer which comprises mainly glycoproteins and water (Vardhanabhuti *et al.,* 2011).

The study by de Hoog *et al.* (2006) measured the friction of an emulsion over a range of surfaces (metal, glass, rubber and pig tongue) and concluded that the softness and roughness of a pig tongue were the most adequate surface properties when investigating tribology in relation to sensory perception. Using a pig tongue and a glass as tribological surfaces, Dresselhius *et al.* (2008) showed that coalescence and aggregation in o/w emulsions occurs due to trapping of oil droplets in the gaps between the papillae. This effect of emulsion destabilisation, which may be expected in a human tongue, was not observed when polydimethylsiloxane (PDMS) surfaces were used. Nevertheless, significant

disadvantages of using a pig tongue were also reported such as poor reproducibility, tissue degradation and limited availability.

By investigating the effects of surface roughness on the friction generated in steel-PDMS contacts, Bongaerts *et al*. (2007) and de Vicente *et al.* (2005) showed that boundary friction decreased with increasing surface roughness. This reduction in friction is expected as the number of asperity contacts (*i.e.* A_r) decreases with increasing roughness and according to the Bowden and Tabor equation, $F_t = A_r\tau$ (Eq. 2.3). Furthermore, the ηU values associated with the mixed-hydrodynamic transition were shown to increase with increasing surface roughness. This effect had also been reported in the previous study by Cassin *et al.* (2001) on steel-silicone contacts.

To best mimic the hydrophobicity and roughness of the oral tissues, Malone *et al.* (2003) used a similar steel-silicone contact and reported a strong correlation between the sensory perception and the friction of o/w emulsions. Based on these results, a steel-on-silicone tribopair is used in the work presented in this present thesis.

2.1.2.5. Lubrication of hydrocolloids in soft-tribological contacts

As previously discussed, soft-tribology is of potential relevance to understanding the physical mechanisms responsible for sensory attributes. As such, studies have investigated the soft-tribology of hydrocolloids in an attempt to determining their behaviour during oral consumption. An example of this is the work of Malone *et al*. (2003) which showed a correlation between the perception of 'slipperiness' and μ of guar solutions in the mixed regime in a steel-silicone contact. Using the same tribological surfaces, Cassin *et al.* (2001) reported a reduction in the mixed-regime μ with increasing concentrations of guar gum and

pig gastric mucin glycoprotein. In this study, evanescent wave spectroscopy was employed to investigate the adsorption properties of the polymers. Results showed that mucin glycoprotein reduced the boundary μ below the values measured for water due to the presence of an adsorbed mucin layer. The reduced boundary μ was suggested to be due to steric or electrostatic repulsion from the mucin adsorbed surfaces. Guar gum, which did not adsorb on surfaces, yielded similar boundary μ. Nevertheless, in the mixed regime, increasing concentrations of guar were shown to decrease μ. A reduction in mixed-regime μ with increasing concentrations of guar gum and xanthan gum was also reported by de Vicente *et al*. (2005) who suggested that the reduced μ was due to viscous and hydrodynamic forces. In this study, the authors introduced a scaling factor representing the effective viscosity in the contact in order to create master Stribeck curves where μ was plotted over entrainment speed multiplied by this scaling factor. Based on the assumption that complete fluid entrainment takes place during testing, this approach allowed the generation of master curves for shear thinning hydrocolloid solutions. Since the shear rate in the contact can not be measured, the use of scaling factor has proven to be a successful solution to generate master curves without having to calculate viscosity.

While studying the lubricating properties of xanthan, pectin, locust bean gum and gellan gum on a soft-tribological contact, Stokes *et al.* (2011) demonstrated that the boundary and mixed regimes are strongly influenced by the adsorbed hydrocolloids. The dry mass of the adsorbed hydrocolloid, which was measured using surface plasmon resonance, was shown to determine the boundary μ for rough surfaces (400 nm rms). For a smooth surface (10 rms), the boundary μ was related to the hydrated wet mass of the adsorbed hydrocolloid, obtained using a quartz crystal microbalance. The mixed-regime μ was reported to be

function of both viscosity and the properties of adsorbed hydrocolloid. From all the studied hydrocolloids, pectin provided the lowest μ as its high viscosity at high shear rates favoured full film hydrodynamic lubrication thereby reducing mixed-regime μ. The thickness of the adsorbed film was the highest for pectin which formed a highly hydrated viscoelastic film yielding low interfacial shear stresses and boundary μ. Locust bean formed a firm film and consequently yielded the highest μ on both rough and smooth surfaces.

2.1.2.6. Lubrication of hydrocolloids fluid gels in soft-tribological contacts

The first study on fluid gel lubrication was carried out by Gabriele *et al.,* (2010). In this work, the lubricating properties of agarose fluid gels ($\approx$100 µm particle size) were investigated using a steel-on-silicone tribopair. A conceptual model was proposed which is represented schematically in Fig. 2.12. This model describes the three distinct lubricating behaviours with increasing speed: At $U = 0$ mm/s, the ball and the disc are in full dry contact as the fluid gel is excluded from the contact area. At low speeds in the mixed regime (zone A), particles remain excluded from the gap as its size is smaller than the size of the particles and the entrainment of the continuous phase reduces μ. As the speed increases, the gap widens until it reaches a size which is the same to the particle size, thus allowing the entrainment of a monolayer of particles. The rolling-sliding motion of the particles in the thin film leads to an increase in μ (zone B). Upon increasing the speed further (zone C), multilayers of particles start to entrain, forcing the two surfaces apart and thus decreasing μ once again. The mechanism of film lubrication is re-established when the gap width surpasses that of the particle size and thus allowing bulk fluid to be entrained.

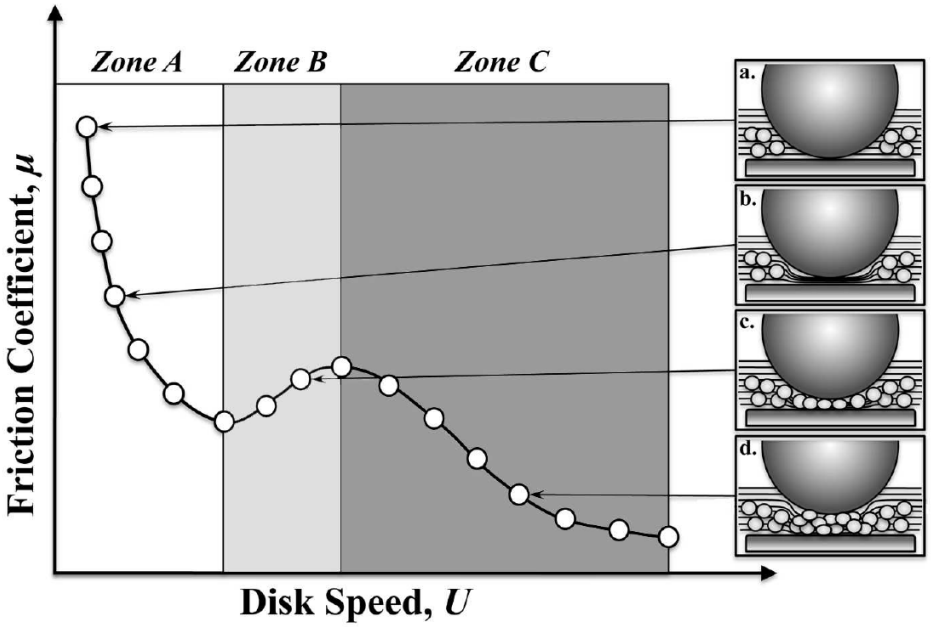

Figure 2.12: Model of fluid gel lubrication based on agar fluid gels with ≈100 µm particles (image from Gabriele et al., 2010).

In the study by Gabriele *et al*. (2010), increasing particle size was shown to increase μ, similar to the findings by de Wijk and Prinz (2005) in custard systems. In the study by Gabriele *et al*. (2010), the critical velocity at which friction starts to increase (U_{entr}), which was related to the onset of particle entrainment, decreased with increasing agar concentration. This inverse relationship between U_{entr} and agar concentration was attributed to the elasticity of the particles, with stiffer particles requiring lower velocities for entrainment. However, it could also be argued that less stiff particles may entrain at lower velocities due to their increased deformability. An alternative hypothesis for the increase in μ is that particles build-up around the ball-on-disc contact thereby preventing the entrainment of the continuous phase.

Using the same tribopair, Mills *et al.* (2013) studied the lubricating properties of agar fluid gels as function of solvent quality and results were explained in terms of the previously

presented model based on exclusion of particles from the contact at low speeds. The μ of water was higher than that of fluid gels at all speeds which suggests particle entrainment was occurring at all speeds. However, an explanation for this behaviour was not provided. The hypothesis of particle entrainment at low speeds for agar fluid gels will be discussed in Chapter 5 – The influence of co-solutes on tribology of agar fluid gels.

The tribology of *k*-carrageenan fluid gels was investigated by Garrec and Norton (2013) who showed that the μ of *k*-carrageenan fluid gels ($\approx$1 µm particle size) was lower than that of water. The Stribeck curve did not display a peak in the mixed regime of lubrication. Thus, it was suggested that *k*-carrageenan particles, being smaller that the surface roughness dimensions, could fit within the surface asperities thereby providing lubrication by entering the contact area at all speeds. In this work, the boundary μ was investigated as function of particle volume fraction (ϕ). As illustrated in Fig. 2.13, the boundary μ of *k*-carrageenan fluid gels decreases with ϕ until a plateau region is reached ($0.3 < \phi < 0.6$). This is followed by a further reduction in μ with increasing ϕ ($\phi > 0.7$). The initial decrease in μ is the result of an increased amount of particles in the contact zone. The fact that a plateau region is observed suggests that the boundary μ dependency on μ relates to the number of particles in the contact, rather than the bulk rheology and inter-particle interaction. Finally, at high ϕ, a multilayer of closely packed particles are entrained to the contact zone and the friction is further reduced. Thus, unlike the fluid gel rheology which greatly depends on the level of inter-particle interactions and hence ϕ, fluid gel tribology is mainly dominated by the elasticity of the particles.

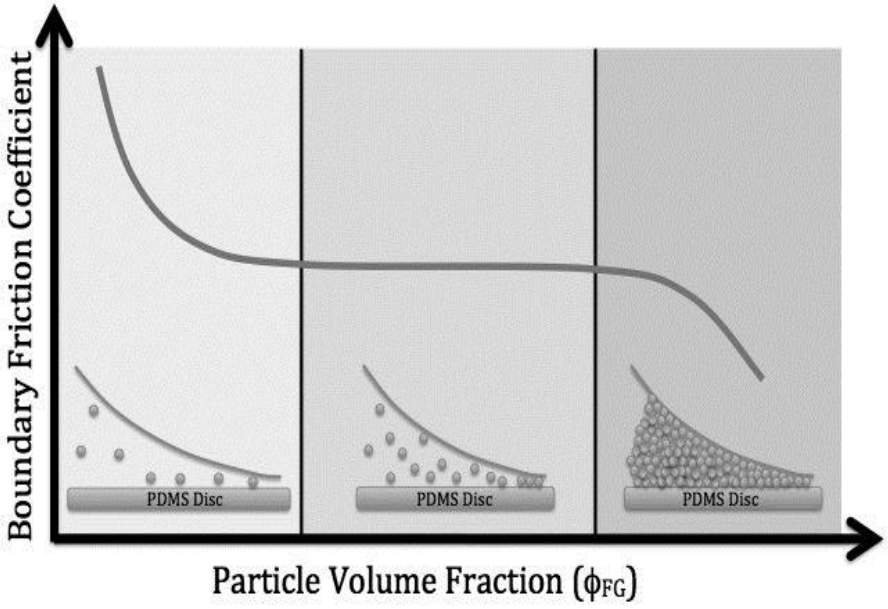

Figure 2.13: Particle entrainment and boundary μ as function of ϕ (adapted image from Garrec and Norton, 2013).

Data obtained from sensory trials revealed that *k*-carrageenan fluid gel particles were not perceived as particles, rather, fluid gels were perceived as 'smooth' (Garrec, 2013). There is therefore an indication that stiffness of fluid gel particles can be manipulated to provide enhanced lubrication while not being detected during consumption. (Fernández Farrés *et al.,* 2014; Section 2.2. - State of the art review).

2.1.2.7. Correlating perceived texture to instrumental data

Over the last decades, there have been several research studies focusing on the development of reliable methods to measure and quantify texture of food in relation to sensory perception. As such, various attempts have been made to correlate instrumental data with in-mouth sensory perception.

Wood (1968) carried out the first systematic investigation of the physical processes controlling perceived viscosity by comparing sensory rates with the shear stress-shear rate profiles of a range of non-Newtonian fluids. From this comparison, it was concluded that the stimulus related to viscous perception is the shear stress created in the mouth at $\dot{\gamma} \approx 50$ s^{-1}. Building on this understanding, Shama and Sherman (1973) studied the perceived viscosity for a range of liquid and semi-solid foods and suggested that a broader range of shear rates (10 – 1000 s^{-1}) are involved during oral processing depending on the food product properties. Results shown that while the viscous perception for thick foods took place at $\dot{\gamma} \approx 10$ s^{-1}, thin foods were assessed at an applied shear stress of $\approx$10 Pa. The conclusion that emerges from this observation is that thick foods are evaluated by the pressure required to induce flow whereas thin materials are assessed by the flow at a constant applied stress.

Technological advances in rheology led to extensive research on rheological properties in relation to the microstructure. Because the structure is not damaged during small deformation tests, they provide better correlations with initial thickness perception than large deformation tests. This was demonstrated by Richardson *et al*. (1989) who showed that small deformation data of complex viscosity (η^*) yielded the best correlation with the thickness perception at an oscillatory frequency of 50 rad/s.

With many results obtained with compression testing (Texture Analysis, T.A.), the general consensus in the literature is that the material properties measured using T.A. are applicable only to attributes related to compression processes. Representative contributions are the study by Bourne (2002) who showed strong correlations between hardness perception and

the maximum compression force and the work by di Monaco *et al.* (2008) who predicted the perception of both hardness and springiness by multicylce compression tests.

Nevertheless, rheology and texture analysis present severe limitations when studying texture perception of fluids and semi-fluid materials where both surface properties and fluid flow play a determining role in perceived textural attributes. The previously accepted notion of thickness being an attribute which can be certainly predicted by rheological tests has been recently under debate. Disagreements have arisen in the literature over the shear rates that prevail during food oral processing which may possibly relate to individual physical and psychological aspects in sensory perception. For example, the thickness perception of xanthan solutions and other fluid foods was shown to correlate best with the viscosity at $\dot{\gamma}$ = 10 s^{-1} whilst poor correlation was shown at $\dot{\gamma}$ = 50 s^{-1} (Culter *et al.,* 1983). Similarly, results by Akhtar *et al*. (2005) suggested that the perception of both thickness and creaminess of o/w emulsions can not be predicted by η at $\dot{\gamma}$ = 50 s^{-1}. More recently, Koliandris *et al.* (2010) have shown that thickness perception of thick hydrocolloid solutions best correlated to η at $\dot{\gamma} \approx$ 500 s^{-1}. Together with the psychophysical aspects involved in food sensory perception, these contradictory findings could arise from a reduction in the length-scale of shear (film thickness) taking place while eating (Chen and Stokes, 2012). Thus, although rheology can effectively describe bulk properties (flow, deformation), these results are insufficient to assess the attributes that are perceived in the thin film as the material is squeezed between oral surfaces.

Jozef Kokini and colleagues pioneered the use of tribology to study the physical processes involved in the sensory perceptions of smoothness, slipperiness, creaminess among other textural attributes (Kokini *et al.,* 1977; Kokini and Cussler, 1983; Kokini, 1987). The authors

proposed an oral lubrication model in which the tongue moves against the palate and the food is sheared whereby lubricating the surfaces. Using this approach, textural attributes of fluids were successfully described by combining friction and viscosity data. The perception of smoothness was shown to relate to μ^{-1} whilst slipperiness related to $(\eta+\mu)^{-1}$. Creaminess was reported to be the collective result of thickness and smoothness, as shown in Fig. 2.14.

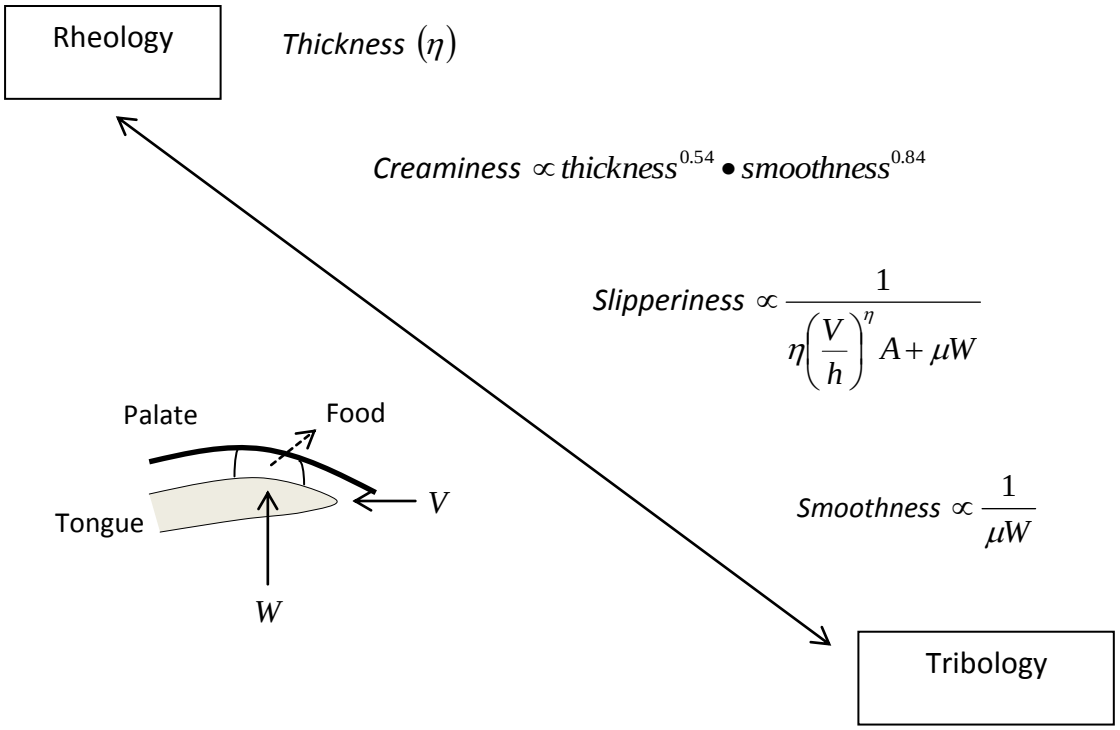

Figure 2.14: Schematic representation of oral lubrication according to Kokini's model (Adapted image from Kokini, 1987) where V is the tongue's velocity.

Since μ was the only parameter involved in the perception of smoothness, smoothness of fluids was suggested to occur at the latest stage of oral processing, before swallowing, due to the formation of a thin layer of fluid residue. This was later confirmed by Adams *et al*. (2007) who, by in-vivo fluorescence imaging measurements, reported the presence of a thin oil layer at the surface of the tongue 30 seconds after consumption.

Slipperiness has been shown to correlate to the mixed-regime friction of o/w emulsions measured in a steel-silicone contact (Malone *et al*., 2003).

Creaminess, because it is a function of both slipperiness and smoothness, is expected to be predicted by tribology to a certain extent. On that basis, de Wijk and Prinz (2005) measured the friction of custards which were shown to effectively correlate to perceived creaminess.

Tribology has recently been used to bring an insight into the mechanisms involved in perceived astringency. Perceived astringency which relates to shrinking, drawing or puckering of the epithelium (ASTM, 2004) is typically regarded in the literature as a tactile sensation (Breslin *et al.,* 1993, Smith *et al*., 1996) although there have been suggestions that it is a fundamental taste quality (Schiffman *et al*., 1992). The general view is that astringency originates from the reduction in lubrication due to the precipitation of salivary proteins as they form complexes with astringent compounds (Charlton *et al.,* 2002; Kallithraka *et al.,* 2001). This notion is supported by Rosetti *et al.* (2009) who used tribology to study the effects of both epigallocatechin gallate (EGCG) and epicatechin on the lubricating properties of saliva. In this study, it was shown that the friction of saliva increased with the addition EGCG due to the depletion of lubricating proteins in contact with the oral mucosa whilst the addition of epicatechin did not change friction. Since both compounds were evaluated as astringent by the sensory panel, the authors suggested that astringency was not only governed by friction and that chemical stimulation may also determine perceived astringency.

In conclusion, rheology and tribology contribute separately to textural perception, thereby constituting two distinct areas within the characterisation of textural attributes. The textural properties that are perceived at the initial stages of food oral processing are

suggested to be controlled by bulk rheology whilst those properties perceived at the later stages relate to the behaviour of the material in the thin film. This includes friction, surface properties and the saliva-material interactions. While rheology is relevant measurement for attributes such as thickness, hardness or elasticity, tribology is relevant for particle size, creaminess, smoothness, slipperiness or astringency. Thus, each technique, rheology and tribology, can be used to predict a particular sensory attributes but both are required for a more complete understanding.

2.1.3. References

Adams, S., Singleton, S., Juskaitis, R., & Wilson, T. (2007). In-vivo visualisation of mouth–material interactions by video rate endoscopy. *Food Hydrocolloids, 21*(5), 986-995.

Akhtar, M., Stenzel, J., Murray, B. S., & Dickinson, E. (2005). Factors affecting the perception of creaminess of oil-in-water emulsions. *Food Hydrocolloids, 19*(3), 521-526.

Amontons, G. (1699). De la résistance causé dans les machines. *Memoires de l'Academie Royale A*, 275–282.

Araki, C. (1956). Structure of the Agarose Constituent of Agar-agar. *Bulletin of the Chemical Society of Japan 29*(4), 543 – 544.

Archard, J. F. (1957). Elastic deformation and the laws of friction. *Proceedings of the Royal Society of London. Series A. Mathematical and Physical Sciences, 243*(1233), 190-205.

Armisen, R., & Galatas, F. (2000). Agar. In G. O. Phillips, & P. A. Williams (Eds.), *Handbook of Hydrocolloids* (pp. 21–40). Cambridge: Woodhead Publishing.

Arnott, S., Fulmer, A. S. W. E., Scott, W. E., Dea, I. C. M., Moorhouse, R., & Rees, D. A. (1974). The agarose double helix and its function in agarose gel structure. *Journal of Molecular Biology, 90*(2), 269-284.

ASTM (2004). Standard definitions of terms relating to sensory evaluation of materials and products, *American Society for Testing and Materials*.

Atkins, E. (1985). Conformations in polysaccharides and complex carbohydrates. *Journal of Biosciences, 8*(1-2), 375-387.

Atkins, E. D. T., Mackie, W., & Smolko, E. E. (1970). Crystalline structures of alginic acids. *Nature, 225*, 626-628.

Bhushan, B. (2010). Modern Tribology Handbook, Two Volume Set. CRC Press.

Blok, H. (1951). Fundamental Mechanical Aspects of Thin-Film Lubrication. *Annals of the New York Academy of Sciences, 53*(4), 779-804.

Bongaerts, J. H. H., Fourtouni, K., & Stokes, J. R. (2007). Soft-tribology: lubrication in a compliant PDMS–PDMS contact. *Tribology International, 40*(10), 1531-1542.

Bourne, M. (2002). Food texture and viscosity: concept and measurement. *Academic Press*.

Bowden, F. P., & Tabor, D. (1954). *The Friction and Lubrication of Solids*, Part 1, Oxford University Press, London.

Bowden, F. P., & Tabor, D. (1964). *The Friction and Lubrication of Solids*, Part 2, Oxford University Press, London.

Braccini, I., & Pérez, S. (2001). Molecular basis of Ca2+-induced gelation in alginates and pectins: the egg-box model revisited. *Biomacromolecules, 2*(4), 1089-1096.

Breslin, P. A. S., Gilmore, M. M., Beauchamp, G. K., & Green, B. G. (1993). Psychophysical evidence that oral astringency is a tactile sensation. *Chemical Senses, 18*(4), 405-417.

Carpick, R. W., & Salmeron, M. (1997). Scratching the surface: fundamental investigations of tribology with atomic force microscopy. *Chemical Reviews,97*(4), 1163-1194.

Carpick, R. W., Agrait, N., Ogletree, D. F., & Salmeron, M. (1996). Measurement of interfacial shear (friction) with an ultrahigh vacuum atomic force microscope. *Journal of Vacuum Science & Technology B, 14*(2), 1289-1295.

Cassin, G., Heinrich, E., & Spikes, H. A. (2001). The influence of surface roughness on the lubrication properties of adsorbing and non-adsorbing biopolymers. *Tribology Letters, 11*(2), 95-102.

Charlton, A. J., Baxter, N. J., Khan, M. L., Moir, A. J., Haslam, E., Davies, A. P., & Williamson, M. P. (2002). Polyphenol/peptide binding and precipitation. *Journal of Agricultural and Food Chemistry, 50*(6), 1593-1601.

Chen, J., & Stokes, J. R. (2012). Rheology and tribology: Two distinctive regimes of food texture sensation. *Trends in Food Science & Technology, 25*(1), 4-12.

Cross, M. M. (1965). Rheology of non-Newtonian fluids: a new flow equation for pseudoplastic systems. *Journal of Colloid Science, 20*(5), 417-437.

Coulomb, C. A. (1785). Theories of simple machines. *Memoires de Mathematique et de Physique de l'Academie Royal, 10*, 161-331.

Cutler, A. N., Morris, E. R., & Taylor, L. (1983). Oral perception of viscosity in fluid foods and model systems. *Journal of Texture Studies, 14*(4), 377-395.

De Hoog, E. H., Prinz, J. F., Huntjens, L., Dresselhuis, D. M., & Van Aken, G. A. (2006). Lubrication of oral surfaces by food emulsions: the importance of surface characteristics. *Journal of Food Science, 71*(7), E337-E341.

De Vicente, J., Stokes, J. R., & Spikes, H. A. (2005). The frictional properties of Newtonian fluids in rolling–sliding soft-EHL contact. *Tribology Letters, 20*(3-4), 273-286.

De Wijk, R. A., & Prinz, J. F. (2005). The role of friction in perceived oral texture. *Food Quality and Preference, 16*(2), 121-129.

Dickinson, E. (2003). Hydrocolloids at interfaces and the influence on the properties of dispersed systems. *Food hydrocolloids, 17*(1), 25-39.

Di Monaco, R., Cavella, S., & Masi, P. (2008). Predicting sensory cohesiveness, hardness and springiness of solid foods from instrumental measurements. *Journal of Texture Studies, 39*(2), 129-149.

Dowson, D., & Higginson, G.R.(1959). A Numerical Solution to the Elastohydrodynamic Problem. *Journal of Mechanical Engineering Science, 1*(1), 6-15.

Dowson, D., & Higginson, G. R. (1961). New Roller Bearing Lubrication Formula. *Engineering, 192*, 158–159.

Dowson, D., & Higginson, G. R. (1966). Elasto-hydrodynamic Lubrication, The Fundamentals of Roller and Gear Lubrication. *Pergamon Press*, Oxford, UK.

Draget, K. I., Simensen, M., Onsøyen, E., & Smidsrød, O. (1993). Gel strength of Ca-limited alginate gels made in situ. *Hydrobiologia, 260*(1), 563-565.

Draget, K. I., Skjåk Bræk, G., & Smidsrød, O. (1994). Alginic acid gels: the effect of alginate chemical composition and molecular weight. *Carbohydrate Polymers*, *25*(1), 31-38.

Draget, K. I., Skjåk-Bræk, G., & Stokke, B. T. (2006). Similarities and differences between alginic acid gels and ionically crosslinked alginate gels. *Food Hydrocolloids*, *20*(2–3), 170-175.

Draget, K. I., Smidsrød, O., & Skjåk-Bræk, G. (2005). Alginates from algae. *Biopolymers Online.*

Dresselhuis, D. M., De Hoog, E. H. A., Cohen Stuart, M. A., & Van Aken, G. A. (2008). Application of oral tissue in tribological measurements in an emulsion perception context. *Food Hydrocolloids, 22*(2), 323-335.

Euler, L. (1750). Histoire de l'Academie Royale des Sciences et Belles-lettres, Berlin, 122.

Fernández Farrés, I., Moakes, R. J. A., & Norton, I. T. (2014). Designing biopolymer fluid gels: A microstructural approach. *Food Hydrocolloids*, *42*, 362-372.

Frith, W., Garijo, X., Foster, T., & Norton, I. (2002). Microstructural origins of the rheology of fluid gels. *Special publication-Royal Society of Chemistry, 278*, 95-103.

Gabriele, A., Spyropoulos, F., & Norton, I. T. (2009). Kinetic study of fluid gel formation and viscoelastic response with kappa-carrageenan. *Food Hydrocolloids, 23*(8), 2054-2061.

Gabriele, A., Spyropoulos, F., & Norton, I. T. (2010). A conceptual model for fluid gel lubrication. *Soft Matter, 6*(17), 4205-4213.

Garrec, D.A. (2013). Understanding fluid gels and hydrocolloid tribology. Doctoral dissertation. University of Birmingham.

Garrec, D. A., Guthrie, B., & Norton, I. T. (2013). Kappa carrageenan fluid gel material properties. Part 1: Rheology. *Food Hydrocolloids, 33*(1), 151-159.

Garrec, D. A., & Norton, I. T. (2012). Understanding fluid gel formation and properties. *Journal of Food Engineering, 112*(3), 175-182.

Garrec, D. A., & Norton, I. T. (2013). Kappa carrageenan fluid gel material properties. Part 2: Tribology. *Food Hydrocolloids, 33*(1), 160-167.

Grant, G. T., Morris, E. R., Rees, D. A., Smith, P. J. C., & Thom, D. (1973). Biological interactions between polysaccharides and divalent cations: The egg-box model. *FEBS Letters*, 32(1), 195-198

Greenwood, J. A., & Williamson, J. B. P. (1966). Contact of nominally flat surfaces. *Proceedings of the Royal Society of London. Series A. Mathematical and Physical Sciences, 295* (1442), 300-319.

Grubin, A. N., & Vinogradova, I. E. (1949). Investigation of the contact ofmachinecomponents. *K. F. Ketova (Ed.). Central Scientific Research Institute for Technology and Mechanical Engineering.*

Hersey, M.D. (1914). The laws of lubrication of horizontal journal bearings. *Journal of the Washington Academy of Sciences, 4*, 542–552.

Hertz, H. (1881). On the contact of elastic solids. *Journal für die reine und angewandte Mathematik*, *92*, 156-171.

IUPAC–IUB (1996). Joint Commission on Biochemical Nomenclature. Nomenclature of carbohydrates.

Johnson, K. L. (1985). Contact Mechanics. Cambridge University Press, Cambridge.

Kallithraka, S., Bakker, J., & Clifford, M. N. (2001). Interaction of (+)-catechin,(−)-epicatechin, procyanidin B2 and procyanidin C1 with pooled human saliva in vitro. *Journal of the Science of Food and Agriculture, 81*(2), 261-268.

Koliandris, A. L., Morris, C., Hewson, L., Hort, J., Taylor, A. J., & Wolf, B. (2010). Correlation between saltiness perception and shear flow behaviour for viscous solutions. *Food Hydrocolloids, 24*(8), 792-799.

Kokini, J. L. (1987). The physical basis of liquid food texture and texture-taste interactions. *Journal of Food Engineering, 6*(1), 51-81.

Kokini, J. L., & Cussler, E. L. (1983). Predicting the Texture of Liquid and Melting Semi-Solid Foods. *Journal of Food Science, 48*(4), 1221-1225.

Kokini, J. L., Kadane, J. B., & Cussler, E. L. (1977). liquid texture perceived in the mouth1. *Journal of Texture Studies, 8*(2), 195-218.

Mackie, W., Perez, S., Rizzo, R., Taravel, F., & Vignon, M. (1983). Aspects of the conformation of polyguluronate in the solid state and in solution. *International Journal of Biological Macromolecules, 5*(6), 329-341.

Malone, M. E., Appelqvist, I. A. M., & Norton, I. T. (2003). Oral behaviour of food hydrocolloids and emulsions. Part 1. Lubrication and deposition considerations. *Food Hydrocolloids, 17*(6), 763-773.

Martin, H. M. (1916). Lubrication of gear teeth. *Engineering (London), 102*, 119-121.

Medin, A. S. (1995). Studies on structure and properties of agarose. Doctoral dissertation. *Acta Universitatis Upsaliensis*, 126.

Meldahl, A. (1941). Contribution to the Theory of the Lubrication of Gears and of the Stressing of the Lubricated Flanks of Gear Teeth. *Brown Boveri Review, 28*(11), 374-382.

Mills, T., Koay, A., & Norton, I. T. (2013). Fluid gel lubrication as a function of solvent quality. *Food Hydrocolloids, 32*(1), 172-177.

Mitchell, J. R., & Blanshard, J. M. V. (1976). Rheological properties of alginate gels. *Journal of Texture Studies*, 7(2), 219-234.

Morris, E. R., & Rees, D. A. (1978). Principles of biopolymer gelation: Possible models for mucus gel structure. *British Medical Bulletin, 34*(1), 49-53.

Morris, E. R., Rees, D. A., & Robinson, G. (1980). Cation-specific aggregation of carrageenan helices: domain model of polymer gel structure. *Journal of Molecular Biology, 138*(2), 349-362.

Myant, C., Spikes, H. A., & Stokes, J. R. (2010). Influence of load and elastic properties on the rolling and sliding friction of lubricated compliant contacts. *Tribology International, 43*(1), 55-63.

Norton, I. T., Frith, W. J., & Ablett, S. (2006). Fluid gels, mixed fluid gels and satiety. *Food Hydrocolloids, 20*(2), 229-239.

Norton, I., Goodall, D., Austen, K., Morris, E., & Rees, D. (1986). Dynamics of molecular organization in agarose sulphate. *Biopolymers, 25*(6), 1009-1029.

Norton, I. T., Goodall, D. M., Morris, E. R., & Rees, D. A. (1979). Kinetic evidence consistent with double helix formation in K-carrageenan solutions. *Journal of the Chemical Society, Chemical Communications, 22*, 988-990.

Norton, I. T., Jarvis, D. A., & Foster, T. J. (1999). A molecular model for the formation and properties of fluid gels*. International Journal of Biological Macromolecules, 26*(4), 255-261.

Peppler, W. (1936). Untersuchungen uber die Druckiibertragung bei belasteten und geschmierten umlaufenden achsparallelen Zylindern, *Maschinenelemente-Tagung Aachen 1935*, Vol. 42.

Phillips, G. O., & Williams, P. A. (Eds.). (2009). *Handbook of Hydrocolloids*. Elsevier.

Pring, J. T. (1982). The Oxford Dictionary of Modern Greek: Greek-English, English-Greek. *Clarendon Press.* Oxford University Press.

Reitsma, M. G., Cain, R. G., Biggs, S., & Smith, D. W. (2006). Wear of a single asperity using Lateral Force Microscopy. *Tribology Letters, 24*(3), 257-263.

Reynolds, O. (1886). On the Theory of Lubrication and Its Application to Mr. Beauchamp Tower's Experiments, Including an Experimental Determination of the Viscosity of Olive Oil. *Proceedings of the Royal Society of London, 40*(242-245), 191-203.

Richardson, R. K., Morris, E. R., Ross-Murphy, S. B., Taylor, L. J., & Dea, I. (1989). Characterization of the perceived texture of thickened systems by dynamic viscosity measurements. *Food Hydrocolloids, 3*(3), 175-191.

Rossetti, D., Bongaerts, J. H. H., Wantling, E., Stokes, J. R., & Williamson, A. M. (2009). Astringency of tea catechins: more than an oral lubrication tactile percept. *Food Hydrocolloids, 23*(7), 1984-1992.

Schiffman, S. S., Suggs, M. S., Sostman, L., & Simon, S. A. (1992). Chorda tympani and lingual nerve responses to astringent compounds in rodents. *Physiology & Behavior, 51*(1), 51-63.

Shama, F., & Sherman, P. (1973). Variation in stimuli associated with oral evaluation of the viscosities of glucose solutions. *Journal of Texture Studies, 4*(2), 254-262.

Smidsrød, O. (1974). Molecular basis for some physical properties of alginates in the gel state. *Faraday Discussions of the Chemical Society, 57*, 263-274.

Smidsrød, O. (1990). Alginate as immobilization matrix for cells. *Trends in Biotechnology, 8*, 71-78.

Smidsrød, O., Glover, R. M., & Whittington, S. G. (1973). The relative extension of alginates having different chemical composition. *Carbohydrate Research, 27*(1), 107-118.

Smith, A. K., June, H., & Noble, A. C. (1996). Effects of viscosity on the bitterness and astringency of grape seed tannin. *Food Quality and Preference, 7*(3), 161-166.

Steginsky, C. A., Beale, J. M., Floss, H. G., & Mayer, R. M. (1992). Structural determination of alginic acid and the effects of calcium binding as determined by high-field NMR. *Carbohydrate Research, 225*(1), 11-26.

Stephen, A. M., & Phillips, G. O. (Eds.). (2014). Food polysaccharides and their applications (Vol. 160). CRC Press.

Stokes, J. R., Macakova, L., Chojnicka-Paszun, A., de Kruif, C. G., & de Jongh, H. H. (2011). Lubrication, adsorption, and rheology of aqueous polysaccharide solutions. *Langmuir, 27*(7), 3474-3484.

Stokke, B. T., Draget, K. I., Smidsrød, O., Yuguchi, Y., Urakawa, H., & Kajiwara, K. (2000). Small-angle X-ray scattering and rheological characterization of alginate gels. 1. Ca-alginate gels. *Macromolecules, 33*(5), 1853-1863.

Stribeck, R. (1902). *Die wesentlichen Eigenschaften der Gleit- und Rollenlager Zeitschrift des Vereins Deutscher Ingenieure, 36* (46), 1341–1348, 1432–1438 and 1463–1470.

Sworn, G., Sanderson, G. R., & Gibson, W. (1995). Gellan gum fluid gels. *Food Hydrocolloids, 9*(4), 265-271.

Tako, M., & Nakamura, S. (1988). Gelation mechanism of agarose. *Carbohydrate Research, 180*(2), 277-284.

Tichy, J. A., & Meyer, D. M. (2000). Review of solid mechanics in tribology. *International journal of Solids and Structures, 37*(1), 391-400.

Vardhanabhuti, B., Cox, P. W., Norton, I. T., & Foegeding, E. A. (2011). Lubricating properties of human whole saliva as affected by β-lactoglobulin. *Food Hydrocolloids, 25*(6), 1499-1506.

Wolf, B., Frith, W. J., Singleton, S., Tassieri, M., & Norton, I. T. (2001). Shear behaviour of biopolymer suspensions with spheroidal and cylindrical particles. *Rheologica Acta, 40*(3), 238-247.

Wood, F. W. (1968). Psychophysical Studies on the Consistency of Liquid Foods. *Rheology and Texture of Food Stuffs, SCI Monograph,* (27), 40-49.

2.2. State of the art review: Designing biopolymer fluid gels

This section is a state of the art review of fluid gel research in the context of food formulation engineering, with focus on the production, rheology and tribology of fluid gels.

This work has been published as:

Fernández Farrés, I., Moakes, R. J. A., & Norton, I. T. (2014). Designing biopolymer fluid gels: A microstructural approach. *Food Hydrocolloids*, *42*, 362-372.

Abstract

Fluid gels are suspensions of gelled particles whose elasticity and physical dimensions can be manipulated to impart a range of material properties. The formation and physical properties of fluid gels are discussed with the focus being on the process-structure relationship.

Recent work in this area has led to the development of new techniques for the production of thermo-stable fluid gels. An overview is provided on these techniques which have been successfully employed to produce thermo-stable fluid gels from both alginate and proteins.

An enhanced understanding of the molecular events occurring during fluid gel formation is outlined which has enabled greater control over the microstructure. This has allowed the production of small (< 10 μm), spherical and reasonably soft particles which resemble oil droplets. These particles when used in emulsion based products to replace a significant proportion of the oil, show rheology matching that of the full fat original product.

Increasing the volume fraction and elasticity of fluid gel particles has been shown to decrease the friction measured at the contact between the soft surfaces of a tribometer. This ability of fluid gel particles to provide lubrication through entrainment to the contact zone suggests that fluid gels have the potential to impart sensory attributes typically associated with fat.

Directions for future research are also discussed which may provide further insights into food structuring and breakdown thereby assisting the design of more complex structures with novel functional attributes.

2.2.1. Introduction

Biopolymers have traditionally been used in the food industry to provide structural stability and to impart desirable texture to a wide range of products including emulsions. The relatively recent rise in health problems associated with obesity and consumer demand for tasty products has led scientists to develop low energy food products that are acceptable in terms of sensory attributes.

Microstructural engineering has emerged as a powerful tool to meet these demands, where polysaccharides are often used to build structures that resemble those of the original product that is to be reformulated. To achieve this, methods have been developed to enable scientists to control and manipulate the physical properties of structuring ingredients. An example of this is the production of suspensions of micro-gelled particles whose strength and physical dimensions are tailored to match the structures of the ingredients they are replacing such as oil droplets. The colloidal properties of those particulate suspensions (*i.e.* fluid gels) allow them to impart desirable properties in emulsion based products.

The production of fluid gels was restricted to polysaccharides, specifically polysaccharides which undergo thermo-reversible ordering transitions, but recent developments have enabled the production of thermally stable fluid gels. This has allowed for a much wider range of applications in the food industry. Thermo-stable fluid gels have been created by calcium-induced gelation of alginates and also with whey protein materials. Methods for the production of those fluid gels will be described in this paper with the focus being on the relationship between processing conditions and the resulting microstructures.

Key requirements for successful design of colloidal structures for fat replacement are advance the understanding of the mechanisms which underlie the functional properties of oil droplets and the ability to predict their behaviour using instrumental techniques. Oil droplets in food products are responsible for desirable sensory attributes such as creaminess and to impart flavour. Textural attributes are strongly dependent upon the level of lubrication provided by the material in the contact generated between the tongue and palate during consumption. For that reason and in order to characterise the lubricating behaviour of fluid gels, soft-tribological techniques have been used, where the friction between the soft surfaces of a ball and disc in relative motion is measured. Tribological results from oil-in-water emulsions were shown to correlate well with sensory data, providing an insight into the processes occurring in the oral cavity during food consumption. This correlation relates to the fact that the structure of the emulsion deforms into a thin film during the last step of food processing in the mouth, specifically as a result of the movement of the tongue against the palate before swallowing. The dimensions of the thin film that is generated during oral processing is similar to that which forms between the ball and the disc of the tribometer at speeds between 10 mm/s and 100 mm/s (Malone *et al.,* 2003). Thus, a good match has been found between sensory measurements and the triobological data obtained at these speeds, when soft rubber materials that resemble the surfaces of the oral cavity are used.

Fluid gels have shown the ability to generate thin film in these flow conditions. As such, fluid gel tribology is specifically relevant to determination and prediction in mouth sensory attributes by studying the ability of fluid gels to provide lubrication.

Recent work on fluid gel lubrication will also be covered, with a focus on aspects that are of importance for microstructural engineering including the influence of particle structure on particle entrainment into the contact zone and the resulting level of lubrication.

A discussion on the areas of future research that are required to gain a better understanding of fluid gel structuring and breakdown in both the mouth and the gastrointestinal (GI) tract is provided. This will enable the design of novel and more complex fluid gel structures. A multidisciplinary approach including knowledge of colloid science, sensory response and physiology will be needed to the exciting challenge of bringing an insight into how foods react to biological processes, how they affect organoleptic perception and their impact on human health.

2.2.2. Fluid gels

2.2.2.1. Thermo-reversible fluid gels from polysaccharides

Fluid gels are formed by the application of a flow field to the gelling biopolymer solution while undergoing conformational transition and subsequent aggregation. For biopolymers undergoing thermally reversible transitions, control over the kinetics of the ordering process is achieved by the manipulation of the cooling rate which determines the final particle physical properties. Kinetic competition between the processes of network formation and shear induced break-up that occurs as the midpoint temperature is approached has a dramatic effect on the resulting particle structure (size, shape) and the intrinsic particle 'reactivity'. At high cooling rates, the gelation process dominates over the applied shear rate and large irregularly-shaped particles are produced. As the conformational ordering kinetics is more closely matched to the time scale of the applied shear rate (*i.e.* at lower

cooling rates) the input from the applied flow field increases, resulting in the formation of small and spherical particles. Consequently, systems exhibit a more fluid-like response (reduced storage modulus) than that of fluid gels produced at higher cooling rates. Under the same applied cooling rate, both particle size and volume occupancy are strongly influenced by the applied shear field: increasing the magnitude of the shear rate leads to smaller particles and lower volume fractions. Work by Gabriele *et al.* (2009) showed that while big and irregularly-shaped particles are produced at low shear rates, small and nearly spherical particles can be obtained at high shear rates for *k*-carrageenan fluid gels produced at the same cooling rates (Gabriele *et al.*, 2009). Therefore, a range of microstructures with significantly different physical properties can be produced from minor changes to the processing parameters whilst using the same material.

Mechanistically, the formation of fluid gels is a nucleation and growth process (Norton *et al.,* 1999). The applied shear forces ensure the initially formed gel nuclei remain separated from each other which limits the molecular ordering to occur within distinct particles.

The resulting particles have a higher polymer density at centre which gradually decreases towards the edge due to the weak interfacial tension acting between the gelled and non-gelled phases of the polymer and also that the input from the flow field is higher at the particle surface. However, as will be discussed later in this paper, the degree to which the applied shear limits molecular ordering depends largely on the nature of the polymer. Both the ordering rate and the cohesive nature of the bonds (*e.g.* weak hydrogen bonds or ionic crosslinking) determine the gelled polymeric network of the individual particles and consequently their stiffness. The polymeric network of thermo-reversible fluid gel particles can be elucidated by comparing the melting profile of a fluid gel with that of the

corresponding quiescently cooled gel. The experimental procedure consists of measuring the thermal transitions when the fluid gel is heated above its melting temperature, then cooled and re-heated again. As such, the disordering transition that occurs during the first heating cycle (melting the fluid gel) can be assessed by comparison with that of its corresponding quiescent gel. Results obtained from *k*-carrageenan fluid gels (Fig. 2.15) have shown that enthalpy of melting for the fluid gel ($\Delta_{m,FG}$ = 0.174 ± 0.003 J/g) is significantly lower than that of the quiescent gel ($\Delta_{m,QG}$ = 0.186 ± 0.002 J/g), indicating fewer number of helical domains in the fluid gel (Garrec and Norton, 2012).

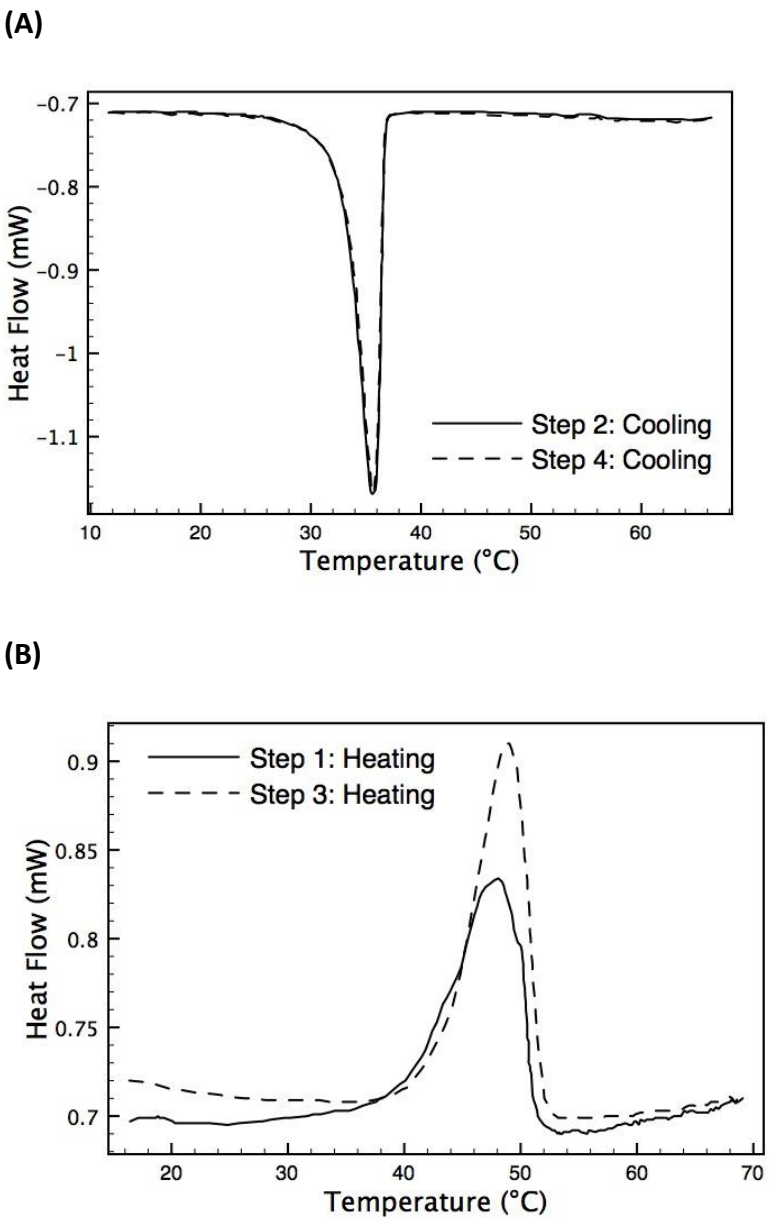

Figure 2.15: (A) Heating and (B) cooling profiles obtained through DSC for initial k-carrageenan (0.5 wt %, 0.3 wt % KCl) fluid followed by quiescent gel. Step 1 shows melting of a previously prepared fluid gel followed by quiescent gelation (step 2). In situ re-melting and gelling of the quiescent gel is then shown in steps 3 and 4 (Garrec and Norton, 2012).

As initially suggested by Norton *et al.* (1999), fewer helical domains and thus smaller helical aggregates are formed at the surface of the particles due to the disruption of the coil-helix transition by the applied shear field. Consequently, the density of the gelled network is lower towards the particle surface where the disruption to the aggregation process results

in later ordering of polymer chain, leading to the formation of particles with 'hairs' (*i.e.* partially retained polymer chains). Unlike *k*-carrageenan, fluid gels produced from agarose display similar melting enthalpies and temperature to those of their counterpart quiescent gels (Norton *et al.* 1999) indicating an equivalent internal structure. This disparity in the calorimetry results for systems produced from *k*-carrageenan compared to those produced from agarose relate to differences in the rate of molecular ordering, being 2-3 orders of magnitude faster for agarose than *k*-carrageenan (Norton *et al*. 1986). The fast ordering transition of agarose kinetically traps the structures into anisotropic shapes and particles typically reach larger dimensions. In contrast to this, fluid gel particles formed from *k*-carrageenan under comparable processing conditions are small (1 μm) and they achieve a thermodynamically favourable spherical shape. Thus, the structural features of the final particles (*e.g.* size, morphology, presence of 'hairs') are strongly dependent on the polysaccharide. These properties have a profound effect on the rheological response of fluid gels, particularly of diluted fluid gels. It is therefore essential to understand the influence of the bulk properties of particles on the degree of dilution, in order to design colloidal structures that will be incorporated into foodstuffs.

The effects of particle shape were addressed in the work of Frith *et al.* (2002) in which the volume fraction dependence of the storage modulus of agarose anisotropic fluid gels was compared with that of model micro-gel suspension of spherical agarose particles. Since both systems were produced from the same hydrocolloid, an equivalent degree of inter-particle interaction was assumed. Spherical particles were achieved by the emulsion route, cooling a water-in-oil emulsion where the gelling polymer is dissolved in the aqueous phase. Initially in this method, a mixture of polymer aqueous solution and oil is sheared while

heating at a temperature above the polymer gelation temperature. This produces droplets with a uniform polymer distribution and a well defined edge at the interface due to the high interfacial tension between the dispersed aqueous phase and the continuous oil phase. Thus, the gelled particles that form upon cooling are spherical particles with homogeneous polymer distribution. Consecutive processes of dilution with water and centrifugation are used to separate the particles from the continuous oil phase. Micro-gel model suspensions are then prepared by dispersing the produced spherical particles in water. As Fig. 2.16 shows, the response to dilution with water of the sheared anisotropic particles is markedly different to that of the uniform spherical particles. The highly irregular and extended morphology of fluid gel particles distribute through the space to a greater degree than the model spherical particles with an equivalent volume. This results in greater inter-particle interaction compared to spherical particles at low volume fractions which leads to the formation of percolated networks although the particles are not aggregated. As such, fluid gels display elastic dominated responses over a broad range of volume fractions (Firth *et al.*, 2002).

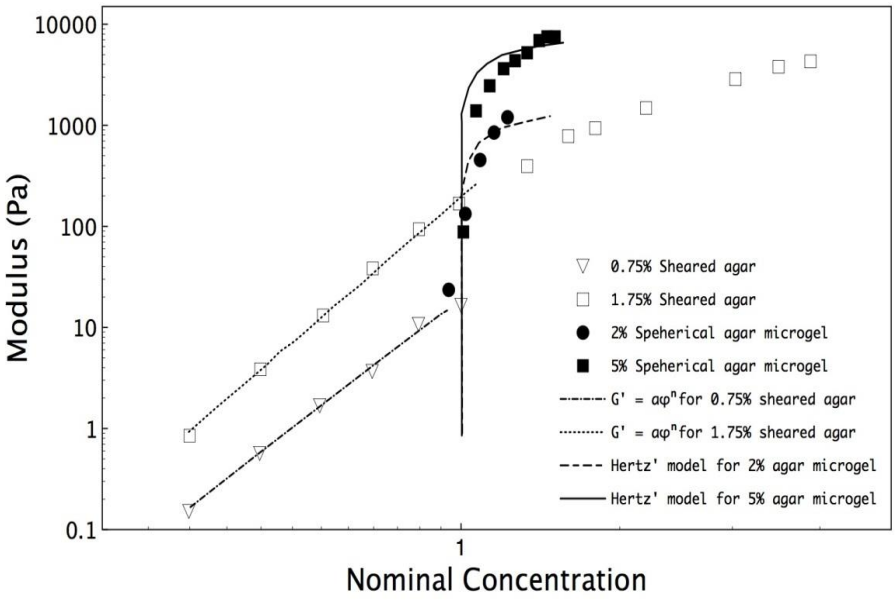

Figure 2.16: Comparative plot for the concentration dependence of the plateau modulus for both sheared and model agar sphere suspensions. Predictions based on the Hertzian interactions between particles have also been illustrated, assuming a particle modulus of 33 KPa (Frith et al., 2002).

In the work of Wolf *et al.* (2001), the influence of particle shape on rheology and the process-morphology relationship was also investigated, where a wider range of microstructures were produced from the sheared gelation of mixtures of polysaccharides (Fig. 2.17). By manipulating the flow conditions during the gelation of one of the polymers, regular spheroidal or cylindrical shaped particles were formed. The use of a rheometer with concentric cylinder geometry allowed the production of uniform and regularly shaped gelled microstructures. Molten mixtures of gellan and *k*-carrageenan were loaded to the rheometer at 60 °C and subjected to a constant stress of 0.05 Pa. Ellipsoidal shapes were achieved by cooling the system below the gelation temperature of the dispersed phase (gellan) whilst applying a constant stress (above 0.05 Pa). Alternatively, cylindrical particles were produced as a result of firstly cooling under small stress (0.05 Pa) and subsequently

increasing the stress up to 0.5 Pa immediately before the gelation of the dispersed phase. Droplets are initially elongated into cylindrical threads, which are then trapped via gelation and prior to being broken up. Kinetic trapping of the structure in controlled and defined shapes is achieved by controlling the time scale of the imposed increase in stress such that the process of droplet break up occurs at a lower rate than gelation. If the gelation rate is too slow, spherical particles are formed due to the complete structural relaxation of the droplet phase.

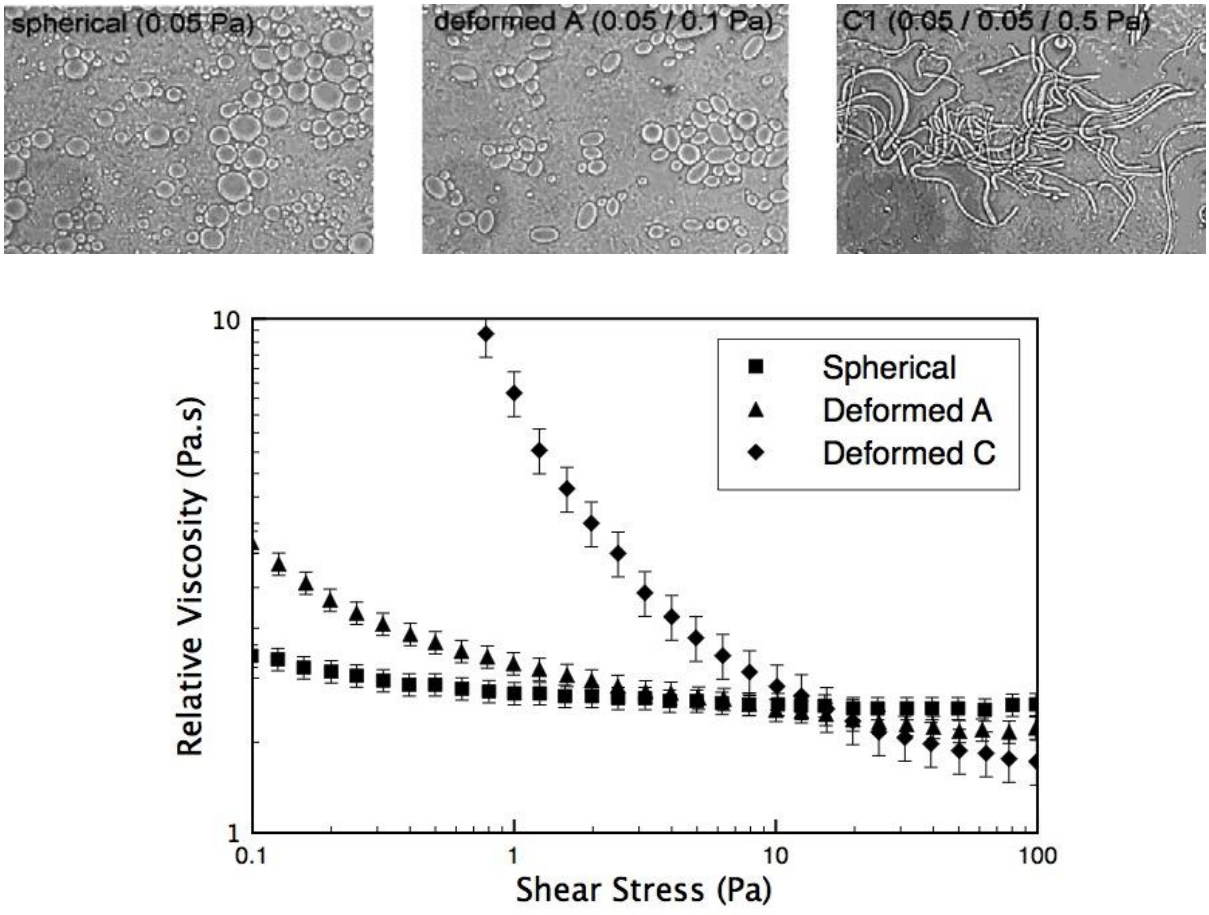

Figure 2.17: Viscosity measurements for particulate asymmetric gel suspensions with varying degrees of aspect ratio. Micrograph inserts depict average particle morphologies for their respective viscometry profile (Wolf et al., 2001).

The shear-induced structuring process in mixed systems requires less energy input than is necessary to produce fluid gels from a solution containing a single biopolymer (Norton *et al.,* 2006). The reason for this lies in the fact that the two phases of mixed polymer systems are not pure such that each polymer exists in both gelled and aqueous state. Thus, only the weak interfacial tension has to be overcome by the applied flow field before inducing gelation. Wolf *et al.* (2001) showed a dramatic effect of particle shape on the relative viscosity, specifically at lower shear stresses where increasing the particle aspect ratio results in suspensions with increased viscosities (Fig. 2.17). At high shear stresses, a greater degree of particle orientation occurs upon increasing the particle aspect ratio, resulting in decreased viscosities. These results also showed that particle entanglements form over time after production due to the greater flexibility of cylindrical particles. Arising from this, particle orientation is suppressed. Moreover, once particle entanglement has occurred application of shear does not orient particles and a reduction in viscosity at higher shear rates is not observed.

It is clear that the evaluation of particle shape and the quantification of particulate volume fraction have led to a more detailed understanding of the relationship between particle morphology and fluid gel properties. In conclusion, both process and formulating parameters can be manipulated in the production of fluid gels from a single polysaccharide so as to create particles with different sizes and shapes. An even wider range of microstructures can be designed in order to achieve novel properties if the gelling polysaccharide is mixed with another polymer. The rheological properties of these particulate structures have potential applications in imparting texture and mouthfeel enhancement when used in emulsion based products. Undoubtedly, in order to establish

whether these rheological behaviours translate into an expected in-mouth performance, an understanding of particle structure in relation to in-mouth sensory perception is required. Current models of the relationship between fluid gel lubrication and sensory response (functionality) involve the use of soft-tribology, recent advances in this area will be discussed later in this paper.

2.2.2.2. Recent developments: thermo-stable fluid gels

Alginate fluid gels

We have discussed the formation of fluid gels from polysaccharides undergoing thermal gelation (*e.g.* agar, *k*-carrageenan and gellan gum) where the conformational ordering kinetics are controlled by the rate of cooling which can be matched the time scale of the applied shear rate (Fig. 2.18.A). In practice, the major difficulty in producing fluid gels from alginate arises from the rapid and temperature independent ordering transition of alginates. As such, controlling the introduction of calcium ions into the alginate solution becomes a key factor when fluid gels are to be produced via diffusion controlled methods (*i.e.* using water soluble salts such as $CaCl_2$).

A technique employing a pin-stirrer device has been developed to produce alginate fluid gels (Fernández Farrés *et al.,* 2013; Chapter 3). Alginate and $CaCl_2$ solutions are separately pumped into the pin-stirrer with the aid of a peristaltic pump and a syringe pump, respectively. The injection point of the $CaCl_2$ is located between the tip of the pin-stirrer and the outer wall so that the two streams merge in the highest energy dissipation zone (Fig. 2.18.B). This allowed production of alginate particles with a diameter < 10 μm.

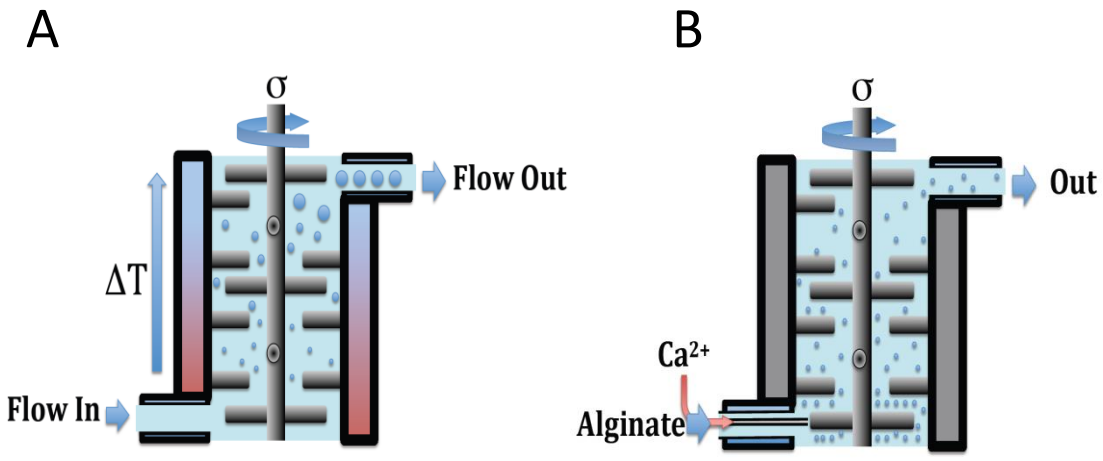

Figure 2.18: Schematic representations of thermally set fluid gels using a temperature gradient to induce gelation whilst applying shear (A) and alginate fluid gel particles produced using a syringe to inject calcium ions directly into the high shear zone (B). The size of the injection syringe is not to scale.

The authors suggested that particles form as a result of both mixing of calcium and network formation competing with the shear induced break-up of the cluster being formed. At decreased polymer concentrations, lower shear stresses act on the initially formed particles due to the reduced viscosity which allows particles to grow to larger dimensions. Additionally, the increased diffusion rate of calcium through the less dense matrix increases the characteristic time for mixing the two liquids at molecular level (micro-mixing). As a result of these mechanisms, gel formation is favoured over the shear controlled breaking process, leading to an increased particle size (Fig. 2.19, Table 2.1).

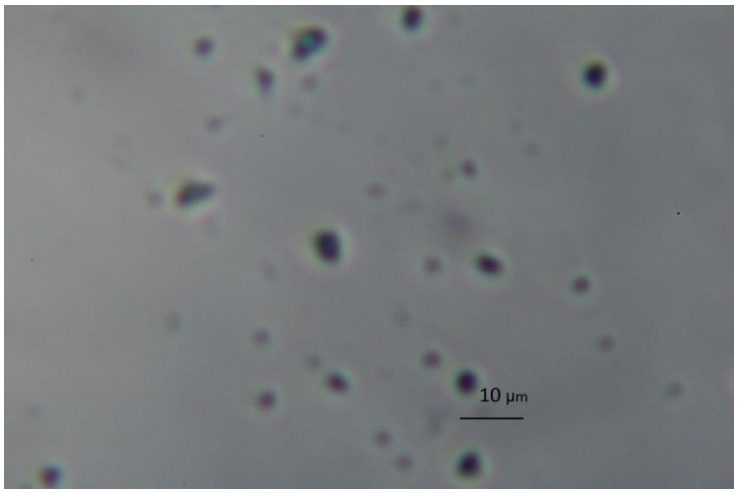

Figure 2.19: Micrograph of diluted 3% (w/w) alginate fluid gel (Fernández Farrés et al., 2013; Chapter 3).

Polymer concentration [w/w %]	Particle diameter [µm]
1	9.5 ± 2
2	8.7 ± 3
3	3.8 ± 4
4	3.4 ± 4

Table 2.1: Particle size of alginate fluid gels produced by diffusion-controlled method (Fernández Farrés et al., 2013; Chapter 3).

This method bears the limitation of poor control on the competing parameters (mixing and gelation) so that the ability to monitor alginate concentration in a single micro-gel particle is still lacking. Because the shear field inside the stirring vessel is not uniform, the size of the particles is strongly affected by the exact location of the injection point.

Hence, a more refined technique using in-situ calcium release has recently been developed that enables production of alginate fluid gels with control over the gelation kinetics (Fernández Farrés and Norton, 2014; Chapter 4). In this method, calcium ions are progressively liberated from an insoluble form of calcium (*e.g.* $CaCO_3$) by reaction with protons from the slow hydrolysis of a glucono-δ-lactone (GDL), as previously used for pectin and alginate gels (Draget, *et al.*, 1990; Ström and Williams, 2003). This gradual introduction

of calcium ions to the alginate solution leads to uniform calcium distribution throughout the system which minimises the formation of inhomogeneous gelled networks and prevents large clusters.

The shear is provided by the rheometer which allows accurate control of the applied shear rate while also monitoring the viscosity so that the kinetics of fluid gel formation can be studied. As shown in Fig. 2.20, systems produced with differing shear rates exhibit indistinguishable Newtonian viscosities before the onset of gelation. Under these conditions of limited calcium, monocomplexes form as a result of the binding of calcium to a single guluronate unit of the polymer chain which decreases the polymer charge density and gives rise to a local charge reversal (Fang *et al.* 2007; Siew *et al.,* 2005). Monocomplexes are well separated from each other; hence remain unaffected by the level of shear. Gel nuclei are also expected to form during these early stages of the ordering process, although their volume fraction is sufficient as to display any crowding effect, thus no change in viscosity occurs. As more calcium ions are released, the pair wise association of monocomplexes leads to the formation of egg-box dimers. These egg-box dimmers subsequently aggregate via inter-cluster association in a process that occurs simultaneously with the shear induced break-up of the network being formed, and fluid gel particles are produced. This simultaneous increase in number and volume fraction of the forming particles results in an increase in viscosity.

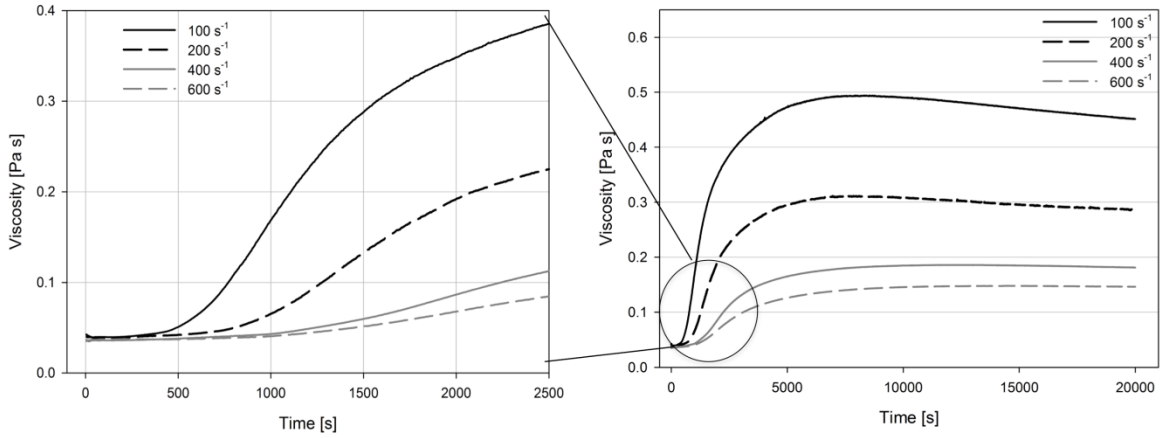

Figure 2.20: Viscosity during fluid gel production as a function of time. Systems were produced at a range of applied shear rates from 1.5 % (w/v) alginate, $CaCO_3$ 22.5 mM, 45 mM GDL and isothermally at 25 °C (Fernández Farrés and Norton, 2014; Chapter 4).

The time at which viscosity starts to increase (*i.e.* onset of gelation) increases upon increasing the level of the applied shear rate, indicating a reduction in the rate of the particle growth (Fig. 2.20). Therefore, the process of particle growth from the initially formed gel nuclei is restricted by the imposed flow field which confirms proposals by Norton *et al.* (1999) who suggested that the shear rate limits the likelihood of an association event occurring between the early formed particles. Further confirmation is obtained by measurements of G' when the shear rate is stopped prior to the completion of fluid gel particle formation. Results have shown increased rates of ordering post-production for systems formed at lower applied shear rates. At this point, intra-particle aggregations under shear change into inter-particle particle aggregations, resulting in quiescent network formation via association of particles. Conversely, when the shear is removed after completion of fluid gel structure, the rate of ordering post-production due to inter-particle interaction is not affected by the magnitude of the applied shear rate during formation (Fernández Farrés and Norton, 2014; Chapter 4).

Similarly to fluid gels made from agar or *k*-carrageenan, alginate fluid gels display a flow behaviour that lies between that of a 'weak' and a 'strong' gel, with G' significantly greater than G'', but more dependent on frequency than in the case of a quiescent gel. Current findings indicate that the stiffness and inter-particle interactions of alginate particle produced via in-situ calcium release can be controlled to give a range of viscoelastic responses.

Another feature that has been identified in alginates and which is commonly observed in thermo-reversible fluid gels is the presence of yield stress, arising from an inter-particle potential that persist post-production. True yield stress values can be determined by subjecting the fluid gels to a constant stress and recording the strain as a function of time. This test is then repeated increasing the stress in intervals. As shown in Fig. 2.21, the material behaves as a solid if the applied stress is below the yield stress and the measured strain is small and independent of time after an immediate elastic response. When the applied stress exceeds the yield stress, the strain tends to infinity until constant strain rate is achieved corresponding to a flow condition in the material. The most likely cause for yield stress behaviour in fluid gels is the presence of hairs at the particle surface which can form bridges between adjacent particles (Norton *et al.,* 1999) until the applied stress is great enough to either break or disentangle them. Increasing polymer concentration results in increases both particulate phase volume and particle stiffness, which promotes inter-particle interaction such that an increased force is required to induced flow via particles sliding past each other (*i.e.* increase in yield stress). As a consequence, the rheological response of alginate fluid gels differs greatly from that of suspensions of hard spheres. The

relatively soft and often 'hairy' nature of fluid gel particles allows them to overlap which prevents close packing behaviour.

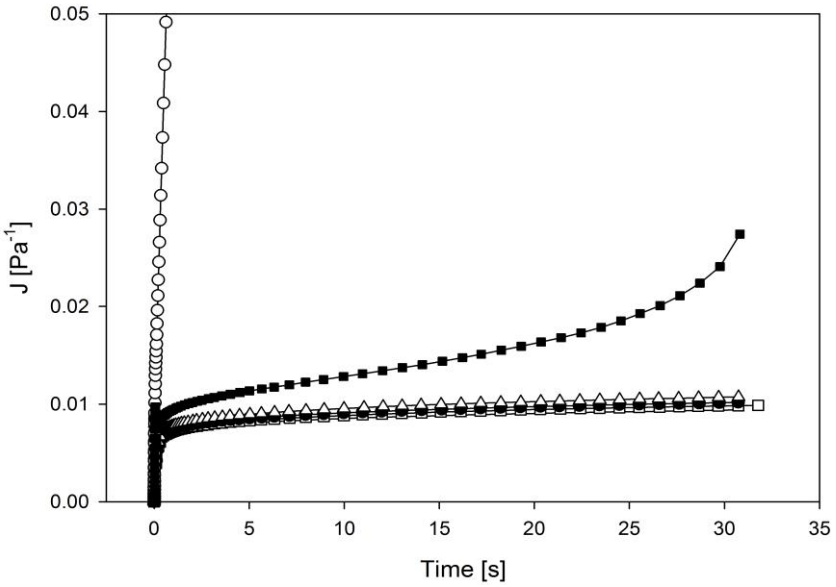

Figure 2.21: *Constant stress (creep) test profile of alginate 2 % (w/w). Applied shear stresses are 15 Pa (□), 17 Pa (●), 19 Pa (△), 21 Pa (▪) and 23 Pa (○). True stress value (21 Pa) is identified as the critical stress causing a significant increase in the creep rate over a short period i.e. minimum stress required for the transition from limited deformation to appreciable flow conditions (Fernández Farrés et al., 2013; Chapter 3).*

Full fat products often contain proteins which confine oil droplets in network structures, which also exhibit yield stresses. From this perspective, alginate fluid gels could potentially be used as fat replacement in food product. Recent findings on the lubrication properties of alginate sheared gel particles are outlined in the following section.

Because of the thermally stable (semi-crystalline) calcium-mediated junction zones, alginate fluid gels do not melt when heated at temperatures commonly used in the food industry (*e.g.* 100 °C, pasteurisation). These characteristics are clearly advantageous over other fluid gels produced from the commonly used *k*-carrageenan, agar or gellan polysacharides which

must be kept and utilised at temperatures below their melting temperatures to preserve the structure.

Protein fluid gels

Current work has begun to apply similar methods to those previously shown, to protein systems. This has led not only to thermo-stable fluid gels as a result of their irreversible denaturation on heating, but delivers the advantage of being nutritionally desirable (Moakes *et al.*, 2015).

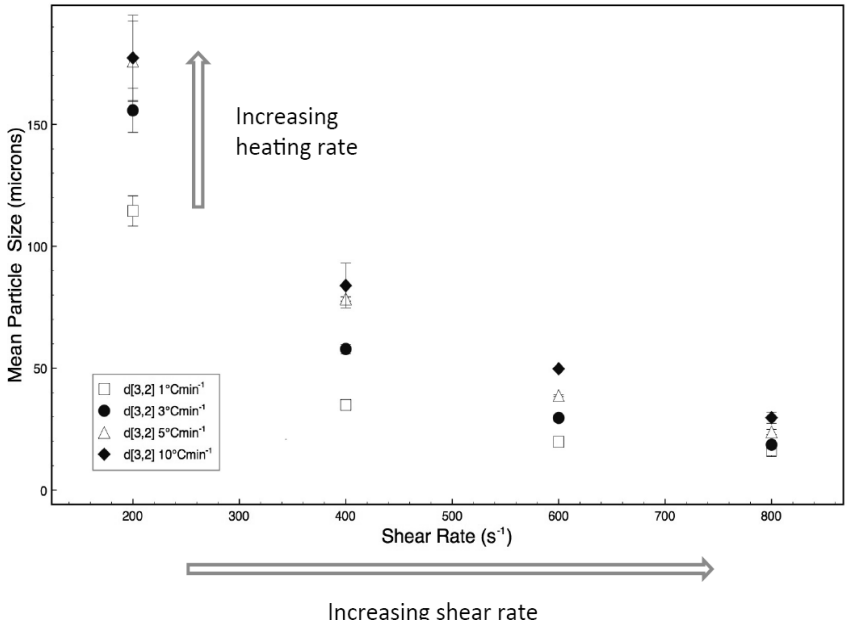

Figure 2.22: Average whey protein fluid gel particle size shown as surface weighted means ($d_{3,2}$). Means were determined using Static Light Scattering (SLS) at varying shear rates as a function of heating rate, (□) 1°C/min, (●) 3 °C/min, (△) 5 °C/min and (◆) 10 °C/min (Moakes et al., 2015).

Viscometry profiles during the formation of fluid gels from whey protein show similar trends to those observed for polysaccharides (Fig. 2.24) with the overriding difference describing structuring occurring on heating as opposed to cooling. Initially, a slight loss in the systems

viscosity occurs due to the heating of the continuous phase, which is followed by a rapid increase in viscosity at a critical temperature (T_g). At T_g, the globular whey protein structure partially denatures whilst retaining its dimeric form. Nuclei form as consequence of the disruption of the secondary structure leading to the formation of oligomers through association of intermolecular β-sheets (Lefèvre and Subirade, 2000). The nuclei grow through a succession of weak interactions and covalent bridging until all native protein within the system is consumed, at which point aggregate size becomes limited by shear. Lastly, post-ordering events occur with particle-particle interactions caused by branching as consequence of sulphide bridging. Further strengthening of the aggregate structures is also observed through increased internal structuring.

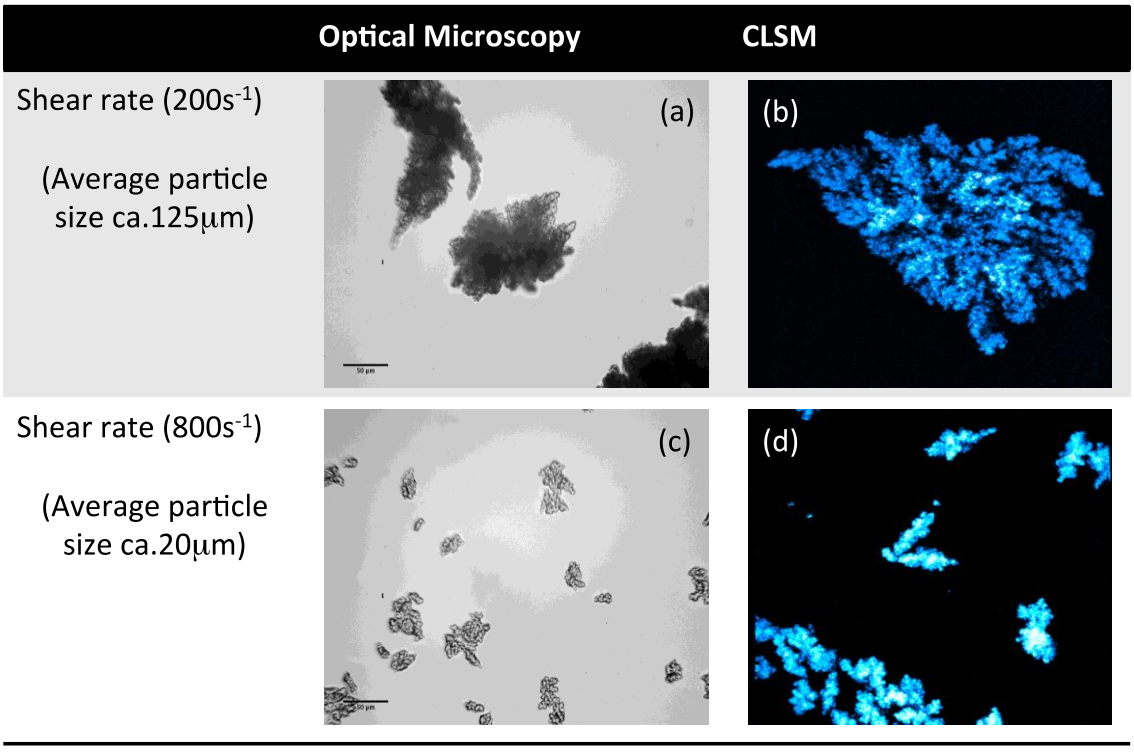

Figure 2.23: Optical (a,c) and confocal light scanning micrographs (b,d) depicting whey protein fluid gel particles (Moakes et al., 2015).

As shown for polysaccharide, the particle size of whey protein fluid gels decreases as a power function with increasing shear (Fig. 2.23). As expected, changing the thermal history of the whey protein systems leads to particle size increase (from low heating rates to higher), also best modelled using a power law. It has been reported that increasing the heating rate applied to the gelling system supports the initiation of an increased number of smaller nuclei (Bromley *et al*., 2006). However, larger aggregates are formed due to the increase of energy being applied to the system. The increase in energy within the system allows a shift from internal structuring to inter-particle bonding to occur. If sufficient energy is applied to overcome the activation energy needed for bond formation within a short time scale, the particle size can shift to being predominantly limited by shear, but also become a function of heating. The kinetics of aggregation can thus be derived from the viscosity increase over time as a function of the gradient, which has been found to increase with increasing heating rate.

Fig. 2.23 shows both optical and confocal micrographs of whey protein fluid gel particles prepared at shear rate of 200 s^{-1} and 800 s^{-1}. The optical micrographs show aggregates with irregular morphology (Fig. 2.23.A, 2.23.C).

The use of three-dimensional stacking with confocal microscopy allowed higher resolution topographical detail of the particles to be obtained. It was shown that at the lower shear rate particles formed a porous network with voids protruding through the structure. This porous matrix appears to have been lost as the particles are subjected to higher levels of shear. It is believed that high shear prevents the ordering of clusters down to a single size, at which further increasing shear has little effect. This cluster (Fig. 2.23.D) then forms the building block for larger aggregates, with porosity being a function of packing efficiency.

Both optical and confocal micrographs show the presence of inter-particle interactions with the weak grouping of particles within localised regions.

Flow and deformational properties of the fluid gels, as previously stated, are closely linked to the microstructure, shape and interactions between particles. The use of image analysis over a large sample (> 1000 particles) has shown the average aspect ratio of the structures to be 1.63 describing an elongated structure. It was found that the change in aspect ratio with increasing shear was minimal, determining that changes in rheology are more closely linked to particle microstructure and interactions than morphology. Increasing shear within the system has shown to decrease the relative viscosity change of the fluid gel following the prevention of bridging between particles. It is also thought that the 'strength' of the material is formed through a combination of both volume fraction and particle elasticity, as shown for alginate fluid gels. Therefore, controlling the resulting microstructure through processing conditions and also volume fraction gives rise to possible control over desired rheological properties. This could lead to the application of protein fluid gels within high-level protein food supplements with thermo-stable behaviour.

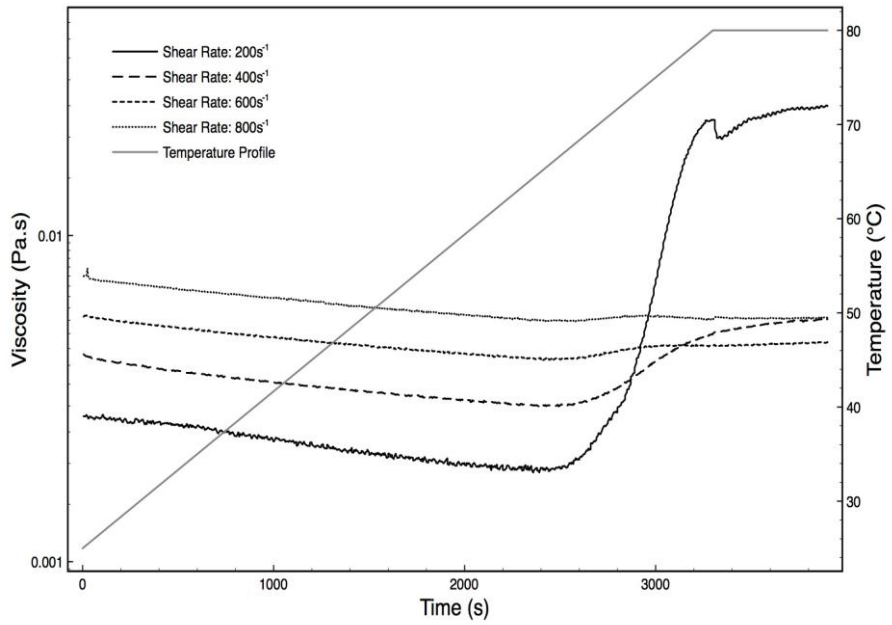

Figure 2.24: Viscometry profiles for a 10 wt % whey protein solution undergoing gelation within a shear field (Moakes et al., 2015).

2.2.3. Fluid gel lubrication

A significant challenge for microstructural engineering of foods is the development of low fat formulations with textural and sensory attributes similar to those of the full fat version. As mentioned earlier, the physical properties and thus textural attributes of fluid gel particles can be manipulated so as to mimic those of the oil droplets that are replaced. Norton *et al.* (2008) showed that the rheological properties of a mayonnaise in which most of the oil droplets were replaced by sheared gel particles matched those of a commercial full fat product.

As can be seen from Fig. 2.25, the sheared gel mayonnaise exhibits both a yield stress and an overall rheological response comparable to that of the full fat version. Yield stress is measured as the finite shear stress at which deformation starts when subjected to a

transient linear stress ramp. The low fat mayonnaise used in this study was produced from sheared agar and 3 % (phase volume) oil was added to impart both flavour and mouth-feel. This is a clear indication that sheared gel particles can replace a significant proportion of the fat droplets in an oil-in-water emulsion with minimal changes to the material properties. In addition to their rheological behaviour, an understanding of the structural changes which occur during oral processing of these food soft materials and their influence on sensory perception is necessary if we are to successfully design structured foods with reduced energy content and are also enjoyable to eat.

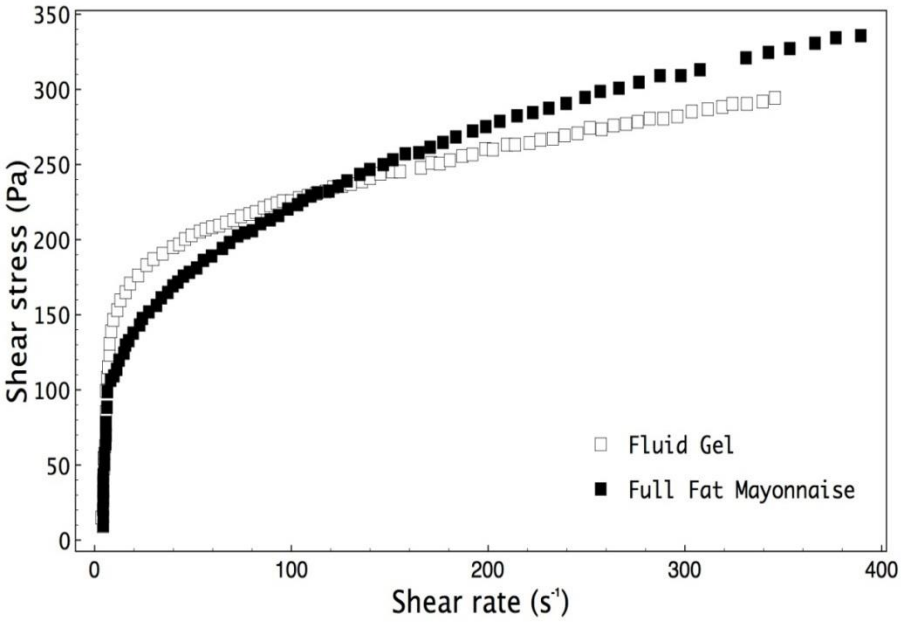

Figure 2.25: Comparative shear stress/shear rate curve of agar fluid gel with a 3 % (phase volume) of oil and a full fat commercial (Hellman's) mayonnaise (adapted image from Cox et al. 2009).

Oil droplets play a determining role in the perception of creaminess (de Wijk and Prinz, 2005) which is also related to thickness (viscosity), smoothness (size, shape and hardness of

particles) and slipperiness (Kokini, 1987; Shama and Sherman; 1973; Tyle, 1993). Tribology (thin film rheology) has emerged in recent years as a powerful technique to study the structure-functionality relationship, allowing major advances in understanding how colloidal systems (including fluid gels) affect lubrication and their influence on in-mouth sensory perception. Malone *et al*. (2003) found a strong correlation between the sensory perception of slipperiness and the friction of an oil-in-water emulsion measured in a soft tribological contact using silicon rubber to mimic the soft surfaces of the mouth. From this correlation, it was determined that speeds between 10 s^{-1} and 100 s^{-1} are involved in the movements between the tongue and the palate during oral processing of food.

A tribometer consists of a rotating ball loaded against a rotating disc at a 45 ° angle creating a sliding/rolling contact and the resulting frictional force at the ball-in-disc contact is measured by a force transducer. On introduction of a lubricant fluid between the surfaces, the fluid pressure increases as the lubricant is gradually drawn into the centre of the contact which partly separates the ball from the disc. As the rotation speed is raised, the increase in volume of lubricant in the contact results in a further surface separation thereby further reducing friction. Stribeck curves are generated by plotting the friction coefficient (μ) over a range of speeds (U), where three different regimes are identified: During boundary lubrication which occurs at the lowest speeds, where the lubricant is excluded from the contact, the load is supported by the asperity contact and μ is independent on U. In the mixed regime, μ decreases with increasing U as the increase in fluid pressure separates the surfaces resulting in both asperity contact and lubricant film supporting the load. At higher speeds, friction increases with U as the fluid volume which is being sheared increases (hydrodynamic regime) although this is not always observed in fluid gel systems.

Gabriele *et al*. (2010) studied the lubrication response of fluid gels produced from agarose with a 100 μm particle size. The obtained Stribeck curves showed an increase in friction coefficient (μ) at low speeds during the mixed regime before the film thickness was great enough so as to induce bulk entrainment. At these low speeds, the lubrication film thickness is lower than the size of the large agarose particles which, as a result, are selectively excluded from the ball-in-disc. The frictional increase was argued to be the result of the lubrication regime provided by the entrainment of a thin monolayer of particles. The proposed mechanism is based on a micro-elastohydrodynamic (micro-ELH) lubrication regime in which the fluid dynamics of particles in the thin film strongly depends on the particle's Young modulus.

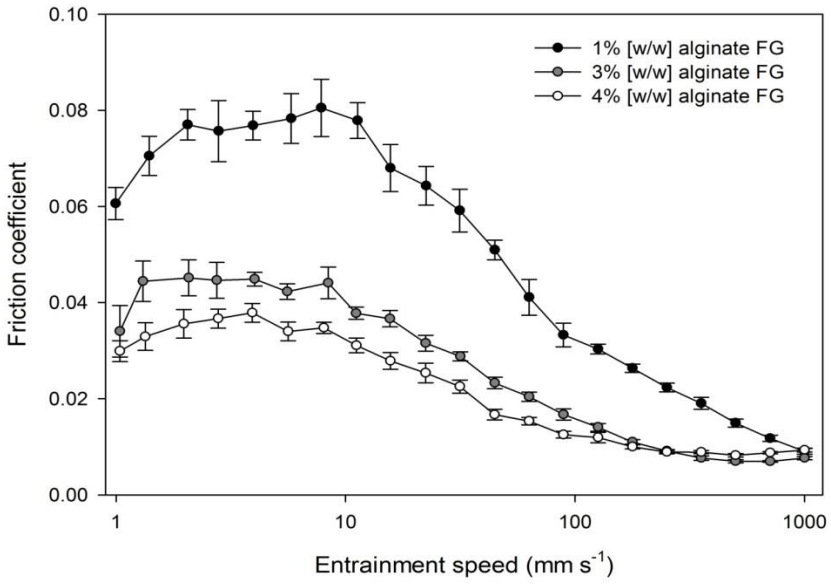

Figure 2.26: Effect of polymer concentration and particle size on lubrication properties of alginate fluid gels. Stribeck curves (ramp up) are presented for applied normal load W of 5 N. The mean frictional increase of the 1 % (w/w) alginate system is roughly twice as large in magnitude compared to that of the 3 % (w/w) and 4 % (w/w) alginate fluid gels (Fernández Farrés et al., 2013; Chapter 3).

An increase in friction at low speeds has also been observed for alginate fluid gels containing particles with a mean average diameters ranging from 3.4 ± 4 μm to 9.5 ± 2 μm. As shown in Fig. 2.26, this peak in friction is less pronounced for the smaller and stiffer alginate particles produced from higher polymer concentrations which also exhibit an overall reduced friction. It is expected that less deformable particles provide lower frictional data as a result of a reduced surface contact due to the stiffer particles greater resistance to compressive forces. The root mean square roughness of the silicone disc surface is approximately 0.8 μm, thus sufficiently small particles (< 1μm) can fit into the disc surface irregularities thereby entering the contact zone via surface roughness. As a result, particle exclusion decreases and systems exhibit a less pronounced peak in friction. This effect was further shown in the work of Garrec and Norton (2013) where *k*-carrageenan fluid gel particles having a diameter equivalent to the surface roughness dimensions (1 μm) provided lubrication at all speeds through particle entrainment, resulting in Stribeck curves without any frictional increase. Because the friction in the boundary lubrication regime was reduced below that of the continuous phase (water) upon increasing the number and stiffness of the particles, particle entrainment was also suggested to occur in boundary conditions.

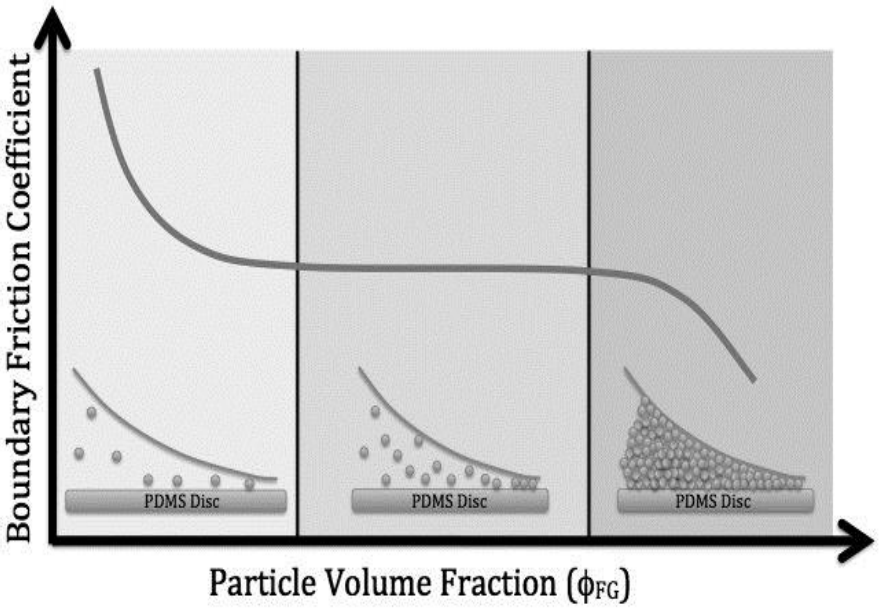

Figure 2.27: Particle entrainment and boundary as function of (adapted image from Garrec and Norton, 2013).

As illustrated in Fig. 2.27, the boundary friction of *k*-carrageenan fluid gels decreases with particle volume fraction (ϕ) until a plateau region is reached ($0.3 < \phi < 0.6$). This is followed by a further reduction in friction with increasing ϕ ($\phi > 0.7$). The initial decrease in μ is the result of an increased number of particles in the contact zone. The fact that a plateau region is observed suggests that the dependence of the boundary friction on volume fraction relates to the number of particles in the contact, rather than the bulk rheology and inter-particle interaction. Finally, at high volume fractions, a multilayer of closely packed particles are entrained to the contact zone and the friction is further reduced. Thus, unlike the fluid gel rheology which greatly depend on the level of inter-particle interactions and hence volume fraction, fluid gel tribology is mainly dominated by the elasticity of the particles.

Data obtained from sensory trials revealed that *k*-carrageenan fluid gel particles were not perceived as particles, rather, fluid gels were perceived as 'smooth' (Garrec, 2013). There is

therefore an indication that stiffness of fluid gel particles can be manipulated to provide enhanced lubrication while not being detected during consumption.

By understanding the microstructure-property relationship the influence of fluid gel lubrication on perceived sensory attributes can be further studied. Tribology as a scientific tool to relate the structural properties to the sensory perception is just starting to develop. Further success will require a combined knowledge of material science and sensory science, along with an understanding of how the processes involved during oral processing (*e.g.* temperature, mixing with saliva, squeezing and shearing between palate-tongue) affect the structure.

2.2.4. New concepts for designing colloidal structures

The production of colloidal gelled structures offers a broad range of material properties that can be modified to the meet a range of product needs. As discussed, controlled structuring processes in which conditions are well defined are used to deliver fluid gel structures with desirable material properties. Fluid gels show promising characteristics for fat replacement as their textural and tribological responses can be controlled to mimic those of oil droplets. The removal of fat in foodstuff not only affects the material properties, but is detrimental to flavour perception.

In order to control and enhance flavour and mouthfeel, novel methods to produce more complex structures are under development. One microstructural approach involves the entrapment of oil droplets within the fluid gel particles, forming a system resembling an oil-in-water emulsion. This would allow fat soluble flavour molecules to be added to the dispersed oil phase so that they could be released as the gel breaks down in the mouth thereby imparting both desirable mouthfeel and flavour attributes. In addition to flavour,

micronutrients could be dissolved in the oil droplets, thus offering the potential for low-energy and nutritionally rich foodstuffs with acceptable organoleptic properties.

The formulation and production process of such structurally complex systems sets the challenge of maintaining the stability of the oil droplets inside the gelled particles. Lipophilic emulsifiers may be required, although it is not yet clear how an interface alters the physical properties. An alternative method for stabilising the oil is the creation of a solid fat interface by adsorption of triacylglyceride particles.

The correct microstructural engineering will be required to ensure that the rupture of the gelled emulsion structure occurs either in the mouth for flavour release or inside the gastrointestinal tract for the release of vitamins or other nutrients.

Another exciting microstructural approach which may allow encapsulation and controlled release of nutrients inside the gastrointestinal tract is building layered fluid gel structures arising from the association between alginate and chitosan. In acidic conditions, alginate gels contract due to reduced solubility of non-ionized carboxyl groups while, in alkaline conditions, the increased hydrophobicity of the ionized carboxyl groups leads to swelling and dissolution. On the contrary, chitosan dissolves in acidic medium due to the hydrophobicity of the protonated amino groups and is insoluble in alkaline conditions. By mixing the two polymers, the electrostatic interaction between the carboxyl groups of alginate and the amino groups of chitosan form a polyelectrolyte complex which is insoluble at pH below 3.5 and dissolves at pH above 6 due to a reduction in charge density of the chitosan (George *et al.,* 2006; Huguet *et al.,* 1996; Tønnesen and Karlsen, 2002). Thus, chitosan coated alginate fluid gel particles should be stable during their passage through the stomach ($1.5 < pH < 3.5$) and subsequently disintegrate in the intestine ($pH \approx 7$) thereby

releasing the encapsulated nutrient. In practical terms, the main challenge will be the formation of a defined chitosan layer which will reduce the porosity of the alginate network hence preventing leakage of encapsulated nutrients.

Alternative mixed biopolymer composites can also be exploited to produce particles with enhanced stiffness as a result of associative interactions between the polymers (*e.g.* carrageenan and locus bean, gelatin and low-methoxy pectin). As a result, novel textural properties could be achieved which may potentially provide enhanced lubrication typically associated with fat content.

Elucidating the function of the interface during the structuring process will be an exciting challenge which will enable the development of predictive models for the microstructure-property relationship of mixed fluid gels.

2.2.5. References

Bromley, E., Krebs, M., & Donald, A. (2006). Mechanisms of structure formation in particulate gels of β-lactoglobulin formed near the isoelectric point. *The European Physical Journal E, 21*(2), 145-152.

Draget, K. I., Østgaard, K., & Smidsrød, O. (1990). Homogeneous alginate gels: A technical approach. *Carbohydrate Polymers, 14*(2), 159-178.

Cox, P. W., Spyropoulos, F., & Norton, I. T. (2009). Effect of Processing on Biopolymer Interactions. Modern Biopolymer Science: *Bridging the Divide between Fundamental Treatise and Industrial Application*, 199.

de Wijk, R. A., & Prinz, J. F. (2005). The role of friction in perceived oral texture. *Food Quality and Preference, 16*(2), 121-129.

Fang, Y., Al-Assaf, S., Phillips, G. O., Nishinari, K., Funami, T., Williams, P. A., et al. (2007). Multiple Steps and Critical Behaviors of the Binding of Calcium to Alginate. *The Journal of Physical Chemistry B, 111*(10), 2456-2462.

Fernández Farrés, I., Douaire, M., & Norton, I. T. (2013). Rheology and tribological properties of Ca-alginate fluid gels produced by diffusion-controlled method. *Food Hydrocolloids, 32*(1), 115-122.

Fernández Farrés, I., & Norton, I. T. (2014). Formation kinetics and rheology of alginate fluid gels produced by in-situ calcium release. *Food Hydrocolloids, 40*, 76-84.

Frith, W., Garijo, X., Foster, T., & Norton, I. (2002). Microstructural origins of the rheology of fluid gels. *Special publication-Royal Society of Chemistry, 278*, 95-103.

Gabriele, A., Spyropoulos, F., & Norton, I. T. (2009). Kinetic study of fluid gel formation and viscoelastic response with kappa-carrageenan. *Food Hydrocolloids, 23*(8), 2054-2061.

Gabriele, A., Spyropoulos, F., & Norton, I. T. (2010). A conceptual model for fluid gel lubrication. *Soft Matter, 6*(17), 4205-4213.

Garrec, D.A. (2013). Understanding fluid gels and hydrocolloid tribology. EngD Thesis. University of Birmingham.

Garrec, D. A., & Norton, I. T. (2012). Understanding fluid gel formation and properties. *Journal of Food Engineering, 112*(3), 175-182.

Garrec, D. A., & Norton, I. T. (2013). Kappa carrageenan fluid gel material properties. Part 2: Tribology. *Food Hydrocolloids, 33*(1), 160-167.

George, M., & Abraham, T. E. (2006). Polyionic hydrocolloids for the intestinal delivery of protein drugs: alginate and chitosan—a review. *Journal of Controlled Release, 114*(1), 1-14.

Huguet, M., Neufeld, R., & Dellacherie, E. (1996). Calcium-alginate beads coated with polycationic polymers: comparison of chitosan and DEAE-dextran. *Process Biochemistry, 31*(4), 347-353.

Kokini, J. L. (1987). The physical basis of liquid food texture and texture-taste interactions. *Journal of Food Engineering, 6*(1), 51-81.

Lefevre, T., & Subirade, M. (2000). Molecular differences in the formation and structure of fine-stranded and particulate β-lactoglobulin gels. *Biopolymers, 54*(7), 578-586.

Malone, M. E., Appelqvist, I. A. M., & Norton, I. T. (2003). Oral behaviour of food hydrocolloids and emulsions. Part 1. Lubrication and deposition considerations. *Food Hydrocolloids, 17*(6), 763-773.

Moakes, R. J. A., Sullo, A., & Norton, I. T. (2015). Preparation and characterisation of whey protein fluid gels: The effects of shear and thermal history. *Food Hydrocolloids, 45*, 227-235.

Norton, I., Goodall, D., Austen, K., Morris, E., & Rees, D. (1986). Dynamics of molecular organization in agarose sulphate. *Biopolymers, 25*(6), 1009-1029.

Norton, I. T., Jarvis, D. A., & Foster, T. J. (1999). A molecular model for the formation and properties of fluid gels*. International Journal of Biological Macromolecules, 26*(4), 255-261.

Norton, I. T., Frith, W. J., & Ablett, S. (2006). Fluid gels, mixed fluid gels and satiety. *Food Hydrocolloids., 20*(2-3), 229-239.

Norton, I. T., Cox, P. W., and Spyropoulos, F. (2008). The role of hydrocolloids in the formation of health foods. *Gums and Stabilizers for the Food Industry 14, 293–305*,Wiliams, P. A. and Phillips, G. O. (eds.). Royal Society of Chemistry Special Publication No. 316, Cambridge.

Shama, F. & Sherman, P. 1973. Identification of stimuli controlling the sensory evaluation of viscosity II. Oral methods. *Journal of Texture Studies, 4*, 111-118.

Siew, C. K., Williams, P. A., & Young, N. W. G. (2005). New Insights into the Mechanism of Gelation of Alginate and Pectin: Charge Annihilation and Reversal Mechanism. *Biomacromolecules, 6*(2), 963-969.

Ström, A., & Williams, M. A. (2003). Controlled calcium release in the absence and presence of an ion-binding polymer. *The Journal of Physical Chemistry B*, 107(40), 10995-10999.

Tyle, P. 1993. Effect of size, shape and hardness of particles in suspension on oral texture and palatability. *Acta Psychologica, 84*, 111-118.

Tønnesen, H. H., & Karlsen, J. (2002). Alginate in drug delivery systems. *Drug Development and Industrial Pharmacy, 28*(6), 621-630.

Wolf, B., Frith, W. J., Singleton, S., Tassieri, M., & Norton, I. T. (2001). Shear behaviour of biopolymer suspensions with spheroidal and cylindrical particles. *Rheologica Acta, 40*(3), 238-247.

Chapter 3 : RHEOLOGY AND TRIBOLOGICAL PROPERTIES OF CA-ALGINATE FLUID GELS PRODUCED BY DIFFUSION-CONTROLLED METHOD

Fernández Farrés, I., Douaire, M., & Norton, I. T. (2013). Rheology and tribological properties of Ca-alginate fluid gels produced by diffusion-controlled method. *Food Hydrocolloids, 32*(1), 115-122.

Abstract

A new method has been developed for the production of alginate fluid gels. By using the turbulent flow field generated within a pin stirrer, fluid gel particles can be produced in a reproducible and controlled manner. Using this approach yielded an average particle diameter smaller than 10 μm for all alginate fluid gels produced.

A weak gel-like behaviour is reported for the produced materials, which displayed a gradual increase of G' upon increasing polymer concentration. Steady shear results revealed the existence of an apparent yield stress, indicating that a significant inter-particle potential persisted after the production process had finished.

Soft-tribology was used to assess the lubrication properties of Ca-alginate fluid gels. The entrainment of particles in the ball-on-disc contact resulted in a localised increase of friction in the mixed regime, which was found to be dependent on both particle intrinsic properties and the surface roughness of the disc. An increase of polymer concentration resulted in an overall decreased friction for systems with similar particle dimensions.

These distinct but complementary functional responses of fluid gels, arising from increasing alginate concentration, offer real possibilities towards building microstructures with enhanced sensory attributes.

3.1. Introduction

Fluid gels are formed by applying an appropriate flow field to a biopolymer solution undergoing gelation; as a result a highly concentrated suspension of gelled particles is formed (Norton *et al.,* 2006). The resulting gelled structures are known to possess physical properties and dimensions resembling those of oil droplets in emulsion based products, which might then be used to deliver enhanced sensory perception in novel foods (Frith *et al.,* 2002; Norton *et al*., 2006).

We report here the first study on fluid gels produced from alginate, a linear polyuronic polysaccharide extracted from brown seaweed (Phaeophyceae), consisting of (1-4)-linked blocks of poly-β-*D*-mannuronic acid and poly-α-*L*-guluronic acid residues of widely varying composition and sequence, in which the calcium binding sites are formed by homopolymeric regions of guluronic acid residues (Draget *et al.,* 1997; Draget *et al.*, 2005; Draget *et al.,* 2006).

So far, published investigations on hydrocolloids fluid gels are restricted to the so called thermo-reversible gels, consisting of a network structure in which the junction zones are of a weak reversible nature and therefore unstable towards heat treatment processes such as pasteurization. Thermal gelation of biopolymers under shear as well as its effects on structural organisation has been widely studied. Norton *et al*. (1999) proposed a nucleation and growth mechanism for fluid gel particles produced by shear cooling of hydrocolloids that form aggregating structures (*e.g.* agar), where both particle size and particle volume fraction are shear rate and concentration dependent. The gelling ability of agar depends on the intra- and inter-molecular hydrogen bonds which take place as the temperature is lowered below the phase transition point. A similar structuring process might also be

responsible for the fluid gel formation from alginate, where inter- and intra-chain distribution of mannuronic and guluronic acid residues is expected.

The production of thermally set fluid gels is possible in processes allowing control of both cooling rate and flow field, such as a jacketed pin stirrer. By modifying the process parameters (*i.e.* cooling rate, flow field), it is possible to match conformational ordering kinetics (reaction characteristic time scale) and time scale of the applied shear. In practical terms, the main difficulty to produce fluid gels from alginates arises from the nearly instantaneous and temperature independent sol-gel transition of the polymer. According to the 'egg-box model', the guluronate residues adopt a 2-fold symmetry giving rise to a buckled chain. Inter-chain association occurs by dimerization of chain sequences with the Ca^{2+} sandwiched within the dimer on specific sites along each of the interior surfaces (Grant *et al.,* 1973; Thom *et al.,* 1982) and it takes place in the millisecond or microsecond timescale (Morris, *et al.,* 1978). An appropriate release of calcium salt is therefore crucial to ensure control of the gelation rate and the resulting fluid gel microstructure.

A setting method using an in-situ release of internal calcium salt (*i.e.* Ca-EDTA, $CaCO_3$) by change of pH could represent an option to gain control over the gelation kinetics. For the purpose of this work and to avoid complexity in the system, a diffusion-controlled release of calcium was employed. The developed technique involves continuous pumping of the polymer and ion solutions into a jacketed pin-stirrer device. The injection of calcium near the impeller of the pin-stirrer allowed particles to be produced with a mean diameter smaller than 10 µm. Reproducibility and control over the crosslinking ion concentration was achieved by using a syringe pump.

Overall, stable polymer microstructures, arising from a strong chelate type of binding, were achieved under specific conditions (*i.e.* polymer concentration and applied shear field). Contrary to thermo-reversible fluid gels, the resulting alginate gelled structures offer the advantage of stability toward heat treatment processes (Hedges and Norton, 1994).

The effects of shearing during gelation of alginates on the resulting microstrucutres have been investigated. These changes in morphology and structural entities appeared to have favourable and determinable consequences on the viscoelastic properties of the final particulate suspensions.

A tribological characterisation was also carried out, which highlighted some common features existing between the lubrication response of Ca-induced alginates and thermo-reversible fluid gels. More specifically, the effect of particle properties (size, elasticity) on the lubrication properties of the fluid gels was examined.

3.2. Materials and methods

3.2.1. Materials

Sodium alginate (W201502) was purchased from Sigma-Aldrich (Sigma-Aldrich Company Ltd., Dorset, UK) and was used with no further purification.

Alginate solutions were prepared by slowly adding the required amount of the biopolymer powder to cold distilled water. The obtained dispersions were then heated and stirred for 45 minutes at 95 °C to ensure complete solubilisation.

Calcium chloride solutions were prepared by dissolving the required amount of $CaCl_2$ (C1016, Sigma-Aldrich Company Ltd., Dorset, UK) in distilled water.

3.2.2. Methods

3.2.2.1. Production of alginate fluid gels

Fluid gel systems were produced in a laboratory scale pin-stirrer heat exchanger. The shear field provided by such equipment has been previously demonstrated to be sufficient to form hydrocolloid fluid gels (Norton and Frith, 2001). Reactants were injected separately in the pin-stirrer device with the aid of a peristaltic pump for the alginate solution and a syringe pump (Cole-Parmer Instruments, London, UK) for the calcium chloride solution. Thus the alginate and calcium streams merged at the time of entering the main channel, inside the stirring vessel.

In order to induce the creation of micro-particles in the early stages of the aggregation process, the calcium chloride solution injection point was located as close as possible to the pin, in the high energy dissipation zone, in order to ensure rapid mixing of the two streams.

An average residence time of 8 minutes and 1550 RPM shaft speed proved sufficient to create micro-particles with a mean particle size below 10 μm.

Regardless of the cold setting properties of alginate gels, material properties of the final gel can be greatly modified by a change in temperature during the sol-gel transition. In order to guarantee reproducibility of the sample preparation, a constant cooling rate was used to cool the samples from $\approx$ 55 °C at the inlet to $\approx$ 10 °C at the outlet of the jacketed stirrer vessel.

3.2.2.2. Rheological measurements

Steady shear and small strain oscillatory shear experiments were carried out in a Bohlin Gemini HR Nano stress-controlled Rheometer (Malvern Instruments Ltd., UK) with a 40 mm diameter, parallel plate geometry and a 1 mm gap. Samples were kept isothermally at 20 °C during all rheological measurements.

Frequency sweep tests were performed at a stress within the linear viscoelastic region, while varying the frequency from 0.01 Hz to 1 Hz. The linear viscoelastic region was determined in a previous rheological characterisation by amplitude sweep measurements at frequency of 1 Hz.

Apparent yield stress values were initially obtained from stress ramp experiments. The applied shear stress was linearly increased at a constant rate for a period of time and the yield stress was calculated by extrapolation of the shear stress-shear rate plots to a zero shear rate. In ramp tests, the yielding process is affected by the applied ramp rate *i.e.* the lower the applied ramp rate, the smaller the critical stress observed (Nguyen *et al.,* 2006). Therefore, stress ramp results were used to estimate an apparent yield stress value prior to creep experiments.

Constant stress (creep) experiments were carried out to identify the 'true' yield stress. Fluid gels were subjected to a constant stress σ [Pa] for 30 seconds and the deformation or strain γ was recorded as a function of time. The above test was repeated increasing the stress in intervals of 1 Pa from 5 Pa to 30 Pa for the 1 % (w/w) and 2 % (w/w) systems and from 20 Pa to 40 Pa for the systems with 3 % (w/w) and 4 % (w/w) concentration. A set of creep curves with a 30 seconds rest period between each creep test were generated at

various applied shear stresses and the compliance $J = \dot{\gamma} / \sigma$ [Pa^{-1}] was plotted against time. The material behaves as a solid if the applied stress is below the yield stress and the measured strain is small and independent of time after an immediate elastic response. When the applied stress exceeds the yield stress of the material, the strain tends to infinity until constant strain rate is achieved corresponding to a flow condition in the material. The yield stress value was identified as the critical stress which produces a large creep rate increase (Fig. 3.3).

3.2.2.3. Friction measurements

A Mini Traction Machine (MTM PCS Instruments, UK) was used to measure friction at a ball-on-disc contact in a mixed rolling-sliding motion.

A 3/4 inch diameter AISI 400 rotating stainless steel ball (PCS Instruments, London) was loaded against the face of a flat surface of a soft (E = 0.5 MPa) silicone elastomer disc (Samco Silicone Products, Warwickshire, UK) at a defined normal load W . Both ball and disc were independently driven to obtain a lubricated contact at a fixed slide-roll ratio (SRR) over a wide range of entrainment speeds. SRR is the ratio of sliding to rolling speeds at the contact and the entrainment speed U is the mean of ball and disc speeds, where velocity and ball speeds are U_{disc} and U_{ball}, respectively (Bongaerts *et al.,* 2007):

$$SRR = U_{disc} - U_{ball}$$

Eq. 3.1

All experiments were conducted at T = 20 °C and a SRR = 50 % and repeated for various normal loads.

Each test consists of 6 runs of alternatively ramping up from U = *1 – 1000 mm·s^{-1}* and then ramping down from U = *1000 – 1 mm·s^{-1}*. Tests were repeated three times for each fluid gel sample. Silicone disks were cleaned by sonication for 10 minutes first in ethanol, followed by 10 minutes in deionised water and then dried prior to usage. A new cleaned silicone disk was used in each test. The stainless steel ball was cleaned between tests by washing with acetone, followed by deionised water.

Friction coefficient data μ of the ramp up and ramp down were separately averaged and plotted against entrainment speed U . Figures are represented in the form of Stribeck curve with the error bar representing the error standard deviation of the 9 runs (Bongaerts *et al.,* 2007; Malone *et al.,* 2003).

Friction coefficient (μ) is a dimensionless parameter defined by equation 3.2, where F_t is the tangential force and W is the applied normal load:

$$\mu = F_t / W$$

Eq. 3.2

3.2.2.4. Particle size analysis

Light scattering techniques could not be used to measure the size of fluid gel particles, because their refractive index is very similar to that of the suspending medium (water). For that reason the size of the particles were determined by microscopic examination using an optical microscope (Brunel Microscopes Ltd SP300F, UK) equipped with a camera (Canon EOS 1000D, Japan). Polarized light was employed to increase the contrast, allowing the average diameter of the micro-gel particle sizes to be measured (over a 50 total) in pixels

using ImageJ software. Pixels were then converted into µm using a conversion factor previously obtained by calibration using a known length graticulate.

3.3. Results and discussions

3.3.1. Design and structural properties of alginate micro-particles

A diffusion-setting process with a nearly instantaneous binding reaction occurs between Ca^{2+} ions and available COO^- groups of alginate chain when directly mixing an active form calcium with the polymer solution (Draget *et al.,* 1990; Stokke *et al.*, 2000).

The particle properties are the result of a competition between shearing and the formation of gelled clusters via ionic crosslinking (mixing and diffusion). Distortion of the microstructure occurs when the timescale associated with flow is smaller than the timescale associated with local scale diffusion (*i.e.* reciprocal of shear rate is smaller than the time for diffusion). Using the Stokes-Einstein relation for diffusivity, this constraint leads to the known dimensionless Péclet number (Choi and Krieger, 1986; Wagner and Russel, 1989), which is defined in hydrodynamics by the ratio of the Brownian diffusion time for a particle diffusing in a suspending fluid and the time for convective movements in the flow field, where R [µm] is the particle radius, η [Pa·s] is the suspending fluid viscosity, K = $1.38 \cdot 10^{-23}$ $J \cdot K^{-1}$ is the Boltzmann constant, T [K] is the absolute temperature and $\dot{\gamma}$ [s^{-1}] is the shear rate:

$$Pe = \frac{\frac{6\pi R^3 \eta}{KT}}{\dot{\gamma}^{-1}}$$

Eq. 3.3

Fluid gels are produced either through mechanical break-up of clusters of the forming gel, for Pe < 1, or via spinodal decomposition, for Pe > 1 (Carvalho and Djabourov, 1997; Gabriele *et al.,* 2009).

A pin-stirrer rotation speed of 1550 RPM with a residence time of 8 min was employed to produce all fluid gel systems. The high shear rate, together with the relatively small mean particle diameter (< 10 μm), implies that particles are produced with a Pe < 1.Thus the main driver for the alginate fluid gel particles formation within this process is via mechanical fracture of a forming gel matrix.

More than 98 % of the molecular ordering process is required to take place under shear in order to produce homogenous and stable fluid gels (Garrec and Norton, 2012). Controlling the introduction of the cross-linking ions was essential to avoid post-production molecular re-ordering and thus to maintain stable alginate fluid gels.

The applied shear rate yielded significantly bigger particle size for the 1 % (w/w) alginate (mean calculated diameter of 9.5 ± 2 μm) than for the more concentrated fluid gels (3 % and 4 % (w/w)) which, from microscopical examination, were found to be of similar dimensions at approximately 3 μm (Table 3.1).

Alginate concentration [w/w %]	Particle diameter [µm]
1	9.5 ± 2
2	8.7 ± 3
3	3.8 ± 4
4	3.4 ± 4

Table 3.1: Physical characteristics of alginate fluid gel particles. Mean particle size and standard deviation are calculated from 50 measurements.

Bulk quiescent gels of increased alginate concentrations are known to resist larger deformation strains before breaking down into smaller particles compared to alginate quiescent gels with lower polymer concentration (LeRoux *et al.,* 1999; Yuguchi *et al.,* 2000). Thus, bigger particles are only to be expected in the case of a gel that forms quiescently and that is subsequently fractured by mechanical forces. Likewise, shearing a quiescent gel typically leads to particles with serrated contours (Ellis and Jacquier, 2009). Conversely, an increased particle size (despite the risk of size overestimation due to particles swelling in dilution) was found for fluid gels produced with lower polymer concentration and particles did not exhibit sharp edges or serrated contours (Fig. 3.1).

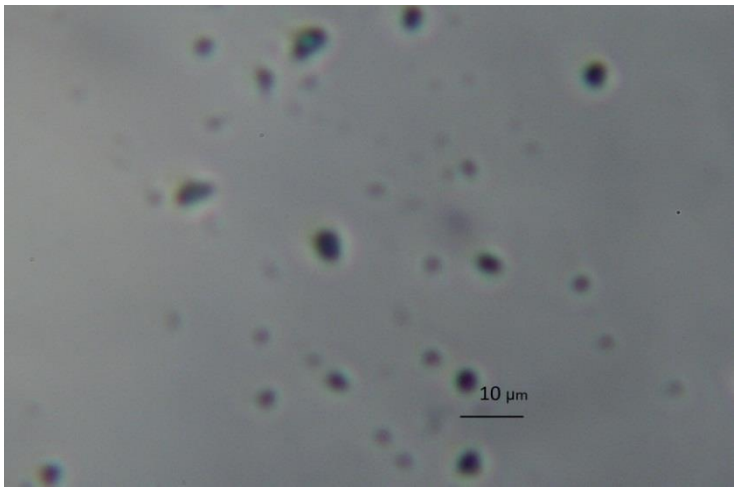

Figure 3.1: Micrograph of diluted 3% (w/w) alginate fluid gels.

Therefore, the author' hypothesis is that both mixing of calcium and network formation compete against the shear induced break-up of the network being formed. In such processes, the local shear stresses experienced by the growing particles control their equilibrium size. Upon decreasing concentration, lower shear stresses would act on the initial gel nuclei due to an overall decreased viscosity. This relates to the concentration of disordered polymer chains in the matrix which, as the particles are formed, is lower for the less concentrated system. Hence, the gross increase in the particulate size as a result of decreasing polymer concentration. In addition, this less dense matrix results in faster diffusion rates of calcium through the gelled matrix. In these conditions, the characteristic time for mixing the two liquid phases at molecular level (micro-mixing) would also increase, due to both low viscosity and increase in diffusion coefficient. These mechanisms therefore give advantage to the gel formation over the breaking process.

The proposed mechanism is then as follows. The gelation is controlled by mixing between alginate and calcium in equilibrium with the breaking up process. If the mixing is fast then bigger and irregularly shaped particles are formed, resulting from the breaking of fast

growing particles. If the mixing is slower, the breaking process dominates and smaller and regular shaped particles are formed (*i.e.* higher concentrated systems). However, this hypothesis should be considered an initial approximation; further time-resolved experiments are needed to clarify the mechanism by which particles form and grow under these applied shear field conditions.

3.3.2. Rheological characterisation of alginate fluid gels

3.3.2.1. Shear viscometry

The effect of polymer concentration on the mechanical response of alginate fluid gels was investigated. The produced fluid gels exhibited similar strong shear thinning behaviour, regardless of the polymer concentration, arising from the gradual break up of inter-particle bridges induced by shear. The microstructural events dictating the shear-thinning rheology are driven by the close approach of particle surface through which particles interact. The flow of a highly concentrated suspension of nearly spherical particles is characterized by the relative flow of particles past one another. Accordingly, the breaking of inter-particle bridges during the rheological measurement implies that the bulk viscosity is a direct function of the intrinsic elasticity and packing of the particles (Frith *et al.,* 2002; Norton *et al.,* 1999; Norton *et al.,* 2000).

The increase of viscosity with alginate concentration would thus be attributed to an increase of both particle intrinsic elasticity and particle volume fraction. Table 3.2 shows the rheological power-law dependency expressed by $\eta = k\dot{\gamma}^n$ of the alginate fluid gels where η is the viscosity [Pa·s], $\dot{\gamma}$ is the shear rate [s^{-1}], k is the consistency constant [$Pa \cdot s^{n+1}$] and n is the power law-index.

Alginate conc (w/w)	*k* [Pa s^{n+1}]	*n*	r^2
1%	1.54	-0.62	0.9975
2%	7.97	-0.65	0.9942
3%	20.25	-0.69	0.9987
4%	35.17	-0.70	0.9980

Table 3.2: Power-law dependency of the rheological behaviour of alginate fluid gels with $\eta = k\dot{\gamma}^n$. k *and* n *are the consistency constant and power-law index, respectively.*

In order to investigate the level of interaction between Ca-alginate particles in the final alginate micro-gel suspensions, the produced fluid gel systems were subjected to a transient linear stress ramp of 100 Pa·min^{-1} during 60 seconds to identify an approximate yield stress value. The steady shear results revealed the existence of an apparent yield stress for all studied range of polymer concentrations (Fig. 3.2), as indicated by a finite shear stress without deformation over the experimental time scales.

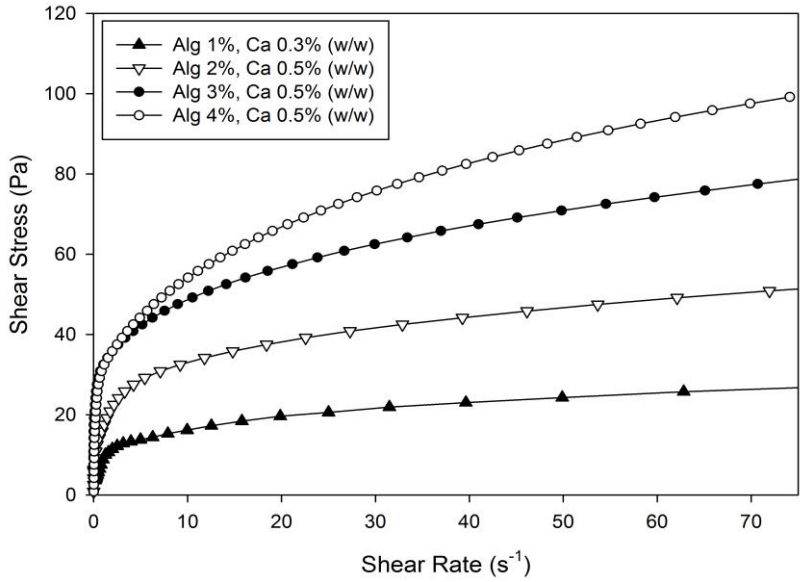

Figure 3.2: Fluid gel behaviour after subjecting samples to a transient shear stress ramp of 100 Pa·min^{-1}. Results show the apparent yield stress dependence as a function of polymer concentration.

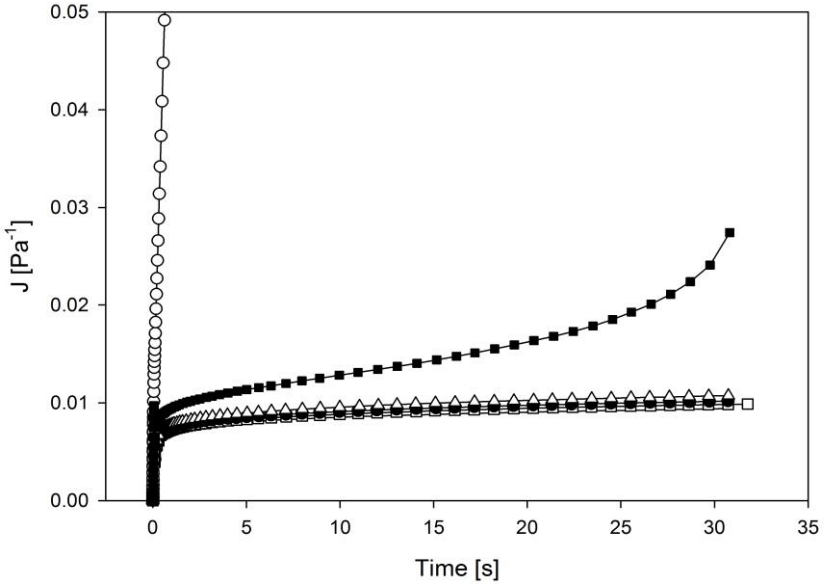

Figure 3.3: Constant stress (creep) test profile of 2 % (w/w) alginate fluid gels. Applied shear stresses are 15 Pa (□), 17 Pa (●), 19 Pa (△), 21 Pa (▪) and 23 Pa (○). True yield stress value (21 Pa) is identified as the critical stress causing a significant increase in the creep rate over a short period i.e. minimum stress required for the transition from limited deformation to appreciable flow conditions.

Alginate concentration [w/w %]	Stress ramp		Creep test	
	Mean σ_γ (Pa)	SD (Pa)	Mean σ_γ (Pa)	SD (Pa)
1	18.1	2.8	11.2	0.8
2	36.4	4.0	21.0	1.0
3	39.3	3.1	24.3	1.5
4	44.5	3.3	29.3	2.5

Table 3.3: Average yield stress values of 3 repeats obtained from stress ramp and creep test techniques.

True yield stress values were then determined by creep experiments as described in Section 3.2.2.2. – Rheological measurements.

The creep profile of the fluid gel at different shear stresses is shown in Fig. 3.3, where stress levels are changed at 30 second intervals. This time was selected as previous stress ramp experiments revealed that the sample would start flowing within such a time frame.

Values obtained from both techniques are presented in Table 3.3 as mean average and standard deviation of three repeat measurements. Creep tests were found to produce more reproducible results than shear ramp tests which rely on extrapolation from steady-shear viscosity data.

The phenomenon of yield stress is generally associated with a three dimensional, rigid network structure that must deform and fail before flow can occur (Mason *et al.,* 1996). However, for suspensions of non-aggregated particles, this strain-to-failure behaviour is an indication of the level of inter-particle potential arising due to a net attractive force between particles.

Calcium induced gelation involves three distinct molecular events; monocomplexation, dimerization, and lateral associations among the dimers occurring involving co-operative interactions between blocks of guluronic residues rather than 'point cross-linking' (Fang *et al.,* 2007; Morris *et al.,* 1973). The monocomplexes formation, which can be regarded as nucleation, decreases electrostatic repulsions by reducing the charge density on alginate chains and by creating positively charged patches (Siew *et al.,* 2005). Applied shear forces presumably limit the molecular transition to occur within distinct particles, while promoting the latter aggregation of monocomplexes. As a consequence, non-ordered chain segments are likely to appear at the surface of these primary particles. These disordered chains partially retained at the particle surface would then be free to form bridges between adjacent particles until the applied stress is great enough to either break or disentangle them. The resulting inter-particle reactivity could then account for the particles not being in a close packed lattice as well as their distinctive yield stress response.

Moreover, an inhomogeneous gel structure with higher polymer distribution at the surface and gradually decreasing towards the centre of the gel forms as a result of the diffusion-controlled gelling kinetics (Draget *et al.,* 2009; Mikkelsen and Elgsaeter, 1995; Rayment *et al.,* 2009; Skjak-Braek *et al.,* 1989; Wright *et al.,* 2009).

The calculated yield stress (σ_γ) increased with increasing both particulate volume and particle stiffness and decreasing particle size, similarly to the increase of G' under the same conditions (Table 3.2). This implies that a greater mechanical energy input is required to unjam the system, as expected for high concentrated particulate suspensions in which a larger force is required to induce the flow via particles 'squeezing' between each other. The

yield stress, however depends on both particle and inter-particle properties, thus a greater gel entanglement between particles is assumed for more concentrated systems.

In summary, the yield stress results have shown that a significant inter-particle reactivity, presumably mediated by Ca^{+2} interactions, persisted post processing and after the gel was set. Therefore, from a rheological perspective, alginate fluid gels may be regarded as a suspension of charged particles whose rheology is dominated by inter-particle interactions over Brownian motion and hydrodynamic forces.

3.3.2.2. Structure and rheological behaviour by dynamic measurements

It is generally accepted that the non-Newtonian behaviour of dense suspensions results from changes in microstructure (position of the suspended particles relative to each other) under shear. To gain further insight into the structural events taking place in such particulate suspensions, a series of dynamic rheology experiments have been carried out. Fig. 3.4 shows the mechanical spectra of Ca-alginate fluid gels at a range of polymer concentration. Qualitatively, frequency sweep measurements indicated the almost uniform gel-like response over the frequency range studied. The application of small oscillatory shear to fluid gels disturbed slightly the microstructure without destroying it which allowed the measured shear modulus to be interpreted in terms of structure and inter-particle energy. The mechanical properties of all produced fluid gels appeared to lie somewhere between those of a 'weak' and 'strong' gel, with G' significantly greater than G'' but more dependent on frequency than in the case of 'strong' or quiescent gel. Likewise, alginate fluid gels exhibited the ability of flowing under low strains and recovering the initial structure and thus the elastic response.

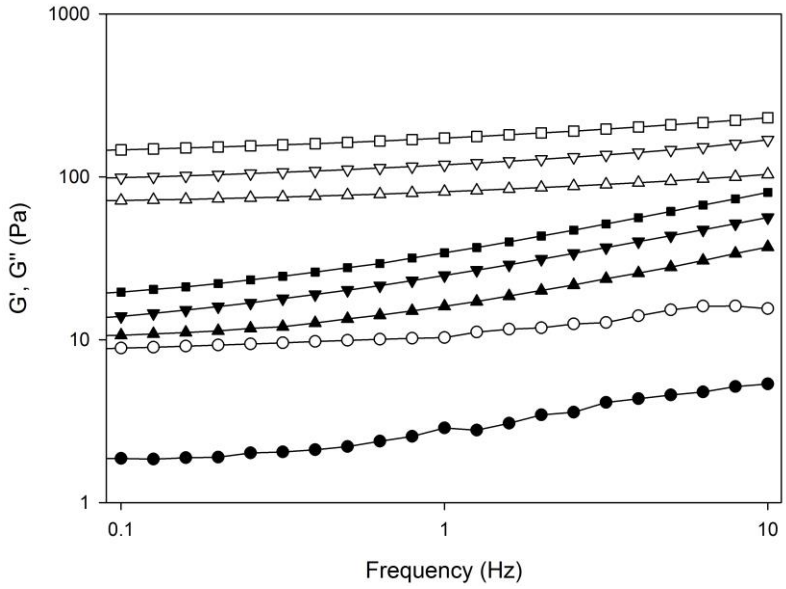

Figure 3.4: : Frequency dependence of G' (white symbols) and G'' (black symbols) of alginate fluid gels in the viscoelastic linear regime. Concentrations are Alg 1 %$_{w/w}$ (○), Alg 2 %$_{w/w}$(△), Alg 3 %$_{w/w}$ (▽), Alg 4 %$_{w/w}$ (□).

As previously mentioned, alterations in alginate concentration are expected to induce effective changes in particle phase volume, and consequently affecting the final suspensions rheology. The relationship between viscoelasticity and polymer concentration was further investigated as to interpret the rheological changes in terms of particle microstructure. Fluid gels were produced from 2 % (w/w) and 2.5 % (w/w) polymer concentrations under the same processing conditions (applied shear rate, cooling rate). Subsequently, a wide range of dilutions were prepared from the two primary fluid gels systems. Further Na^{+}-Ca^{2+} exchanges that could diminish the viscoelastic response were prevented by using deionized water for sample preparation and conditioning. The plateau storage modulus (G') at 0.1 Hz of both diluted systems was recorded from oscillatory testing.

A concentration comparison can be assessed by plotting G'/c_p^2 as function of normalised concentration (c/c_p), where c is overall alginate concentration and c_p is concentration of

alginate at preparation, as explained by Frith *et al.* (2002). It is assumed that sheared particle moduli scales with the quiescent particle moduli (*i.e.* a concentration square law (Clark and Ross-Murphy, 1985).

The particle volume fraction, which was determined by centrifugation (Cassin *et al.,* 2000) was found to be ϕ = 0.35 for both fluid gel systems. Contrary to the steep increase predicted from models developed for rigid particles suspensions (Jeffrey and Acrivos, 1976; Russel, 1978), fluid gels displayed a gradual increase of G' upon increasing normalized concentration with an approximately power law behaviour (Fig. 3.5).

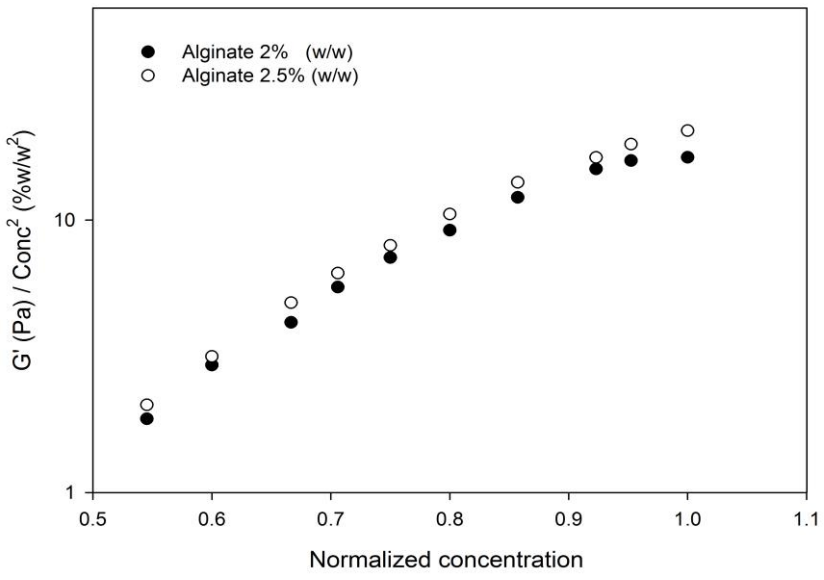

Figure 3.5: Dependence of the normalised plateau storage modulus $\left(G'/c_p^2\right)$ *at 0.1Hz on the normalised concentration* $\left(c/c_p\right)$ *for 2% and 2.5% sheared alginate.*

These results suggest that alginate particles have the ability to behave as deformable entities, similar to fat droplets in an o/w emulsion.

Systems also showed similar responses to dilution, with both sets of data almost superimposing at a given concentration. A suspension containing stiffer particles (2.5 %

(w/w)) displayed slightly higher G' for the same normalised concentration. Higher G' values would imply that either bigger irregularly shaped particles are formed or that more inter-particle bridging occurs within the suspension. That no difference in particle size and particle phase volume (degree of space filling) was found suggests that only particle elasticity and interparticle potential contributed to the enhanced moduli of the 2.5 % (w/w) system.

This technique bears the limitation of poor control on the competing parameters (mixing and gelation process) so that the ability to monitor alginate concentration in a single micro-gel particle is still lacking. However, results have demonstrated that equivalent particulate phase volumes can be obtained through processing (*i.e.* applied shear), and thus similar material properties. The applied shear rate during production, which is thought to limit the crosslinking process, leads to anisotropic particulate suspensions instead of homogeneous networks. The employed high rotation speeds (1550 RPM) have proved to greatly influence the particle properties (shape, size), particulate volume and consequently the final viscoelastic response. It has been shown that similar structures from different polymer concentrations can be obtained through controlling processing parameters.

As a conclusion of this rheological study, the produced alginate fluid gels have been characterised as suspensions comprising essentially non-aggregated particles which despite not being in a close packed lattice, displayed a markedly gel-like behaviour and which can only flow past one another appreciably if a large enough stress (greater than the apparent yield stress) is applied. These unique properties can be advantageously be used to form materials with enhanced sensory attributes in many food engineering processes. Concretely, it can be utilized as the dispersed aqueous phase in fat continuous spreads allowing the

inclusion of destabilizing ingredients as these are 'captured' in the micro-gels (Hedges and Norton, 1994).

3.3.3. Lubrication properties of alginate fluid gels

Contrary to rigid particle suspensions, the gradual increase of the viscoleastic properties with concentration has demonstrated that particles behaved as deformable entities, as would oil droplets in an o/w emulsion. These results imply that the produced fluid gels could ultimately be used to deliver enhanced sensory attributes or to replace fat content whilst keeping a similar microstructure to that of the original product. In-mouth sensory perception however can't be explained only in terms of bulk rheology. Overall thickness sensation can be measured in elongational deformation along with shear rate due to the heterogeneous shear field occurring in the mouth during consumption (Lillford, 2000).

Further characterisation of the created fluid gels has been performed by the means of soft tribology. The low contact pressures provided by the deformable surfaces used in this study have been reported to greatly mimic oral conditions, thus yielding frictional data with strong correlations to in-mouth sensory attributes (Malone *et al.,* 2003). Specifically, the lubricating abilities of alginate fluid gels as a function of hydrocolloid concentration were investigated. This was assessed by measuring the friction coefficient obtained by initially ramping up and subsequently ramping down the entrainment speeds, U .

Three different regimes (boundary, mixed and hydrodynamic) are identified when friction coefficient is plotted as function of U , obtaining what is typically known as a Stribeck curve. In the boundary regime, which occurs at low speeds, the normal load is supported by the contacting asperities. Low film thickness and a negligible fluid entrainment into the contact

area describe the lubrication under these conditions. In the mixed regime of lubrication, the rate of fluid flow in the contact zone is large enough to partially separate the ball from the disk while the lubricant film thickness and length of the surface asperities are of similar sizes. This implies that, in the mixed regime, both bulk lubricant rheology and surface properties have an influence on the friction response. Finally, at high entrainment speeds, a film of lubricant fully separates the surfaces and the friction coefficient increases with U as the lubricant is sheared. The friction coefficient under these lubrication conditions (hydrodynamic regime) is influenced by the bulk rheological properties of the lubricant and it is fairly independent of surface characteristics.

Fig. 3.6 shows the Stribeck curves for the produced Ca-alginate fluid gels. Some common features have been identified between the lubrication behaviour of the alginate fluid gels and that of pure non-ionic fluid gels (agarose) in the sense that a peak in friction coefficient is found in the ramp up of the Stribeck curve and an hysteresis between ramping up and ramping down is also identified in the mixed regime of the 1% (w/w) alginate system.

(A)

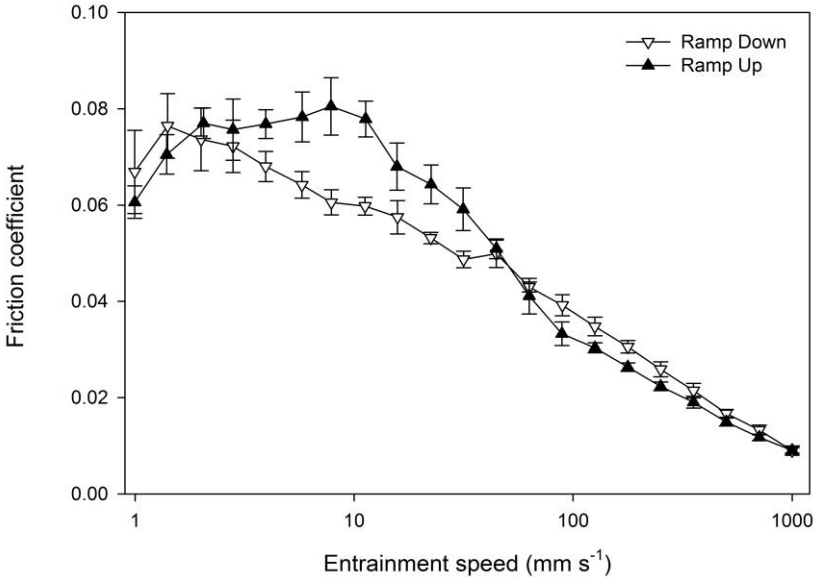

(B)

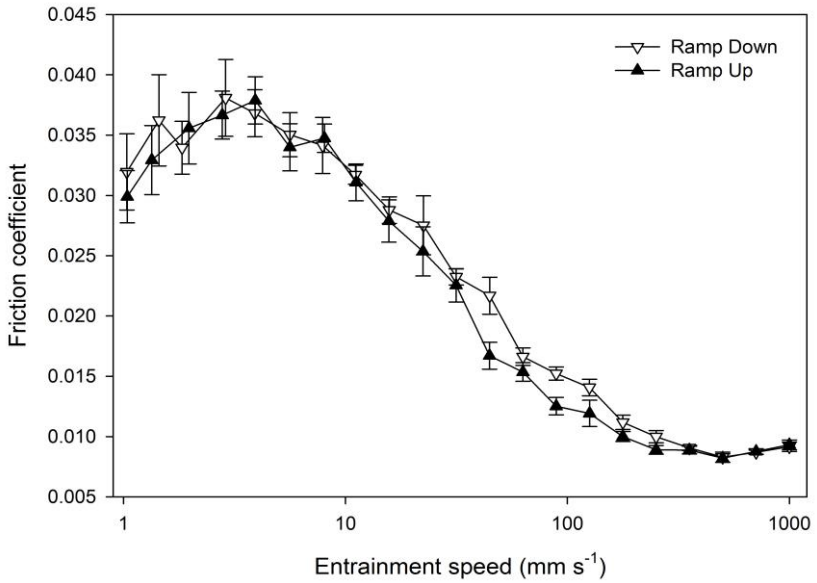

Figure 3.6:(A) Stribeck curve for 1% (w/w) alginate fluid gel, with 9 µm average particle size. Test was performed with applied normal load W of 5 N. (B) Stribeck curve for 4 % (w/w) alginate fluid gel, with 3 µm average particle size. Test was performed with applied normal load W of 5 N.

The dependence of friction on the direction of the applied speed ramp has been previously reported for fluid gels made from agarose (Gabriele *et al.,* 2010). This hysteresis behaviour was argued to be a consequence of the entrainment of particles into the gap between the surfaces. Concretely, the localised increase of friction of the ramp up was ascribed to a critical velocity, U_{entr}, at which particles begin to enter the ball-on-disc contact. At these speeds, the lubrication film thickness appeared to be lower in comparison to the size of individual agarose particles, whose Sauter mean diameter was $\approx$ 100 µm. These reasonably big particles were selectively excluded to the gap until the shift from film lubrication to a lubrication regime occurred due to a greater film thickness, which allowed particles to be entrained.

The Elastomer Silicone disc surfaces used in this study have a root mean square roughness of order 699 nm to 1004 nm, whereas the roughness of the Stainless steel ball is 43.2 nm. Sufficiently small particles ($\approx$ 1 µm) could then fit into the disc irregularities thus entering the ball-on-disc contact zone via surface roughness, leading to overall less particle exclusion at these low speeds. In addition, the thin monolayer of small particles which now holds the surfaces is expected to give a lower increase in friction than would a thin monolayer of the same particles with bigger size. Hence, a less pronounced peak was found for the ramp up of the Stribeck curve for the fluid gel system containing particles with decreased particle size (alginate 4 % (w/w)). This experimental finding agrees with previous work on silica particles (De Wijk *et al.,* 2006) in starch-containing custard desserts and with a more recent study on agarose fluid gel particles (Gabriele *et al.,* 2010) in which systems with smallest particles yielded lower friction coefficients. Further increase in *U* allowed for more particles to be entrained and a decrease in the system's friction was observed. Under these velocity

conditions ($U > U_{entr}$), a multilayer of particles is expected to enter the gap as the mechanism of film lubrication is restored.

The Stribeck curves (ramping up) as a function of concentration are presented in Fig. 3.7. The difference in the curve trend can be clearly identified when comparing the alginate 1 % (w/w) to both 3 % (w/w) and 4 % (w/w) fluid gels within the same integration scale. As already mentioned, a sharper peak in the ramping up curve is shown in the system with bigger particles, with a mean friction increase being roughly twice as large in magnitude compared to that of the 3% (w/w) and 4% (w/w) alginate fluid gels. The results also showed that as particle elasticity increased (through alginate concentration), the U_{entr} was reduced, suggesting that higher polymer concentration was able to promote particle entrainment. According to classical hydrodynamic theory, this behaviour is expected simply due to the alginate viscosity in the inlet zone, where the shear rates are still relatively moderate, which plays a role in helping to entrain particles into the contact. This is consistent with earlier work on agarose fluid gel particles (Gabriele *et al.,* 2010) or on fluid entrainment of guar solutions (Cassin *et al.,* 2001) which reported similar frictional responses upon varying polymer concentration. Finally, the behaviour of a thin monolayer of alginate particles was found to be dependent on particle stiffness in a way that an increase in alginate concentration resulted in an overall reduction in friction coefficient.

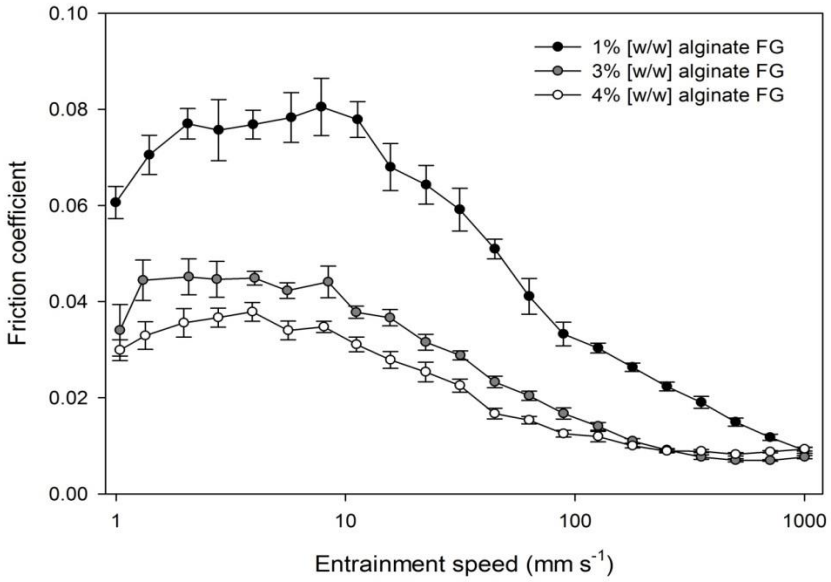

Figure 3.7: Effect of polymer concentration and particle size on lubrication properties of alginate fluid gels. Stribeck curves (ramp up) are presented for applied normal load W of 5 N.

Overall, the micro-fluid dynamic of the particles in the thin film and consequently the lubrication response appeared to be considerably affected by surface roughness and particle intrinsic properties (size, elasticity). This experimental finding agrees to what has been described for a highly concentrated (particle phase volume) suspensions by Meeker *et al*. (2004). This study mathematically demonstrated that a micro-elastodynamic lubrication regime establishes between micro-particles and the tribopair surfaces, with particle elasticity, surface roughness and lubrication layer between particle-surface dictating the local fluid dynamics.

In summary, enhanced viscosity and particle elasticity, through raising alginate concentration, has been shown to lower friction. Likewise, small particles were driven to the gap between the ball and the disk without increasing friction. These results suggest the advantageous impact that the presence of small (ideally less than 10 μm) alginate gelled

particles would have upon lubrication and reinforces the idea of using fluid gel particles to replace oil droplets in an o/w emulsion.

3.4. Conclusions

This study has reported for the first time the rheological and tribological properties of thermally stable alginate fluid gels. Overall, a simple straightforward methodology has been developed to consistently produce fluid gels from alginate with variable functional properties.

It is concluded that the competing mechanisms responsible for the particles formation are the break-up of gelled clusters and the formation of those clusters via ionic crosslinking. When increasing polymer concentration, slower calcium diffusion through the gelled matrix and the non-gelled suspension occurs due to the higher viscosity. As a consequence, there is more breaking up of the forming particles and less ionic crosslinking, which explains the decreased particle dimensions upon increasing alginate concentration.

Applying shear during gelation of Ca-alginate systems greatly alters the resulting morphology of the structural entities, allowing the microstructure to be manipulated through controlling processing parameters. In this way, similar fluid gel structures yielding comparable material properties were obtained from different alginate concentrations. From rheological perspective, the produced fluid gels were described as suspensions of interactive gelled particles dispersed in a non-gelled matrix, displaying a weak gel-like flow behaviour and high-shear limiting viscosities. An increase of polymer concentration resulted in higher yield stress and higher viscosities once fluid gels started flowing.

The lubrication response of alginate fluid gels was also examined. A localised increase of friction corresponding to a critical entrainment velocity was found upon increasing entrainment speed U. This velocity at which particles are fully entrained, U_{entr}, was found to be inversely proportional to particle elasticity and particle size. However, further research is needed to elucidate the influence of crosslink density, which is presumed to have a determining role on the rheological and lubrication responses of the final suspensions.

3.5. References

Bongaerts, J. H. H., Fourtouni, K., & Stokes, J. R. (2007). Soft-tribology: Lubrication in a compliant PDMS–PDMS contact. *Tribology International, 40*(10–12), 1531-1542.

Carvalho, W., & Djabourov, M. (1997). Physical gelation under shear for gelatin gels. *Rheologic Acta*, *36*(6), 591-609.

Cassin, G., Appelqvist, I., Normand, V., & Norton, I. T. (2000). Stress-induced compaction of concentrated dispersions of gel particles. *Colloid and Polymer Science*, *278*(8), 777-782.

Cassin, G., Heinrich, E., & Spikes, H. A. (2001). The Influence of Surface Roughness on the Lubrication Properties of Adsorbing and Non-Adsorbing Biopolymers. *Tribology Letters*, *11*(2), 95-102.

Choi, G. N., & Krieger, I. M. (1986). Rheological studies on sterically stabilized model dispersions of uniform colloidal spheres: II. Steady-shear viscosity. *Journal of Colloid and Interface Science*, *113*(1), 101-113.

Clark, A. H., & Ross-Murphy, S. B. (1985). The concentration dependence of biopolymer gel modulus. *British Polymer Journal*, 17(2), 164-168.

De Wijk, R., Terpstra, M., Janssen, A., & Prinz, J. (2006). Perceived creaminess of semi-solid foods. *Trends in Food Science & Technology*, *17*(8), 412-422.

Draget, K. I., Østgaard, K., & Smidsrød, O. (1990). Homogeneous alginate gels: a technical approach. *Carbohydrate Polymers*, *14*(2), 159-178.

Draget, K.I., Phillips, G., & Williams, P. (2009). Alginates. *Handbook of Hydrocolloids*, 807-828.

Draget, K. I., Skjak-Braek, G., & Smidsrod, O. (1997). Alginate based new materials. *International Journal of Biological Macromolecules*, *21*(1-2), 47-55.

Draget, K. I., Skjåk-Bræk, G., & Stokke, B. T. (2006). Similarities and differences between alginic acid gels and ionically crosslinked alginate gels. *Food Hydrocolloids*, *20*(2), 170-175.

Draget, K. I., Smidsrød, O., & Skjåk-Bræk, G. (2005). Alginates from Algae. *Biopolymers Online*: Wiley-VCH Verlag GmbH & Co. KGaA.

Ellis, A., & Jacquier, J. C. (2009). Manufacture and characterisation of agarose microparticles. *Journal of Food Engineering*, *90*(2), 141-145.

Fang, Y., Al-Assaf, S., Phillips, G. O., Nishinari, K., Funami, T., Williams, P. A., & Li, L. (2007). Multiple Steps and Critical Behaviors of the Binding of Calcium to Alginate. *The Journal of Physical Chemistry B, 111*(10), 2456-2462.

Frith, W., Garijo, X., Foster, T., & Norton, I. (2002). Microstructural origins of the rheology of fluid gels. *Special publication-Royal Society of Chemistry, 278*, 95-103.

Gabriele, A., Spyropoulos, F., & Norton, I. T. (2009). Kinetic study of fluid gel formation and viscoelastic response with kappa-carrageenan. *Food Hydrocolloids, 23*(8), 2054-2061.

Gabriele, A., Spyropoulos, F., & Norton, I. T. (2010). A conceptual model for fluid gel lubrication. *Soft Matter, 6*(17), 4205-4213.

Garrec, D. A., & Norton, I. T. (2012). Understanding fluid gel formation and properties. *Journal of Food Engineering, 112*(3), 175-182.

Hedges, N. D., & Norton, I. T. (1994). Fluid composition: EP Patent 0,432,835.

Jeffrey, D., & Acrivos, A. (1976). The rheological properties of suspensions of rigid particles. *AIChE Journal, 22*(3), 417-432.

LeRoux, M. A., Guilak, F., & Setton, L. A. (1999). Compressive and shear properties of alginate gel: Effects of sodium ions and alginate concentration. *Journal of Biomedical Materials Research, 47*(1), 46-53.

Lillford, P. J. (2000). The materials science of eating and food breakdown. *MRS Bulletin, 25*(12), 38-43.

Malone, M. E., Appelqvist, I. A. M., & Norton, I. T. (2003). Oral behaviour of food hydrocolloids and emulsions. Part 1. Lubrication and deposition considerations. *Food Hydrocolloids, 17*(6), 763-773.

Mason, T., Bibette, J., & Weitz, D. (1996). Yielding and flow of monodisperse emulsions. *Journal of Colloid and Interface Science, 179*(2), 439-448.

Meeker, S. P., Bonnecaze, R. T., & Cloitre, M. (2004). Slip and Flow in Soft Particle Pastes. *Physical Review Letters, 92*(19), 198302.

Mikkelsen, A., & Elgsaeter, A. (1995). Density distribution of calcium-induced alginate gels. A numerical study. *Biopolymers, 36*(1), 17-41.

Morris, E. R., Rees, D. A., & Thom, D. (1973). Characterization of polysaccharide structure and interactions by circular dichroism: order-disorder transition in the calcium alginate system. *Journal of the Chemical Society, Chemical Communications*(7), 245-246.

Morris, E. R., Rees, D. A., Thom, D., & Boyd, J. (1978). Chiroptical and stoichiometric evidence of aspecific, primary dimerisation process in alginate gelation. *Carbohydrate Research, 66*(1), 145-154.

Nguyen, Q. D., Akroyd, T., De Kee, D. C., & Zhu, L. (2006). Yield stress measurements in suspensions: an inter-laboratory study. *Korea-Australia Rheology Journal, 18*(1), 15-24.

Norton, I. T., & Frith, W. J. (2001). Microstructure design in mixed biopolymer composites. *Food Hydrocolloids, 15*(4–6), 543-553

Norton, I. T., Frith, W. J., & Ablett, S. (2006). Fluid gels, mixed fluid gels and satiety. *Food Hydrocolloids, 20*(2-3), 229-239.

Norton, I. T., Jarvis, D. A., & Foster, T. J. (1999). A molecular model for the formation and propertiesof fluid gels. *International Journal of Biological Macromolecules, 26*(4), 255-261.

Norton, I. T., Smith, C. G., Frith, W. J., & Foster, T. J. (2000). The production, properties and utilisation of fluid gels. In K. Nishinari (Ed.), *Hydrocolloids* (pp. 219-227). Amsterdam: Elsevier Science.

Rayment, P., Wright, P., Hoad, C., Ciampi, E., Haydock, D., Gowland, P., & Butler, M. F. (2009). Investigation of alginate beads for gastro-intestinal functionality, Part 1: In vitro characterisation. *Food Hydrocolloids*, *23*(3), 816-822.

Russel, W. B. (1978). The rheology of suspensions of charged rigid spheres. *Journal of Fluid Mechanics, 85*(02), 209-232.

Siew, C. K., Williams, P. A., & Young, N. W. G. (2005). New Insights into the Mechanism of Gelation ofAlginate and Pectin: Charge Annihilation and Reversal Mechanism. *Biomacromolecules, 6*(2), 963-969.

Skjak-Braek, G., Grasdalen, H., & Smidsrod, O. (1989). Inhomogeneous polysaccharide ionic gels. *Carbohydrate Polymers, 10*(1), 31-54.

Stokke, B. T., Draget, K. I., Smidsrød, O., Yuguchi, Y., Urakawa, H., & Kajiwara, K. (2000). Small-angle X-ray scattering and rheological characterization of alginate gels. 1. Ca-alginate gels. *Macromolecules, 33*(5), 1853-1863.

Thom, D., Grant, G. T., Morris, E. R. & Rees, D. A. 1982. Characterisation of cation binding and gelation of polyuronates by circular dichroism. *Carbohydrate Research, 100*, 29-42.

Wagner, N. J., & Russel, W. B. (1989). Nonequilibrium statistical mechanics of concentrated colloidal dispersions: Hard spheres in weak flows with many-body thermodynamic interactions. *Physica A: Statistical Mechanics and its Applications, 155*(3), 475-518.

Wright, P. J., Ciampi, E., Hoad, C. L., Weaver, A. C., van Ginkel, M., Marciani, L., Gowland, P., Butler, M. F. & Rayment, P. (2009). Investigation of alginate gel inhomogeneity in simulated gastro-intestinal conditions using magnetic resonance imaging and transmission electron microscopy. *Carbohydrate Polymers, 77*(2), 306-315.

Yuguchi, Y., Urakawa, H., Kajiwara, K., Draget, K. I., & Stokke, B. T. (2000). Small-angle X-ray scattering and rheological characterization of alginate gels. 2. Time-resolved studies on ionotropic gels. *Journal of Molecular Structure, 554*(1), 21-34.

Chapter 4 : FORMATION KINETICS AND RHEOLOGY OF ALGINATE FLUID GELS PRODUCED BY IN-SITU CALCIUM RELEASE

Fernández Farrés, I., & Norton, I. T. (2014). Formation kinetics and rheology of alginate fluid gels produced by in-situ calcium release. *Food Hydrocolloids, 40*, 76-84.

Abstract

The formation and properties of alginate fluid gels produced using in-situ calcium release and a defined shear field are investigated. Results show that, while the rate of particle growth during formation increases significantly upon lowering the shear rate, the rate of inter-particle interaction post-production remains unaffected by the magnitude of shear.

The longer polymer chain allows a greater number of possible sites for calcium crosslinking per chain which enhances the formation of a percolating network and increases the number of rheologically-effective network crosslinks. As a result, high M_w alginate fluid gels exhibit faster gelation kinetics and greater viscosities than those of low M_w alginate fluid gels.

Particle stiffness increases with increasing $CaCO_3$ concentration until a critical value is reached. Quiescent gels display the same $CaCO_3$ critical value, suggesting that the number of crosslinks within an individual fluid gel particle is equivalent to that of their counterpart quiescent gel. This is due to the fast coil-dimer transition which, under the applied shear field, leads to kinetically trapped fluid gel structures. However, their textural response differs from that of a quiescent gel which is likely caused by the bridging between fluid gel particles.

In addition to advancing the understanding of the production of fluid gels from alginates, this work shows for the first time how the ordering kinetics and the resulting particle properties can be manipulated by the choice of alginate M_w and $CaCO_3$ concentration, potentially allowing the design and delivery of specific structures with desirable attributes.

4.1. Introduction

Alginates are linear polyuronic polysaccharide extracted from brown seaweed (Phaeophyceae), consisting of (1-4)-linked blocks of poly-β-D-mannuronic acid (M) and poly-α-L-guluronic acid (G) residues at different proportions and with different sequential occurrence (Draget *et al.*, 2006; Stokke *et al.*, 2000).

Quiescent gelation of alginates with different M/G ratios has been extensively studied, where alginates with high content of guluronate have been shown to form strong, brittle gels, whereas alginates rich in manuronate residues give softer and more elastic gels (Draget, *et al*., 1994; Matsumoto *et al.*, 1992; Smidsrød, 1974). In that regard, recent molecular model investigations have demonstrated that calcium ions preferentially bind to the G-blocks which are stiffer and possess a more extended chain conformation compared to the M-blocks due to a greater hindered rotation around the glycosidic linkages (Braccini *et al.*, 1999; Braccini and Pérez, 2001). The effects of both calcium and alginate M/G ratio on the rheological behaviour of alginate gels are discussed in great detail in the work of Mitchell and Blanshard (1976).

However, little attention has been paid to the influence of polymer molecular weight (M_w) on the time dependent gelation mechanism of alginate gels and, to our knowledge, no study has reported the effect of polymer M_w and calcium on the formation of suspensions of alginate micro-gelled particles (*i.e.* fluid gels). Thus, the aim of the present work is to investigate the structural events dictating the formation of such particulate structures and the different properties that emerge from varying either processing conditions or the material (alginate M_w and calcium concentration).

Fluid gels are formed by application of a sufficiently energetic flow field to the polymer solution whilst undergoing conformational transition and consequent aggregation (Norton *et al.*, 1999; Norton *et al.*, 2000). In the case of alginates, the production of micro-particles is particularly complicated due to the fact that the ordering process is not controlled by temperature and it occurs over the millisecond to seconds time scale (Goodall and Norton, 1987). A new developed technique employing a Pin-stirrer device has been recently used to produce alginate fluid gels. This technique involves the injection of a soluble form of calcium (*e.g.* $CaCl_2$) near the impeller of the Pin, in the high energy dissipation zone, so that the alginate and calcium streams are quickly mixed inside the stirred vessel, thereby preventing large particles to form (Fernández Farrés *et al.*, 2013; Chapter 3).

By directly introducing an active form of calcium into the alginate solution and under shear, the rapid crosslinking reaction between the carboxyl groups of the polymer chain and the cations leads to the formation of anisotropic gelled particles with broad size distributions. This is due to differences in the diffusion rate of calcium throughout the system, that is, the diffusion rate of calcium through the gelled matrix is slower than the diffusion rate of calcium through the aqueous continuous phase.

Poor control over the gelation kinetics characteristic to such diffusion-controlled methods can be overcome by gradually releasing the crosslinking ion from a less soluble form of calcium (*e.g.* $CaCO_3$, $Ca_3(PO_4)_2$) triggered by the reaction with protons from the hydrolysis of a glucono-δ-lactone (GDL). This method (internal gelation), as previously described by Draget, *et al.*, (1990) and Mitchell and Blanshard (1976), has been employed in the present study because it allowed the rate of ordering transition to be matched to the time scale of the imposed shear field. This shear field required to form fluid gels was provided by the

rheometer, which enabled manipulation of the intensity of applied shear rate and monitoring of the viscoelastic response during processing. By using the rheometer in combination with internal gelation method the kinetics of fluid gel formation could be evaluated.

In this work, alginates with different M_w and equivalent G/M were used to produce a range of fluid gels. The structural changes occurring during fluid gel formation due to variations in shear rate, amount of calcium and alginate molecular weight were investigated by rheological techniques. Compression tests on quiescent gels were also used to further elucidate the binding mechanism of calcium to alginate, and the consequences on particle elasticity. This allowed the material properties of fluid gels to be described in relation to the particle structure and inter-particle interactions.

4.2. Materials and methods

4.2.1. Materials and sample preparation

Medium viscosity sodium alginate (W201502), $CaCO_3$ (C6763) and glucono-δ-lactone (G2164) were purchased from Sigma–Aldrich (Sigma-Aldrich Company Ltd., Dorset, UK) and were used without further purification.

Two sodium alginate samples having different molecular weight were also purchased from Sigma-Aldrich (Sigma-Aldrich Company Ltd., Dorset, UK). These two polymers are extracted from the alga Macrocystis pyrifera which has an M/G ratio of 1.6, obtained from FTIR spectroscopic analysis (Gómez-Ordóñez and Rupérez, 2011; Mackie, 1971).

The weight average molecular weight (M_w) was reported to be $1.43 \cdot 10^5$ g·mol^{-1} for low viscosity alginate (A2158) and $3.5 \cdot 10^5$ g·mol^{-1} for high viscosity alginate (A2033) (Pamies *et al*., 2010).

Alginate solutions were prepared by dispersing the biopolymer powder in double distilled water and then stirred while heating to 90 °C until dissolved. $CaCO_3$ in powder form was dispersed in alginate solutions and sonicated for 10 minutes in order to decrease particle size. Freshly made aqueous solutions of a slowly hydrolyzing glucono-δ-lactone (GDL) were added to the alginate and $CaCO_3$ mixtures immediately prior to sample loading, resulting in a range of final target concentrations.

The $CaCO_3$ concentrations for 0.5 % (w/v), 1 % (w/v), 1.5 % (w/v) and 2 % (w/v) alginate systems used in this study were 7.5 mM, 15 mM, 22.5 mM and 30 mM, respectively.

4.2.2. Fluid gel production in a rheometer

A range of fluid gels were produced from the mixtures of alginate, $CaCO_3$ and GDL in a Kinexus Rheometer (Malvern Instruments Ltd., UK) using a four bladed vane (25 mm diameter) in cup (27 mm diameter) under shear controlled and isothermal (T = 25 °C) conditions.

This technique allows control of the applied shear rate as well as monitoring of the rheological response during experimentation. The vane geometry was used to avoid slip effects. In addition, the vane geometry allowed relatively large amount of sample to be produced and analysed repeatedly in subsequent tests.

Shear viscosity was monitored during fluid gel production with data points recorded every 5 seconds. The onset time of gelation was identified as the time when a minimum of 7 successive data points showed an increase of more than 0.2 % in shear viscosity. The completion time was identified as the time when a minimum of 7 successive data points showed less than 0.08 % change in shear viscosity.

4.2.3. Dynamic oscillatory measurements of fluid gels

The structure and particle interactions of the fluid gels were elucidated by dynamic oscillatory measurments performed on a Kinexus Rheometer (Malvern Instruments Ltd., UK) using a cone and plate geometry (4 ° cone angle, 40 mm diameter) at *25 °C*.

The evolution of the dynamic storage modulus (G') after production was monitored at a constant stress of 10 mPa and 1 Hz frequency. The viscoelastic properties of the produced fluid gels were measured by small amplitude oscillatory experiments at a fixed strain of 0.2 %, which was within the linear region.

Strain sweep measurements were performed at 1 Hz on fluid gels 48 hours after the production process was finished.

4.2.4. Polarimetry

Measurements of optical rotation were performed using a Gyromat Automatic Polarimeter (Anton Paar, GmbH) with a sample cell of 5 cm path-length.

4.2.5. Texture analysis of quiescent gels

Compression tests were carried out on quiescent gels using a TA.XT.plus Texture Analyser (Stable Micro Sustems Ltd., UK) with a 40 mm diameter cylindrical aluminium probe. All gel cylinders had a height of 10 mm and a diameter of 23.04 mm. The rate of compression was 1 mm·s^{-1} for all samples.

Equations 4.1 - 4.4 were used to calculate the true stress σ_T and true (Hencky) strain ε_H values from the force/distance data, where H_0 and A_0 are the initial height and cross-sectional area, h and F are the height and the compression force applied, ε_E and ε_H are the engineering strain and true (Hencky) strain and σ_E and σ_T are the engineering stress and true stress (Moresi and Bruno, 2007):

$$\sigma_E = F / A_0$$

Eq. 4.1

$$\varepsilon_E = (h - H_0) / H_0$$

Eq. 4.2

$$\varepsilon_H = \ln(1 + \varepsilon_E)$$

Eq. 4.3

$$\sigma_T = \sigma_E(1 + \varepsilon_E)$$

Eq. 4.4

The Young's modulus (E) was calculated as the slope of the initial linear region of the true stress/true strain curves as described elsewhere (Norton *et al.*, 2011).

4.3. Results and discussion

4.3.1. Kinetics of alginate fluid gel formation

4.3.1.1. Applied shear rate dependence

The internal gelation technique was utilised throughout this work, where a stoichiometric equivalent of glucono-δ-lactone (GDL) was used to ensure that a pH = 7 was held constant, thus avoiding the formation of alginic acid gels. Evidence for the GDL hydrolysis was obtained by polarimetry. Fig. 4.1 shows the change in optical rotation of linearly polarized light induced by transition from GDL to a mixture of δ-lactone, γ-lactone and gluconic acid as a 365 nm light beam was passed through the $CaCO_3$-GDL system.

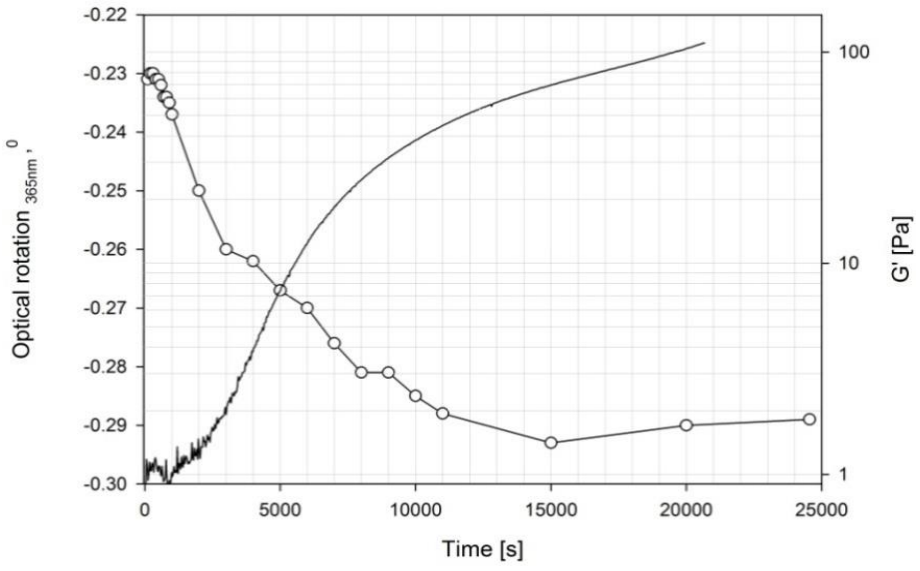

Figure 4.1: Optical rotation (white circles) according to the GDL hydrolysis for 7.5 mM $CaCO_3$, 15 mM GDL mixtures. Evolution of G' (line) for a quiescent gel produced from 0.5 % (w/v) alginate, 7.5 mM $CaCO_3$, 15 mM GDL.

The release of protons from the GDL hydrolysis gradually liberates calcium ions from the insoluble $CaCO_3$ salt in an acid-based reaction. The Ca^{2+} ions then trigger the association of the polyguluronate sequences of the alginate chain by dimerization mechanism, giving rise to aligned ribbon-like assemblies with cavities into which calcium ions are located (*i.e.* egg box dimers) (Grant *et al.*, 1973). As the extent of association increases through aggregation of ordered dimers, clusters expand in size until they form a continuous three-dimensional crosslinked network. This increases the relative contribution of the storage modulus, G'(Fig. 4.1).

The progressive introduction of calcium ions to the aqueous phase allows uniform distribution of ions throughout the system which will prevent large clusters and will minimise the formation of inhomogeneous gelled networks when producing fluid gels.

The shear required to form fluid gels was provided by the rheometer, where the instantaneous viscosity was measured as a function of time for a range of applied shear rates. As shown in Fig. 4.2, all solutions displayed virtually Newtonian behaviour before the onset time of gelation. This is ascribed to the binding of calcium to a single guluronate unit that occurs under limited calcium conditions, prior to the formation of egg-box dimers. As a result, monocomplexes are formed, decreasing the charge density on the polymer chain and giving rise to local charge reversal (Fang *et al.*, 2007; Siew, *et al.*, 2005). These monocomplexes are well separated from each other, hence remaining relatively insensitive to the shear. For high M_w alginates, the formation of such compact structures resulted in a significant decrease of viscosity, as will be further discussed later in this paper.

As more calcium ions become available, the pair wise association between monocomplexes forms one-dimensional egg-box dimer structures which then aggregate via inter-cluster

associations in a process that occurs simultaneously with the shear induced break-up of the network being formed. As a consequence of these competing mechanisms, micro-gelled particles are formed.

Norton *et al.* (1999) proposed a nucleation and growth mechanism for fluid gel particle formation, where the initial clusters (*i.e.* gel nuclei) can grow through enrichment from the non-gelled continuous phase or via coalescence/agglomeration of those gel nuclei.

Assuming that gel nuclei form at the beginning of the kinetic experiment, their initial volume fraction would not be great enough as to display any crowding effect and the viscosity would remain Newtonian, as it is shown in Fig. 4.2. The subsequent increase in viscosity is attributed to a simultaneous increase in number and volume fraction of particles (Norton *et al.*, 1999).

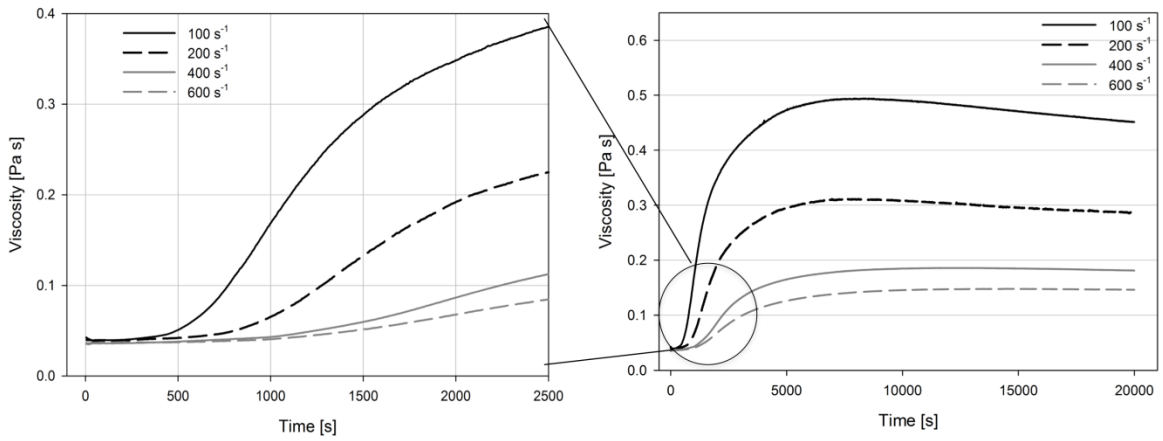

Figure 4.2: Viscosity during fluid gel production as a function of time. Systems were produced at a range of applied shear rates from 1.5 % (w/v) alginate, $CaCO_3$ 22.5 mM, 45 mM GDL and isothermally at 25 °C.

	ONSET		COMPLETION	
Shear rate [1/s]	T_o [s]	η_o [Pa s]	T_c [s]	η_c [Pa s]
100	405	0.044	6690	0.492
200	660	0.045	6655	0.309
400	1000	0.043	6540	0.176
600	1175	0.043	6410	0.136

Table 4.1: Onset times (T_o) and completion times T_c of gelation for alginate fluid gels produced at a range of shear rates. All systems were prepared from 1.5 % (w/v) alginate, 22.5 mM $CaCO_3$ and 45 mM GDL.

The time at which this process starts (onset time of gelation) increases as the magnitude of the applied shear force is increased (Fig. 4.2, Table 4.1) which indicates a reduction in the rate of particle growth. This suggests that the applied shear rate limits the likelihood of an association event to occur between the early formed particles. In addition, these results represent the first experimental evidence for the shear rate dependence of the rate of particle growth. Further data supporting this view are provided later in this study.

Viscosity change ($\Delta\eta$) during formation as a function of the applied shear rate ($\dot{\gamma}$) is presented on a double logarithmic plot in Fig. 4.3. The data was fitted to the power law equation previously used with agarose and *k*-carrageenan sheared gels (Emanuele and Palma-Vittorelli, 1992; Gabriele *et al.*, 2009):

$$\Delta\eta = B(\dot{\gamma})^{-D}$$

Eq. 4.5

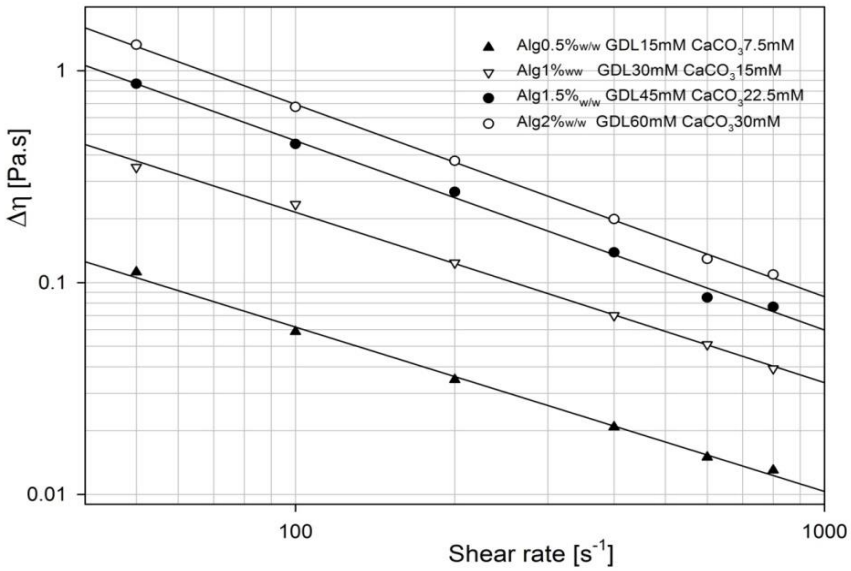

Figure 4.3: Viscosity change as a function of applied shear rate during formation of alginate fluid gels. Data is presented in a double logarithmic plot.

Parameters	B	D	R^2
Alg 0.5 %, GDL 15 mM, $CaCO_3$ 7.5 mM	2.19	0.776	0.997
Alg 1 %, GDL 30 mM, $CaCO_3$ 15 mM	8.71	0.804	0.996
Alg 1.5 %, GDL 45 mM, $CaCO_3$ 22.5 mM	28.51	0.893	0.996
Alg 2 %, GDL 60 mM, $CaCO_3$ 30 mM	45.53	0.908	0.998

Table 4.2: Parameters of the power law equation (Eq. 4.5) describing the dependence of viscosity increase on applied shear rate for fluid gels produced at a range of alginate concentrations.

As shown in Table 4.2, both parameters B and D increase with increasing polymer concentration. For fluid gels produced with same molar ratio calcium to alginate, the following empirical equation describing the increase of B with polymer concentration was found, where c is alginate concentration:

$$B = 9.99c^{2.24}$$

Eq. 4.6

The effect of the applied shear rate was further explored by performing frequency sweeps on the fluid gels 48 hours after production. Fluid gels produced at the lowest shear rate (50 s^{-1}) displayed the highest G' values as one would expect due to increased inter-particle contact of a suspension with large particles and a high particulate phase volume (Fig. 4.4).

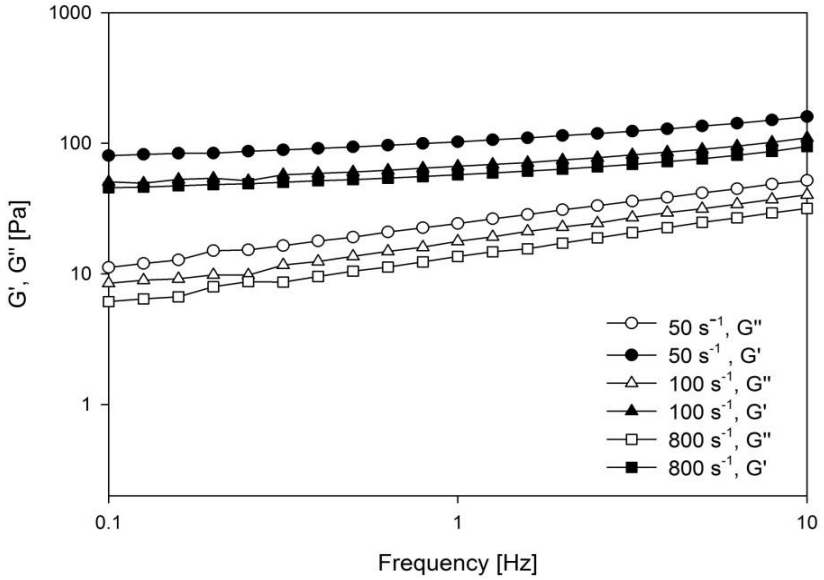

Figure 4.4: Mechanical spectra of 1 % (w/v) alginate fluid gels produced at different applied shear rates. Tests were conducted at strains within the linear viscoelastic regime.

An increase in particle size for fluid gels produced with lower shear rates has been reported in previous works on agar and *k*-carrageenan fluid gels (Gabriele *et al.*, 2009; Norton *et al.*, 1999). Thus, throughout this work, shear rates above 50 s^{-1} were employed so as to prevent the formation of large aggregates of particles.

In contrast to the system produced at 50 s^{-1}, the effect of shear rate on storage modulus was reduced when the shear rate was increased from 100 s^{-1} to 800 s^{-1}. Furthermore, the small differences measured in G' were not mirrored by measurements of shear viscometry,

as all systems exhibited virtually identical viscosities across all shear rates (Fig. 4.5). This suggests a comparable elasticity/deformability of particles which in turn determines the flow of these particles past one another.

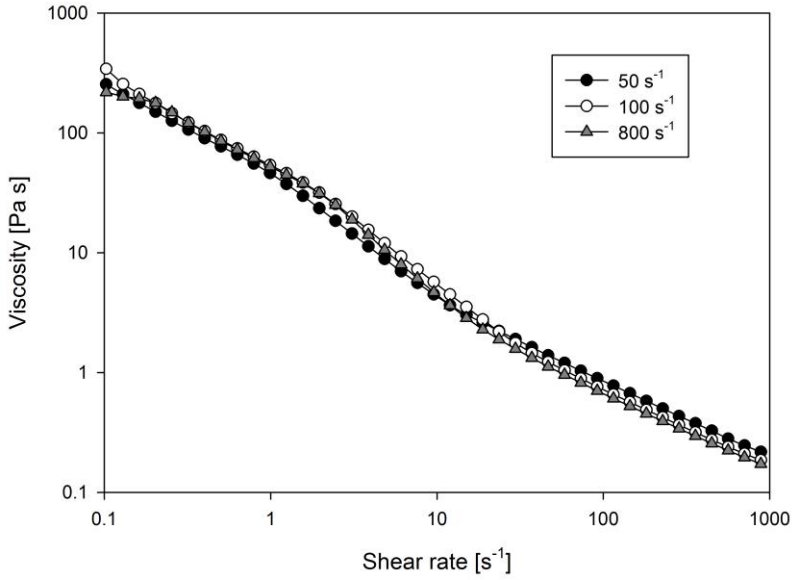

Figure 4.5: Flow curves of the alginate fluid gels produced at different shear rates. Measurements were conducted 48 hours after the production process.

The reason for this is that the fluid gel system, once formed, continues to evolve via inter-particle interaction. It has been argued in the literature that the complete ordering of gels made from aggregating polysaccharide may occur over a time scale of an hour to days (Arnott *et al.,* 1974). Thus, it is expected that the re-ordering process which occurred quiescently (*i.e.* in the absence of shear) for 48 hours led to systems with similar properties. Similarly to agar, it is expected that the applied shear kinetically captures the alginate particle structures into anisotropic morphologies rather than the more thermodynamically favourable spherical shape due to the rapid coil-dimer transitions. These anisotropic shapes

favour inter-particle interaction, allowing the material to form a percolated network, thus determining the elasticity of the fluid gel system.

As will be demonstrated later in this paper, the quiescent structuring process due to inter-particle interaction is mainly controlled by calcium concentration rather than the magnitude of the applied shear rate.

4.3.1.2. Effect of calcium concentration and polymer molecular weight

We have shown that to a certain degree the level of applied shear affects the kinetics of ordering transition in alginate. This conversion rate from disordered polymer coils to a fluid gel structure is expected to strongly depend on calcium concentration as well as the physicochemical properties of the polymer.

In this study, two alginate samples with different molecular weights (M_w) and equivalent fraction of guluronic acids (F_G) were used to produce fluid gels with a range of $CaCO_3$ concentrations. Thus, variations in their rheological behaviour could be attributed exclusively to differences in molecular assemblies arising from changes in the number of cross-links per polymer chain.

From Fig. 4.6.A-4.6.B it can be seen that the viscosity decreases prior to the onset time of gelation due to the formation of monocomplexes. This is more significant when high M_w alginates are used, most likely due to the greater flexibility of the long polymer chains, allowing them to contract/shrink to a greater extent.

The data presented in Fig. 4.6.A-4.6.B also shows that high M_w alginates have greater viscosities and increased ordering rates compared to the low M_w systems. The higher rate

of viscosity increase arises from a greater length scale affected by the same G/Ca interactions compared to the low M_w alginates. This enhances the formation of a percolating network along with an increasing the number of rheologically-effective network crosslinks for the same number of molecular cross-links at higher polymer molecular weight.

(A)

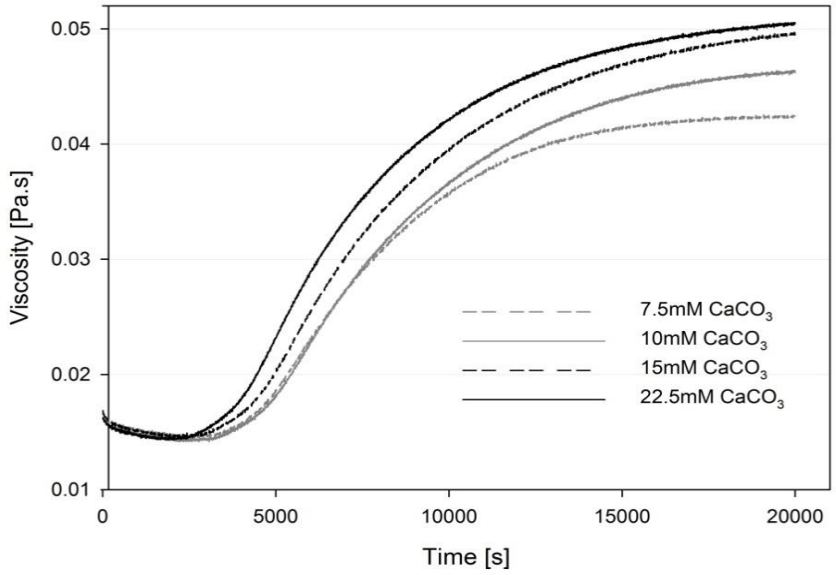

(B)

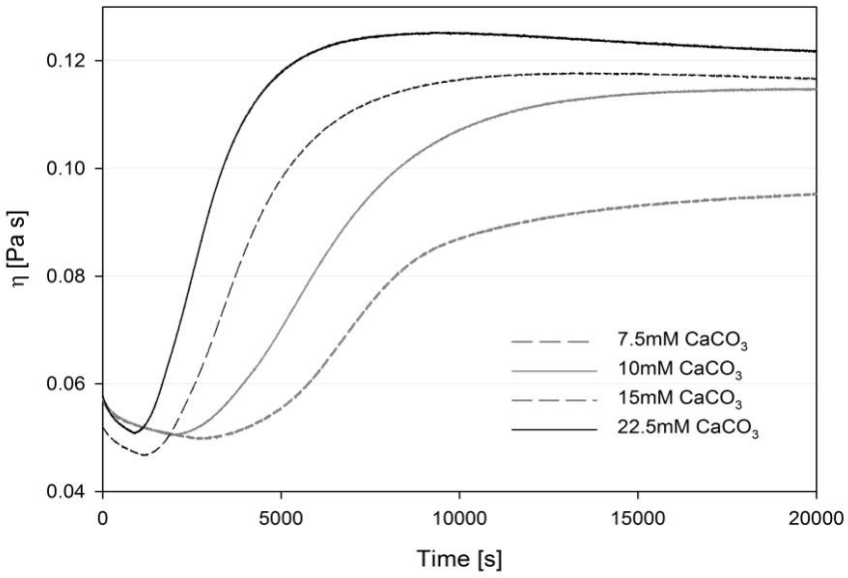

Figure 4.6: (A) Viscosity curve during formation of low M_w alginate 1% (w/v) fluid gels produced at 800 s^{-1}, 30 mM GDL and at a range of calcium concentrations. (B).Viscosity curve during formation of high M_w alginate 1% (w/v) fluid gels produced at 800 s^{-1}, 30 mM GDL and at a range of calcium concentrations.

The decreased number of loose chain ends of the high molecular weight alginates could also contribute to this behaviour, probably to a lesser extent, by enabling more calcium ions to be rapidly accommodated between adjacent G-blocks.

This strong influence of polymer M_w is not surprising considering that gelation via in-situ calcium release occurs in a calcium-limited environment and thus the chain characteristics are expected to greatly affect the calcium binding to the alginate chain. The calcium binding mechanism and its consequences on the particle's structural properties will be further discussed in Section 4.3.3. – Textural properties of alginate fluid gels.

Within the framework of particle growth occurring by augmentation from the surrounding continuous phase, the faster gelation kinetics measured as a result of increasing calcium concentration is ascribed to an increase of the rate of both coil-dimer transition and dimer-aggregated dimer transition. Even at shear rates as high as 800 s^{-1}, the structuring process occurs more rapidly and to a greater extent when more calcium ions are available. This progressive increase in ordering rate is an indication that the release of calcium is rate limited by the $CaCO_3$ dissolution rather than the GDL hydrolysis. The reason for this is that the reasonably big $CaCO_3$ particles (19 µm average particle size) dissolve at a slower rate than the process of GDL hydrolysis. This is in agreement with Ström and Williams (2003) findings which showed that while the H^+ and Ca^{2+} release rates for systems containing 1.7 µm $CaCO_3$ particles and GDL were comparable, the Ca^{2+} release rates of 5 µm and 10 µm $CaCO_3$ particles were slower than the H^+ release rate and dependent on $CaCO_3$ particle size.

4.3.2. Particle growth and inter-particle interactions in the absence of shear

In order to further investigate the effect of processing conditions on particle growth and inter-particle interaction, the dynamic storage modulus was measured at a frequency of 1 Hz and applied stress of 10 mPa after fluid gels were produced. The results obtained for fluid gels produced from 1.5 % (w/v) alginate, 22.5 mM $CaCO_3$, 45 mM GDL at a range of shear rates are presented in Fig. 4.7.

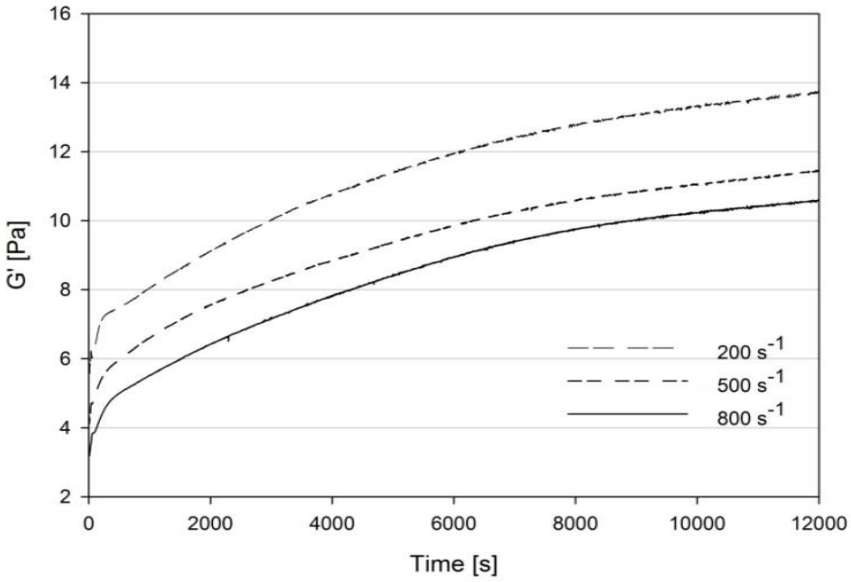

Figure 4.7: G' as a function of time and applied shear rate measured after a production process of 6 hours. Fluid gels were produced from 1.5 % (w/v) alginate, 22.5 mM $CaCO_3$, 45 mM GDL.

$G'(t) = G'_{\infty} - (G'_{\infty} - G'_0)\exp^{-k_i t}$			
$\dot{\gamma}$ [s^{-1}]*	200	500	800
G'_0 [Pa]	6.72	5.44	4.24
G'_{∞} [Pa]	14.73	12.51	11.51
k_i [s^{-1}]	0.0002	0.0002	0.0002
R^2	0.998	0.996	0.998

Table 4.3: Model parameters from the exponential equation (Eq.4.7) describing the inter-particle interactions after production of fluid gels at different applied shear rates. Concentrations of sodium alginate, $CaCO_3$ and GDL were fixed at 1.5% (w/v) and 22.5mM and 45 mM, respectively.

** $\dot{\gamma}$ [s^{-1}]: applied shear rate*

The resultant time dependence curve of G' was reduced empirically to the exponential growth equation (Eq. 4.7) previously used in agarose fluid gels (Gabriele *et al.*, 2009):

$$G'(t) = G'_{\infty} - \left(G'_{\infty} - G'_{0}\right)\exp^{-k_i t}$$

Eq. 4.7

Where k_i is the kinetic constant, G'_0 is the initial storage modulus immediately after stopping the shear and G'_{∞} the storage modulus at infinite time. The calculated values are shown in Table 4.3.

The most interesting result to emerge from this analysis is that the relative rate of ordering k_i remains unaffected by the magnitude of applied shear rate. That is, once the shear is removed, the rate at which the structure is strengthening is independent of the applied mechanical forces. This behaviour occurs when the processing time is greater than the gelation time so that complete molecular ordering occurs under shear, thus the ordering process post-production is driven by inter-particle interactions.

A possible explanation for the equal rates of inter-particle interaction is that particles with similar surface properties are formed at the experimental range of shear rates. The proportion of disordered coils at the particle surface that form due to late polymer ordering (Norton *et al.,* 1999) are expected to play a determining role in the extent of inter-particle bridging.

When comparing the evolution of G' for systems produced from different M_w alginates and under the same conditions of shear rate and processing time, different responses were observed: while the behaviour of the high M_w system can be described by the previously

proposed exponential grow model, the best fit for the data obtained from low M_w alginates is the following linear function:

$$G'(t) = G'_0 + k_g t$$

Eq. 4.8

This result is explained by the fact that the final particulate structure was not completely formed when the shear was removed thus mainly quiescent particle growth drives the evolution of G' over time. This idea is in agreement the previous results which showed lower reaction rates for the low M_w alginates.

Low M_w alginate	$G'(t) = G'_0 + k_g t$							
	7.5mM $CaCO_3$		10mM $CaCO_3$		15mM $CaCO_3$		22.5mM $CaCO_3$	
$\dot{\gamma}$ [s^{-1}]*	200	800	200	800	200	800	200	800
G'_0 [Pa]	1.89	1.24	3.46	2.49	3.65	2.84	4.69	3.07
k_g [s^{-1}]	0.0003	0.0002	0.0004	0.0003	0.0009	0.0008	0.001	0.0009
R^2	0.965	0.947	0.971	0.969	0.999	0.993	0.998	0.997

Table 4.4: *Model parameters from the polynomial first order equation (Eq. 4.8) calculated by fit to the data of low M_w alginates produced at different $CaCO_3$ and applied shear rates. The concentrations of alginate and GDL were kept constant at 1 % (w/v) and 30 mM, respectively.*

* $\dot{\gamma}$ *[s^{-1}]: applied shear rate*

High M_w alginate	$G'(t) = G'_\infty - (G'_\infty - G'_0)\exp^{-k_i t}$							
	7.5mM $CaCO_3$		10mM $CaCO_3$		15mM $CaCO_3$		22.5mM $CaCO_3$	
$\dot{\gamma}$ [s^{-1}]	200	800	200	800	200	800	200	800
G'_0 [Pa]	5.51	2.95	8.54	5.01	12.82	10.14	13.34	12.82
G'_∞ [Pa]	11.42	7.77	13.89	10.89	23.51	21.13	24.32	23.51
k_i [s^{-1}]	0.0001	0.0001	0.0001	0.0001	0.0002	0.0002	0.0002	0.0002
R^2	0.996	0.998	0.991	0.996	0.998	0.995	0.942	0.998

Table 4.5: Model parameters from the exponential equation (Eq.4.7) calculated by fit to the data of high M_w alginates produced at different $CaCO_3$ and applied shear rates. The concentrations of alginate and GDL were kept constant at 1 % (w/v) and 30 mM, respectively.

* *$\dot{\gamma}$ [s^{-1}]: applied shear rate*

As shown in Table 4.4, the ordering rates (k_g) increased as the applied shear rate was decreased for all systems. Under these conditions where particle growth rather than particle interaction controls the rate of ordering, these results confirm that particles grow at a faster rate as the magnitude of the applied shear is lowered.

Conversely, the crosslinking process of the high M_w system appeared to have already occurred to its full extent after 4 hours of processing. Hence, no particle growth occurred once the shear was removed and the rate of ordering was determined by inter-particle interaction and, consequently, was independent on the shear rate (Table 4.5).

This hypothesis is further supported by comparing the effect of calcium concentration on the relative rate of ordering between the low and high M_w systems. The data reveals that

when the shear environment is stopped before completion (low M_w alginate), the ordering rate (particle growth) increases significantly with calcium concentration (Table 4.4), as would be expected due to an increased rate of coil-dimer transition. Differently, only a minor calcium concentration effect is measured when the ordering rate is driven by inter-particle interaction (Table 4.5).

Thus, it is concluded that when the process of particle growth is completed under shear, the rate at which particles interact post-processing is not dependent on applied shear rate, but slightly on calcium concentration. When the shear is removed before the gelled particles are completely formed, the rate of particle growth is controlled by both the applied shear rate and calcium concentration.

4.3.3. Textural properties of alginate fluid gels

As shown in this study, the viscosity increases during formation with increases in calcium concentration. This may be due to the formation of stiffer (less deformable) particles arising from more alginate chains being bound together in junction zones by multiple Ca^{2+} ions which leads to a higher density of crosslinking.

This hypothesis was tested by performing oscillatory strain sweeps at a frequency of 1 Hz on the produced fluid gels 48 hours after production. Results showed greater limiting strains for particles produced with reduced calcium concentrations (Fig. 4.8). That is, the effect of progressively decreasing $CaCO_3$ concentration from 22.5 mM to 10 mM is to increase the deformability of particles such that they can withstand larger strains before flow occurs.

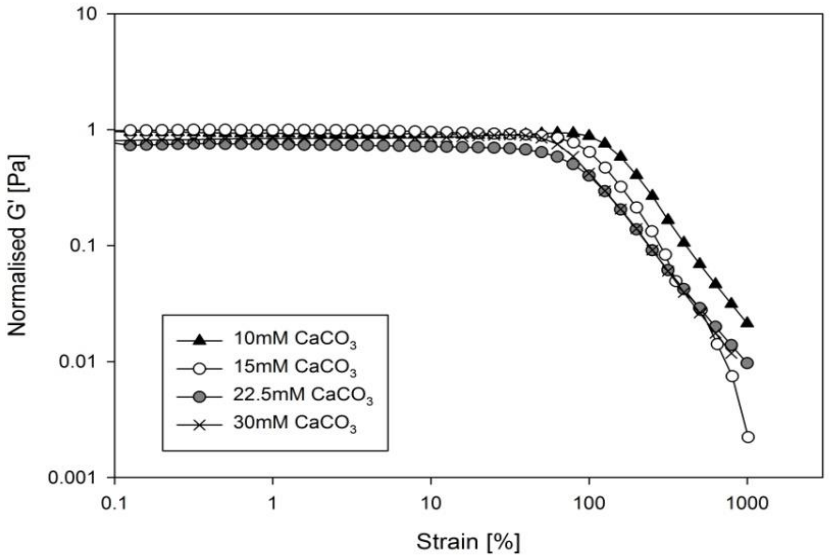

Figure 4.8: Normalised storage modulus versus strain of low M_w alginate 1 % (w/v) fluid gels produced at a range of $CaCO_3$ concentration.

However, the limiting strain of particles produced with 30 mM $CaCO_3$ is higher than expected. This abrupt reduction in particle stiffness is attributed to an excess calcium which restrains the packing of chains into perfectly aligned dimers, leading to both inter-chain and intra-chain binding (Smidsrød, 1974). These heterogeneous binding sites create junctions between chains that are kinetically more stable towards dissociation.

Thus, it appears to be a saturated $CaCO_3$ concentration above which the formation of egg-box dimers and hence particle gelled network is disrupted. For the 1 % low M_w alginate fluid gel, this critical $CaCO_3$ concentration was 22.5 mM.

To gain further insight into the crosslinking mechanism, the strengths of quiescent gels formed at a range of calcium concentrations were measured. These results are presented in Fig. 4.9, where the Elastic Young's modulus (E) was determined as the slope of the initial

linear region of true strain/true stress diagram (details on this analysis are provided in the methodology section).

A steady increase of the Young's Modulus is seen between 10 mM and 22.5 mM $CaCO_3$ which is followed by a sharp increase with the increased degree of crosslinking from 22.5 mM up to 45 mM $CaCO_3$ (Fig. 4.9). These results are consistent with those of Moe *et al.* (1992) who argued that calcium ions, after being liberated from the $CaCO_3$, are accommodated within the longest junction zones before creating new ones. The general view is that G-bocks dimerize in such a way that the alginate chains are bound together by multiple cations in long junction zones rather than distinct, point-like crosslinks (Stokke *et al.,* 1991, Grant *et al.,* 1973).

From Fig. 4.9 it can also be seen that decline in gel strength occurs for concentrations above 45 mM $CaCO_3$ which, for the 2 % (w/v) alginate quiescent gel, corresponds to the same critical molar ratio CaCO3:alginate that has been shown earlier for fluid gels.

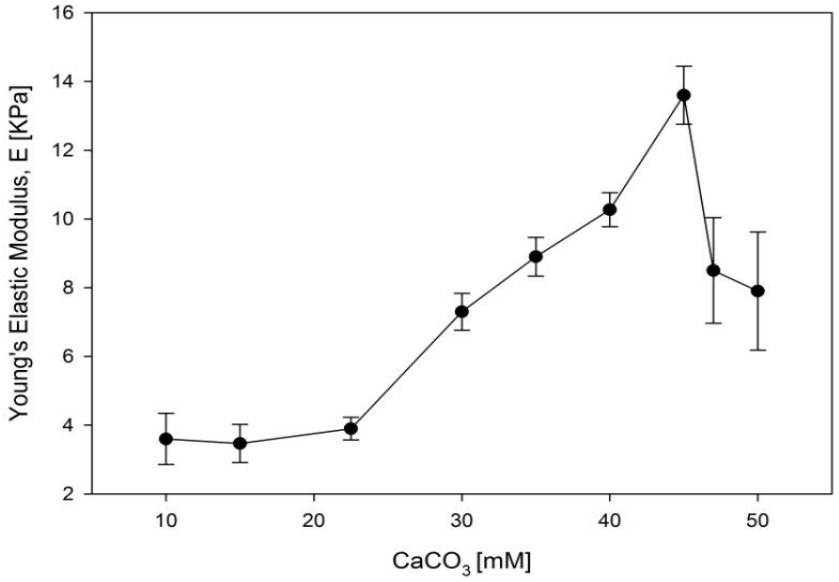

Figure 4.9: Young's Elastic Modulus as function of $CaCO_3$ concentration for 2 % (w/v) low M_w alginates quiescent gels. The GDL concentration was kept constant at 30 mM for all systems.

Assuming that the gel strength is determined by the number of crosslinks per unit volume (Stokke *et al.,* 1991), the fact that both fluid and quiescent gels yield exhibit the same critical molar ratio $CaCO_3$:alginate suggests that similar degree of crosslinking occurs in both sheared and quiescent gelation. Hence, the polymeric gelled network within an individual fluid gel particle is equivalent to that of their counterpart quiescent gel. This is likely to be due to the almost instantaneous coil-dimer transition of alginate in the presence of calcium which, under the imposed shear field, leads to kinetically trapped dimer structures. These results are consistent with those of Frith *et al.* (2002) who demonstrated that the elasticity of individual agarose fluid gel particles is the same as that of their equivalent quiescent gel. Similarly to alginates, the coil-helix transition of agarose occurs on a millisecond timescale (Norton *et al.,* 1986), so it seems that the potential to form kinetically trapped fluid gel

structures is a common feature of aggregating polysaccharides with fast molecular ordering transitions.

Nonetheless, the response of alginate fluid gels appears to differ from their corresponding quiescent gels with respect to the calcium concentration effect on gel strength. The dynamic storage modulus (G') of fluid gels showed an initial abrupt rise as the crosslink density increased with increasing $CaCO_3$ concentration from 10 mM to 22.5 mM, followed by a moderate increase from to 22.5 mM to 45 mM (Fig. 4.10).

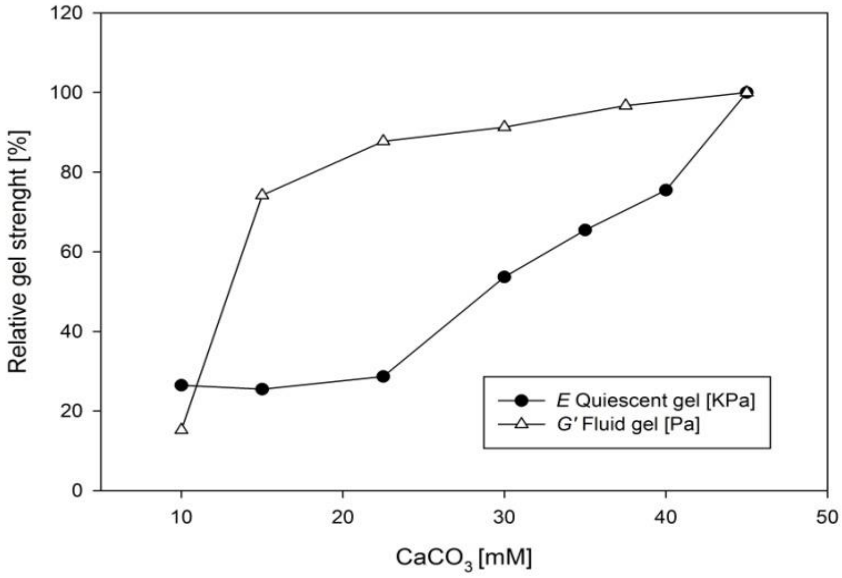

Figure 4.10: Young's Modulus and G' as function of $CaCO_3$ concentration for quiescent and fluid gels. Relative data is calculated by setting the highest strength value to 100 %.

In contrast to quiescent gels whose elasticity is only determined by the mechanism of calcium chelation into junction zones, the formation of percolated networks due to particle interactions is influenced to a greater extent by the particle surface (*e.g.* presence of disordered coils) than the calcium concentration. Thus, in comparison to the Young's elastic

modulus (E) of quiescent gels, G' of fluid gels has a lower dependence on $CaCO_3$ concentration between 22.5 mM to 45 mM.

4.4. Conclusions

The kinetics of alginate fluid gel formation has been studied using in-situ calcium release and under controlled shear conditions. The negative correlation between the viscosity increase and the applied shear rate during production was described using a power law equation.

Rheological results showed that the onset time of gelation increased with increasing the applied shear rate which suggests faster rates of particle growth. These results were confirmed by measurements of G' when shear was removed before completion of fluid gel particle formation. The rate of particle growth increased significantly as a result of either reducing the level of shear or increasing calcium concentration.

On the contrary, when the shear was removed after completion of the fluid gel structure, the rate of re-ordering due to inter-particle interaction appeared not to be affected by the magnitude of applied shear.

Changes in the gelation kinetics and rheological response of fluid gels produced with alginates having different M_w confirmed the significant influence of the chain length and fraction of polymer loose-ends on the degree of crosslinking. High M_w alginate fluid gels exhibited faster formation kinetics, enhanced viscosities and greater G' than those of fluid gels produced with low M_w alginate.

Similarly, increasing calcium concentration increased fluid gel particle stiffness such that lower limiting strains were measured. A saturated calcium concentration, corresponding to a critical $CaCO_3$:alginate molar ratio, was identified for both quiescent and fluid gel systems. This suggested that sheared and quiescent gels have similar network connectivity and equivalent numbers of polysaccharides arranged in egg-box dimers, probably due to the fast dimerization process which kinetically captures the fluid gel structure.

With regard to the calcium concentration effect on the gel strength, the fluid gel's response appeared to be different to that of a quiescent gel at $CaCO_3$ below the critical value. The distinct textural response of fluid gels is ascribed to the interaction between particles that enables an elastic network to form with less dependence on calcium concentration than seen in quiescent gels.

Overall, this work has shown that the kinetics of fluid gel formation and the resulting particle properties can be manipulated by the alginate M_w and calcium concentration, even using the same guluronic/mannuronic block composition. Thus, the ability to control them can ultimately allow the design of alginate fluid gels with specific textural properties.

4.5. References

Arnott, S., Fulmer, A., Scott, W. E., Dea, I. C. M., Moorhouse, R., & Rees, D. A. (1974). The agarose double helix and its function in agarose gel structure. *Journal of Molecular Biology*, *90*(2), 269-284.

Braccini, I., Grasso, R. P., & Pérez, S. (1999). Conformational and configurational features of acidic polysaccharides and their interactions with calcium ions: a molecular modeling investigation. *Carbohydrate Research*, *317*(1), 119-130.

Braccini, I., & Pérez, S. (2001). Molecular basis of Ca2+-induced gelation in alginates and pectins: the egg-box model revisited. *Biomacromolecules, 2*(4), 1089-1096.

Draget, K. I., Skjåk Bræk, G., & Smidsrød, O. (1994). Alginic acid gels: the effect of alginate chemical composition and molecular weight. *Carbohydrate Polymers*, *25*(1), 31-38.

Draget, K. I., Skjåk-Bræk, G., & Stokke, B. T. (2006). Similarities and differences between alginic acid gels and ionically crosslinked alginate gels. *Food Hydrocolloids*, *20*(2–3), 170-175.

Draget, K. I., Østgaard, K., & Smidsrød, O. (1990). Homogeneous alginate gels: A technical approach. *Carbohydrate Polymers*, *14*(2), 159-178.

Emanuele, A., & Palma-Vittorelli, M. B. (1992). Time-resolved experimental study of shear viscosity in the course of spinodal demixing. *Physical Review Letters*, *69*(1), 81-84.

Fang, Y., Al-Assaf, S., Phillips, G. O., Nishinari, K., Funami, T., Williams, P. A., & Li, L. (2007). Multiple Steps and Critical Behaviors of the Binding of Calcium to Alginate. *The Journal of Physical Chemistry B*, *111*(10), 2456-2462.

Fernández Farrés, I., Douaire, M., & Norton, I. T. (2013). Rheology and tribological properties of Ca-alginate fluid gels produced by diffusion-controlled method. *Food Hydrocolloids*, *32*(1), 115-122.

Frith, W. J., Garijo, X., Foster, T. J. & Norton, I. T. 2002. Microstructural origins of the rheology of fluid gels. In: WILLIAMS, P. A. & PHILLIPS, G. O. (eds.) *Gums and stabilisers for the food industry 11*. 95–103

Gabriele, A., Spyropoulos, F., & Norton, I. T. (2009). Kinetic study of fluid gel formation and viscoelastic response with kappa-carrageenan. *Food Hydrocolloids*, *23*(8), 2054-2061.

Gómez-Ordóñez, E., & Rupérez, P. (2011). FTIR-ATR spectroscopy as a tool for polysaccharide identification in edible brown and red seaweeds. *Food Hydrocolloids, 25*(6), 1514-1520.

Goodall, D. M., & Norton, I. T. (1987). Polysaccharide conformations and kinetics. *Accounts of Chemical Research*, *20*(2), 59-65.

Grant, G. T., Morris, E. R., Rees, D. A., Smith, P. J. C., & Thom, D. (1973). Biological interactions between polysaccharides and divalent cations: The egg-box model. *FEBS Letters*, 32(1), 195-198.

Mackie, W. (1971). Semi-quantitative estimation of the composition of alginates by infra-red spectroscopy, *Carbohydrate Research, 20*, 413–415.

Mitchell, J. R., & Blanshard, J. M. V. (1976). Rheological properties of alginate gels. *Journal of Texture Studies*, 7(2), 219-234.

Moe, S. T., Draget, K. I., Skjåk-Bræk, G., & Simdsrød, O. (1992). Temperature dependence of the elastic modulus of alginate gels. *Carbohydrate polymers*, *19*(4), 279-284.

Moresi, M., & Bruno, M. (2007). Characterisation of alginate gels using quasi-static and dynamic methods. *Journal of Food Engineering*, *82*(3), 298-309.

Norton, A. B., Cox, P. W., & Spyropoulos, F. (2011). Acid gelation of low acyl gellan gum relevant to self-structuring in the human stomach. *Food Hydrocolloids*, *25*(5), 1105-1111.

Norton, I. T., Goodall, D. M., Austen, K. R. J., Morris, E. R., & Rees, D. A. (1986). Dynamics of molecular organization in agarose sulphate. *Biopolymers, 25*(6), 1009-1029.

Norton, I. T., Jarvis, D. A., & Foster, T. J. (1999). A molecular model for the formation and properties of fluid gels. *International Journal of Biological Macromolecules*, *26*(4), 255-261.

Norton, I. T., Smith, C. G., Frith, W. J., & Foster, T. J. (2000). The production, properties and utilisation of fluid gels. In N. Katsuyoshi (Ed.), *Hydrocolloids* (pp. 219-227). Amsterdam: Elsevier Science.

Pamies, R., Schmidt, R. R., Martínez, M. D. C. L., & Torre, J. G. D. L. (2010). The influence of mono and divalent cations on dilute and non-dilute aqueous solutions of sodium alginates. *Carbohydrate Polymers*, *80*(1), 248-253.

Siew, C. K., Williams, P. A., & Young, N. W. G. (2005). New Insights into the Mechanism of Gelation of Alginate and Pectin: Charge Annihilation and Reversal Mechanism. *Biomacromolecules*, *6*(2), 963-969

Smidsrød, O. (1974). Molecular basis for some physical properties of alginates in the gel state. *Faraday Discussions of the Chemical Society, 57*, 263-274.

Stokke, B. T., Draget, K. I., Smidsrød, O., Yuguchi, Y., Urakawa, H., & Kajiwara, K. (2000). Small-angle X-ray scattering and rheological characterization of alginate gels. 1. Ca-alginate gels. *Macromolecules, 33*(5), 1853-1863.

Stokke, B. T., Smidsroed, O., Bruheim, P., & Skjaak-Braek, G. (1991). Distribution of uronate residues in alginate chains in relation to alginate gelling properties. *Macromolecules, 24*(16), 4637-4645.

Ström, A., & Williams, M. A. K. (2003). Controlled calcium release in the absence and presence of an ion-binding polymer. *The Journal of Physical Chemistry B*, *107*(40), 10995-10999.

Chapter 5 : THE INFLUENCE OF CO-SOLUTES ON TRIBOLOGY OF AGAR FLUID GELS

Fernández Farrés, I., & Norton, I. T. (2015). The influence of co-solutes on tribology of agar fluid gels. *Food Hydrocolloids, 45,* 186-195.

Abstract

The effects of glucose and glycerol on the lubrication properties of agar fluid gels have been studied using soft tribology. A novel approach using the sediment and supernatant of centrifuged fluid gels has allowed investigation of the distinct contributions of both the gelled particulate phase and the continuous phase on fluid gel tribology. The friction coefficient of both the particulate phase and fluid gels was significantly lower than that of the continuous phase across the three lubrication regimes. This indicates that particle entrainment occurs at all entrainment speeds, enhancing lubrication by prevention of surface contact.

Softer fluid gel particles produced with intermediate levels of glycerol (up to 30 %) show increased friction as would be expected for an increased contact area between the tribological surfaces. At high levels of glycerol, the friction does not increase. It is proposed that soft particles are produced, but the increasing friction is overcome with the increased lubrication from the more highly viscous continuous phase. In contrast, the presence of intermediate levels of glucose (up to 30 %) increases the friction of the aqueous continuous phase, but does not affect the particle properties. Texture analysis, rheology and light scattering techniques were used to elucidate the structural changes of the fluid gels induced by the addition of co-solutes and the influence this has upon lubrication.

5.1. Introduction

Fluid gels are concentrated suspensions of micro-gel particles dispersed in a continuous medium, typically water, and are produced by applying a shear field to the hydrocolloid solution while the sol-gel transition is taking place (Norton *et al*., 1999; Norton *et al.*, 2006). Application of fluid gels is of increasing interest to the food industry because of their ability to generate film thickness in the flow conditions that prevail during food processing in the mouth, potentially imparting desirable mouthfeel and texture attributes (e.g. smoothness) (Malone *et al.,* 2003). The lubrication properties of fluid gels, which have been shown to be greatly influenced by the physical properties of particles (e.g. size, elasticity) (Gabriele *et al.,* 2010; Mills *et al.*, 2013), can be measured using tribology (thin-film rheology).

In this work, we used fluid gels produced from agar which is a seaweed hydrocolloid composed by mixtures of neutral agarose and charged agaropectin, in proportions that vary depending on both the production process and the raw material (Araki, 1956; Phillips and Williams, 2009). Agarose is the polysaccharide with the gelling capability of agar and consists in alternating units of 3-linked β-D-galactopyranose and 4-linked 3, 6-anhydro-α-L-galactopyranose (Araki, 1956). The gelling temperature of agar varies depending on the degree of methoxylation of the agarose chain which is characteristic of the seaweed speces from which the agar has been extracted (Armisen and Galatas, 2000).

As the gelling temperature of agar is approached, intra-molecular hydrogen bonds start to form between the agarose chains, followed by the formation of inter-molecular hydrogen bonds between the two distinct polysaccharide chains (Tako and Nakamura, 1988). The mechanism for gelation involves a coil to double helix transition and a subsequent

aggregation of these helical domains to create a three dimensional structure (Arnott *et al.,* 1974; Morris, 1986; Schafer and Stevens, 1995).

Upon cooling the agar solution under shear below the agar transition temperature, kinetic competition between the process of gel network formation and the shear induced break-up of the network occurs. The result of these two competing mechanisms determines the physical properties of the resulting fluid gel particles as well as the extent of inter-particle interactions. The control over the conformational ordering kinetics is achieved by the applied cooling rate such that a range of viscoelastic properties can be produced by manipulation of the processing conditions.

The fluid gel formation is kinetically controlled by the number of available junction zones, where the rate of ordering is a function of polymer concentration, temperature and solvent quality. Thus, it is expected that changes in the degree of solvation of the hydrocolloid due to the presence of co-solutes will greatly affect the structure of the fluid gel particles and hence their lubricating properties. Although the effects of sugars and polyols on the material properties of quiescent agar gels have been widely reported in the literature, no published study has investigated the formation and lubrication properties of fluid gels mixed with such co-solutes.

The first objective of this work is to provide a comprehensive understanding of the mechanisms underlying the lubrication properties of agar fluid gels. The lubricating behaviour of agar fluid gel was investigated by Gabriele *et al.,* (2010) who proposed a conceptual model for fluid gel lubrication. However, in order to rationalize these findings in terms of particle properties, it is required to decouple the relevant contributions of both the

continuous phase and the particulate phase to fluid gel lubrication. To this end, we have employed a new approach using the supernatant and the sediment of centrifuged fluid gels to evaluate the different contributions.

The second objective of our study is to investigate the effects of co-solutes on fluid gel lubrication by using the proposed approach. In this work, glucose and glycerol were used to modify the solvent quality and the resulting changes in both particle structure and fluid gel properties were measured using tribology, rheology, texture analysis and light scattering techniques. Results show the substantial effect that both the continuous phase and particulate phase have on fluid gel lubrication. The observations from this study also suggest that controlling particle properties allows the lubrication properties to be manipulated, potentially enabling desirable sensory properties to be produced.

5.2. Materials and methods

5.2.1. Fluid gel production

Agar (A1296), D-glucose (G7021) and glycerol (49781) were purchased from Sigma Aldrich and used without further purification.

Agar was dispersed in distilled water at room temperature ($\approx$ 20 °C) and then heated while stirring to 90 °C until completely dissolved. The temperature was then lowered to approximately 70 °C and co-solutes were dissolved into the hot solution.

Fluid gels were produced by pumping the hot solutions into a jacketed pin-stirrer device at a constant flow rate of 25 ml/min. The temperature of the cooling unit was kept at 15 °C and

the pin-stirrer was operated at a shear rate of 2000 RPM which is the maximum operation speed of the equipment.

Fluid gels with more than 30 % glucose could not be produced reproducibly and thus data is not presented.

5.2.2. Tribology of fluid gels

The friction of the produced fluid gels was measured using a mini traction machine (MTM, PCS Instruments, London). The tribometer was equipped with an elastomer disc (Samco Silicone Products) and a ¾ inch diameter AISI 400 stainless steel ball (PCS Instruments, London) as contact surfaces. These specific materials were selected since they have been previously shown to provide data with correlations to sensory perception (Malone *et al.,* 2003). Fresh silicone discs were used for each test after cleaning by sonication for 5 minutes in ethanol followed by 5 minutes in distilled water. The stainless steel ball was cleaned with acetone and distilled water.

A normal load (W) of 2 N and a speed and slide-roll ratio (SRR) of 50 % were used for all the experiments as they were found to yield the most reproducible data. Stribeck curves were generated by measuring the friction upon increasing the speed from U = 1 - 1000 mm/s followed by decreasing the speed from U = 1000 - 1 mm/s until a total of 6 runs were completed. Each test, consisting of 3 ramps up and 3 ramps down, was repeated 3 times. The error bars represent the 1 standard deviation of the mean of the 18 tests per fluid gel sample.

5.2.3. Particle size measurements

Particle size distribution was obtained using a Malvern Mastersizer 2000 with a water dispersion unit. A refractive index of 1.42 was used for the agar fluid gel particles, as previously reported by Gabriele *et al.* (2010).

5.2.4. Texture analysis

Compression tests were performed on quiescently cooled agar gels using a TA.XT.plus Texture Analyser (Stable Micro Systems Ltd., UK) with a 40 mm diameter cylindrical aluminium probe. The height and diameter of the gel cylinders was 10 mm and 23 mm, respectively and the compression rate was 1 mm/s. The true stress σ_T and true (Hencky) strain ε_H were calculated using the following equations, as described elsewhere (Moresi and Bruno, 2007; Norton *et al.,* 2011):

$$\sigma_E = F / A_0$$

Eq. 5.1

$$\varepsilon_E = (h - H_0) / H_0$$

Eq. 5.2

$$\varepsilon_H = \ln(1 + \varepsilon_E)$$

Eq. 5.3

$$\sigma_T = \sigma_E(1 + \varepsilon_E)$$

Eq. 5.4

where H_0 and A_0 are the initial height and cross-sectional area, h and F are the height and the compression force applied, ε_E and ε_H are the engineering and true (Hencky) strain and σ_E and σ_T are the engineering and true stress.

5.2.5. Rheological tests

Dynamic oscillatory measurements were performed on a Kinexus Rheometer (Malvern Instruments Ltd., UK) using a cone and plate geometry (4 ° cone angle, 40 mm diameter).

Strain and stress sweep tests were carried out at 1 Hz on fluid gels at 25 °C, 48 hours after production.

5.3. Results and discussion

5.3.1. Effect of co-solutes on quiescent gels

Previously reported DSC studies on agar fluid gels produced using the method outlined in this paper showed that the enthalpy of melting of fluid gels is comparable to that of their quiescently cooled counterparts (Norton *et al.,* 1999). This indicates that the intrinsic polymeric network and therefore the textural properties of the agar fluid gel particles are the same as those of the corresponding quiescent gels, as suggested by Frith *et al*. (2002). Thus, in order to elucidate the effects of glycerol and glucose on gel particle stiffness, compression tests on quiescent gels were carried out.

Fig. 5.1.A, 5.1.B and 5.1.C show the true stress-true strain profile for the quiescent gels produced with 1 % [w/w] agar and increasing concentrations of glucose and glycerol. The changes in the textural properties of the gels were assessed in terms of the strain at failure

and the Young's Modulus (E) which was obtained as the slope of the initial linear region of the curve (below 0.05 strain), as described in the work of Norton *et al.* (2011).

The addition of glucose (up to 30 %) leads to stiffer agar gels, as indicated by the gradual increase in E. The strain at failure also increases, indicating that gels become more deformable (less brittle) (Fig. 5.1.A).

(A)

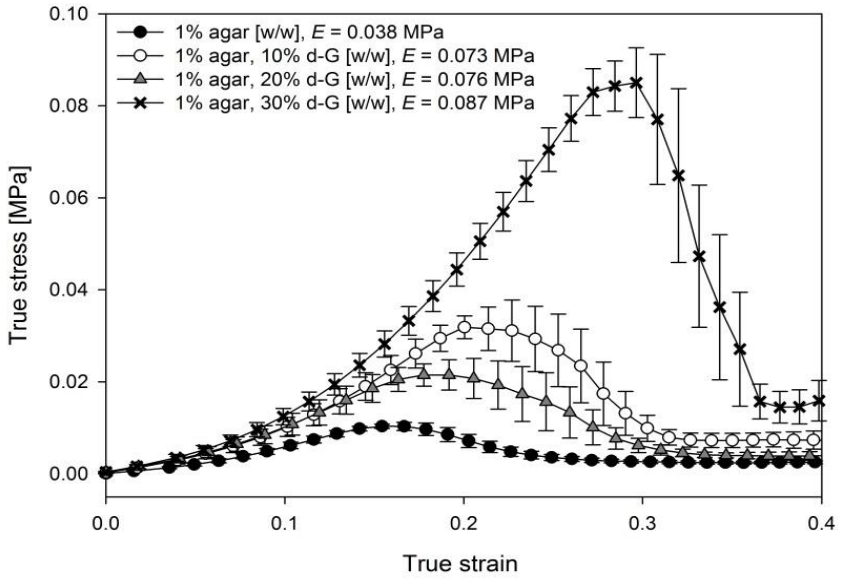

(B)

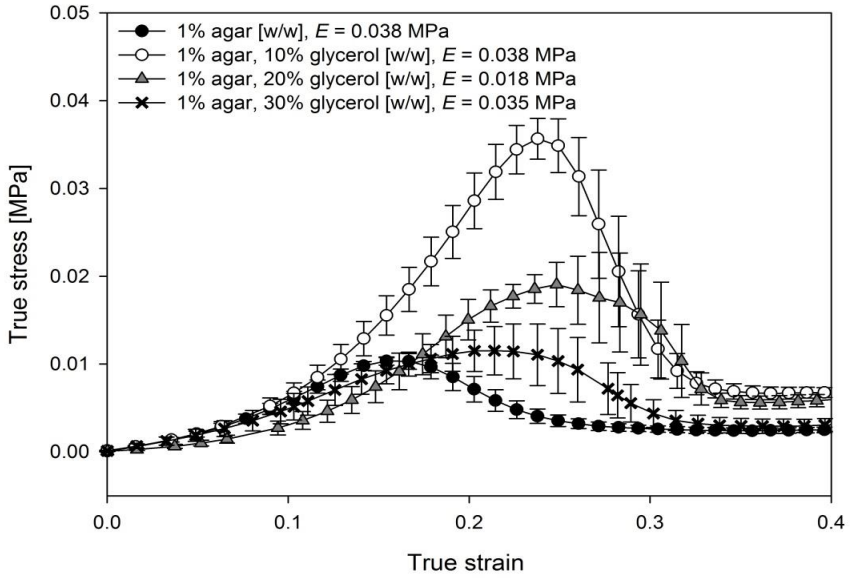

(C)

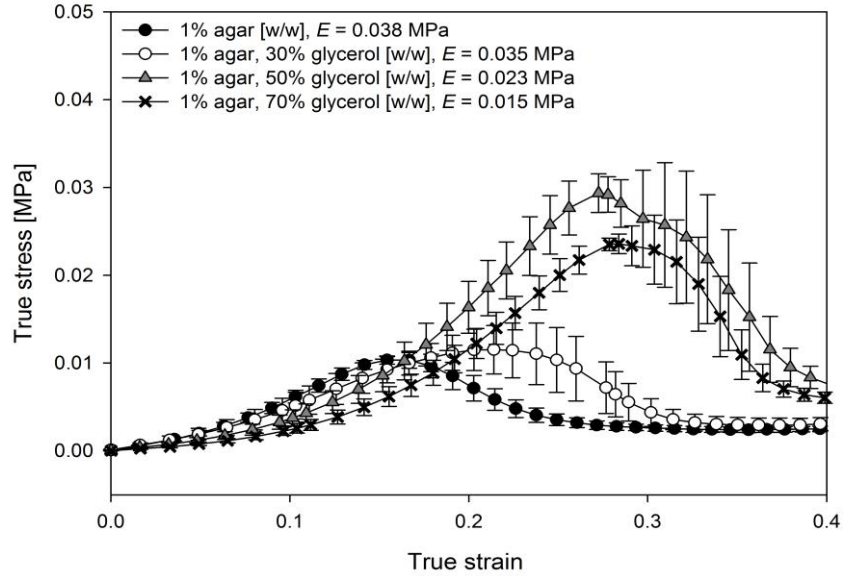

Figure 5.1: True stress/true strain profiles for 1% [w/w] agar quiescent gel as function of glucose concentration (A) and glycerol concentration (B-C).

Although several studies have investigated the influence of sugars on the mechanical properties of polysaccharide gels, the underlying molecular mechanisms are still under debate in the literature. Small deformation tensile tests on agarose gels showed an increase in E with increasing the amount of added sucrose up to 15 % (Nishinari *et al.,* 1992). The authors used the model developed by Oakenfull and Scott (1986) to estimate the size of junction zones. From rubber elasticity theory, Oakenfull and Scott (1986) derived the following equation relating the shear modulus (G) to the polymer concentration:

$$G = -\frac{RTC}{M}\frac{M[Z]-C}{M_Z[Z]-C}$$

Eq. 5.5

Where M is the number average molecular weight of the polymer, M_z is the number average molecular weight of the junction zones, Z is the number of junction zones, C is the weight concentration of polymer and R is the gas constant. The molar concentration of junction zones was calculated from $[Z] = Z / N_A$ where N_A is the Avogadro number. Assuming that G equals to 1/3 of E, theoretical plots of G versus agarose concentration as function of added sucrose were produced. Results indicated that the presence of sucrose leads to an increase in the number of junction zones but to the detriment of their size.

Watase *et al.* (1990) reported an increase in E as well as an increase in both melting temperature (T_m) and the melting enthalpy (ΔH_m) with addition of either glucose or sucrose up to a critical sugar concentration, beyond which a reduction in the extent of ordering was measured. It was suggested that sugars, due to their hydroxyl groups, increase the hydrogen bonding thereby promoting both the formation and aggregation of helical domains. The helix structure of agarose is stabilised by hydrogen bonds with water, where

some of the water molecules occupy the inner part of the helix (Foord and Atkins, 1989). Thus, a decrease in the extent of order (i.e. lower E and ΔH_m) is expected to occur at excessive sugar concentrations as the level of free water becomes insufficient to form thermodynamically stable junction zones.

The stabilisation of the agarose structure was later found to be dependent on the number of equatorially attached hydroxyl groups (*n*(e-OH)) present in sugars, where an increase in E, T_m and setting temperature (T_s) was observed with increasing *n*(e-OH) (Watase *et al.,* 1992).

A zipper model approach to the gel-to-sol transition of thermo-reversible gels was proposed by Nishinari *et al*. (1990). This approach describes the heat capacity of gels as function of the number of zipper (junction zones), the number of parallel links in a zipper, the rotational freedom of a parallel link and the energy enquired to open a link. Based on the zipper model approach, Watase *et al.* (1992) attributed the effect of increased E, T_m and T_s with increasing *n* (e-OH) to an increase in the number of junction zones and a reduction in both the size of each junction zone and the rotational freedom of a parallel link in a junction zone.

The suggestion of junction zones becoming smaller, but more numerous provides an explanation for the increase in E at the intermediate level of glucose (up to 30 %) measured in our work. However, the mechanism responsible for the increase in fracture strain at these glucose concentrations is not completely understood.

Similar to the results shown in our study, Normand *et al*. (2003) reported an increase in E as well as an increase in both the strain and stress at failure with the addition of sucrose (up

to 60 %) to agarose gels. The turbidity and the wavelength exponent were shown to decrease with increasing added sucrose which was ascribed to a reduction in the degree of helix association, leading to finer (i.e. smaller cross-section radii) and greater number of bundles. This idea was supported by TEM micrographs which showed a more homogeneous network with smaller pore size for the agarose gels with added sucrose. The authors suggested that the increase in viscosity due to the presence of sucrose reduces the mobility of the polymer chains thereby limiting the aggregation of helices. An alternative explanation was that sucrose increases the solvent quality such that the increased affinity of the agar helices for the solvent limits helix aggregation.

The effects of glucose on the textural properties of agar gels measured in our present work may be the result of the previously described mechanisms: 1. Formation of H-bonds between the OH groups present in both agar and sugars. 2. Change of the water structure. Both of these mechanisms are expected to take place simultaneously. However, the question remains as to which is dominant.

In this present work, a transition from a brittle to a deformable gel is also seen with an increasing level of glycerol (Fig. 5.1.B, 5.1.C). However, the evolution of E with the addition of glycerol differs from that of glucose. Addition of up to 10 % glycerol has no effect on the E values. At glycerol concentrations above 10 %, reduction in the E is observed with further increase in glycerol concentration. Glycerol is a polyol compound consisting of a 3-Carbon chain with 3 hydroxyl groups. As such, its ability to stabilise the agar gel structure is lower than glucose which, in solution, exists in equilibrium with several cyclic isomers containing equatorially attached hydroxyl groups.

The idea of reduced stabilisation by glycerol is supported by Watase *et al.* (1992) who found that, unlike glucose, addition of glycerol to agarose gels reduces both T_m and T_s. However, the height of the endothermic peak associated to the gel-to-sol transition was shown to increase with increasing concentrations of glycerol which led the authors to explain the reduced thermal stability in terms of an increased rotational freedom of the parallel links constituting a junction zone.

Overall, our results indicate an increase in both stiffness and deformability (as opposed to brittleness) with addition of glucose and a reduction in stiffness and increase in deformability with addition of glycerol.

5.3.2. Effect of co-solutes on fluid gels

The effects of glucose and glycerol on the structure of fluid gels have been investigated by small-strain dynamic oscillation measurements and light scattering experiments. Amplitude sweep tests were performed on the produced fluid gels and the obtained results are reported in Fig. 5.2, where a normalised G' is plotted as function of complex strain. Fluid gels produced with greater glycerol concentrations withstand larger strains before flowing which suggests increased particle deformability.

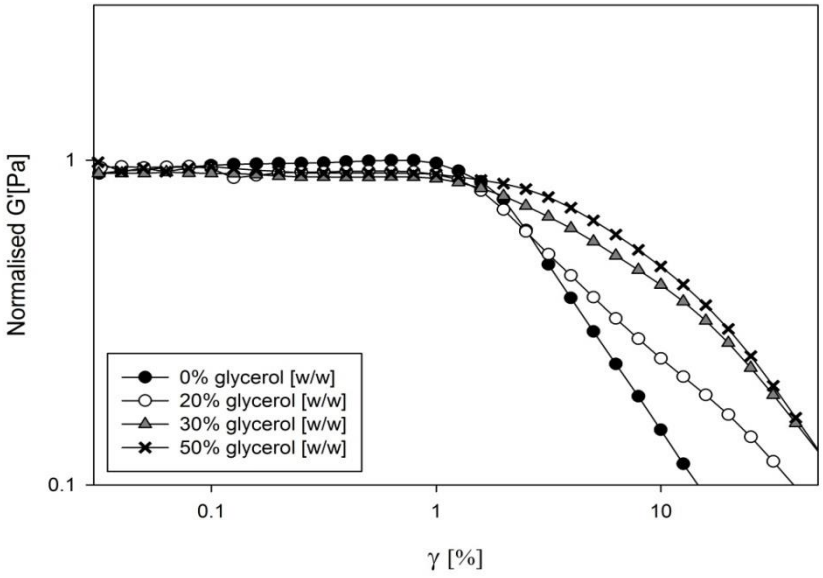

Figure 5.2: Normalised elastic modulus vs complex strain of 1 % agar fluid gels (pin stirrer) mixed with glycerol.

The particle stiffness and degree of inter-particle interaction were evaluated by stress sweep rheological measurements. The reduction in G' with increasing the level of glycerol (Fig. 5.3.A) suggests that softer particles are produced. The yield stress, which can be inferred from the stress at which G' starts to decrease, also decreases with increasing glycerol content, indicating a lower degree of inter-particle interactions.

(A)

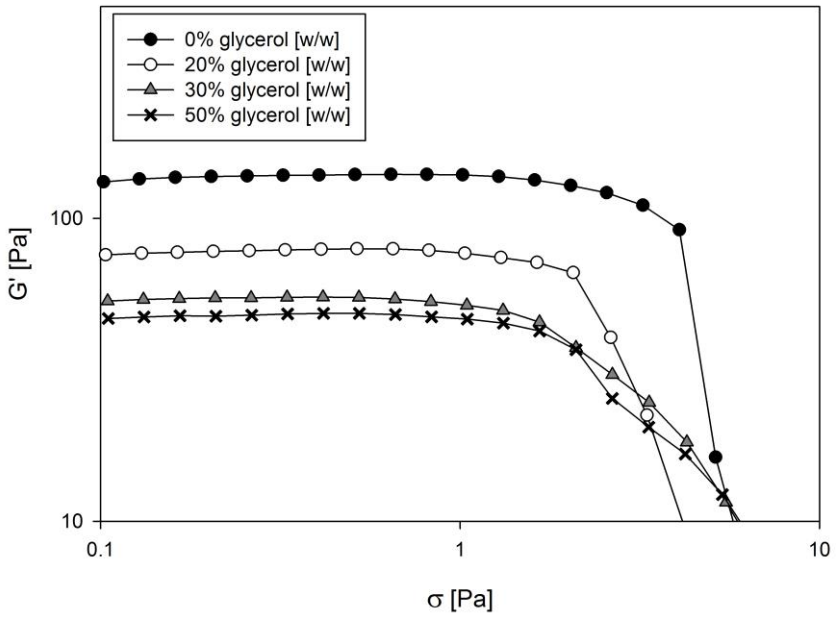

(B)

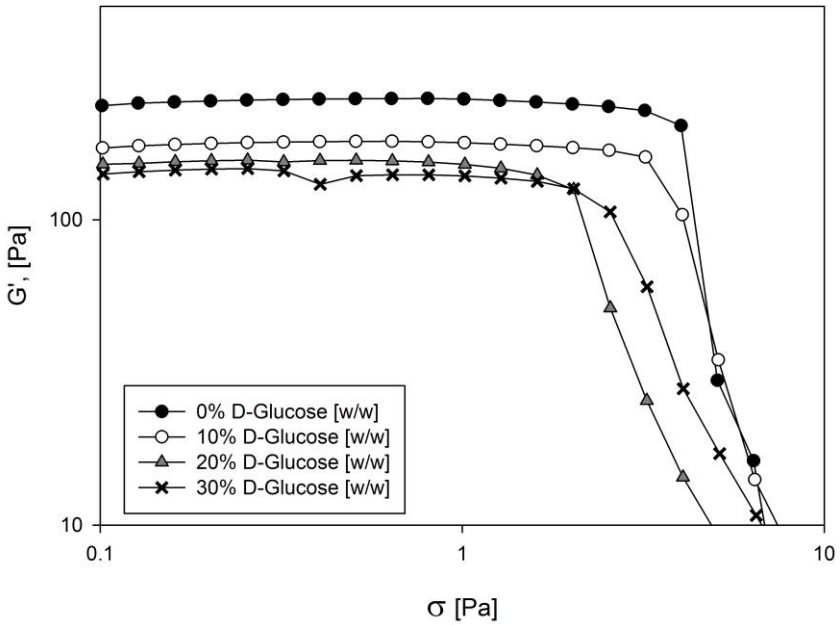

Figure 5.3: Stress sweep at 1 Hz for 1 % agar fluid gels as function of glycerol concentration (A) and glucose concentration (B).

The decrease in particle stiffness with addition of glycerol is consistent with the reduction in E previously discussed for quiescent gels. It has been shown that the solubility of agar is higher in water than in a water-polyol mixture (Nishinari and Watase, 1987). The reduced degree of solvation of agar in a water-glycerol solvent is expected to change the ordering transition, possibly leading to faster rates of polymer aggregation. This would lead to larger, softer and more deformable particles as the gelation process dominates over the applied shear rate in the kinetic competition during fluid gel formation.

Fluid gels exhibit a small progressive increase in gel particle size upon increasing the level of glycerol (Fig. 5.4.A) which is in agreement with the idea of more rapid gelation and low shear impact.

Similar to glycerol, addition of glucose leads to fluid gels with reduced G' and reduced yield stress values (Fig. 5.3.B). However, the reduction in G' is proportionally smaller for glucose than for glycerol. This decrease in G' does not correlate with the increase in E measured for quiescent gels with added glucose. Thus, the decrease in both G' and yield stress is attributed to a reduction in the degree of inter-particle interaction rather than changes to the physical properties of the particles with added glucose. This is supported by particle size distributions which show only slight differences in particle size with increasing glucose concentration (Fig. 5.4.B).

(A)

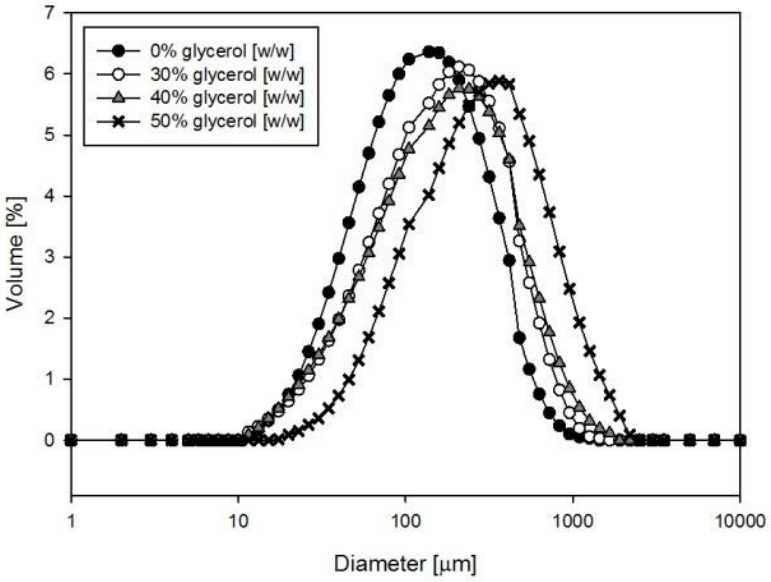

(B)

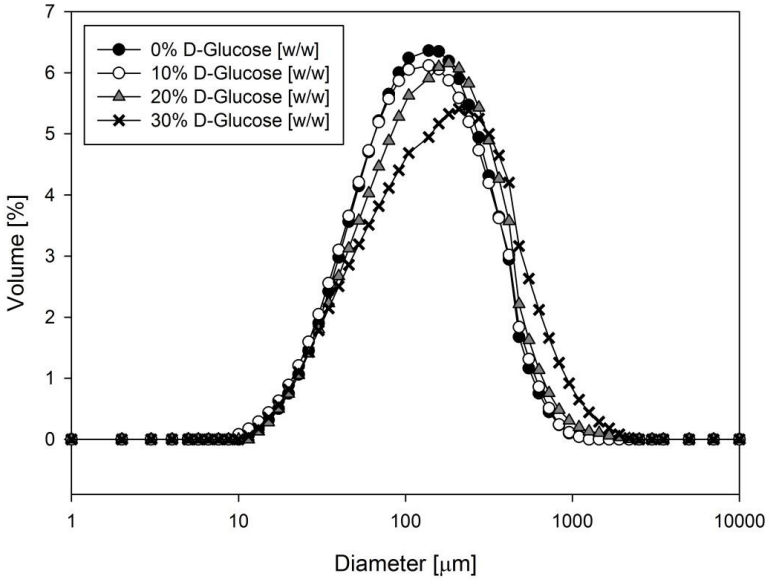

Figure 5.4: Particle size distribution for 1 % agar fluid gels as function of glycerol concentration (A) and glucose concentration (B).

Agar is formed by a mixture of neutral agarose and negatively charged agaropectin. Thus, interactions between the weakly charged agar particles are expected to occur primarily due to van der Waal forces. An increased solvent quality for the agar polymer chains in solution with glucose would increase the affinity of the polymer for the solvent. This change of affinity may also impact upon the behaviour of the fluid gel particles in improved solvent quality. The increased solvent quality for the fluid gels with added glucose is expected to reduce the level of the van der Waal forces acting between the particles.

In conclusion, the structural properties of fluid gel particles are not influenced by the addition of glucose. The presence of glycerol leads to a slight increase in particle size and a significant reduction in particle stiffness. The influence of the reduced stiffness of the particles on the lubricating properties of fluid gels will be discussed in Section 5.3.4. – Lubrication of agar fluid gels with added co-solutes.

5.3.3. Lubrication of agar fluid gels

Fig. 5.5 shows a comparison of the friction of water, the continuous phase, the gelled phase and fluid gels produced from 1 % agar. The curve for fluid gels presents a behaviour that has been previously reported (Gabriele *et al*., 2010). That is, the friction decreases with increasing speed until reaching a critical speed in the mixed regime after which friction starts to increase until again decreasing at high speeds. A lubrication mechanism describing the three distinctive behaviours with increasing speed was suggested by Gabriele *et al*. (2010): At the starting condition, the ball and the disc are in dry contact with both particles and continuous phase excluded from the contact area. As the speed starts to increase, friction decreases due to the entrainment of the continuous phase. Particles remain

excluded from the gap between the contacting surfaces as its size is smaller than the size of the particles (≈ 100 µm). Upon increasing the speed further, the gap widens until it reaches a size which is similar to the size of the particles, thereby allowing a monolayer of particles to enter the contact zone. This monolayer causes an increase in friction from the rolling-sliding motion of particles. At the highest speeds, multilayers of particles are entrained which further forces the two surfaces apart hence reducing friction again until reaching hydrodynamic regime where bulk fluid is entrained.

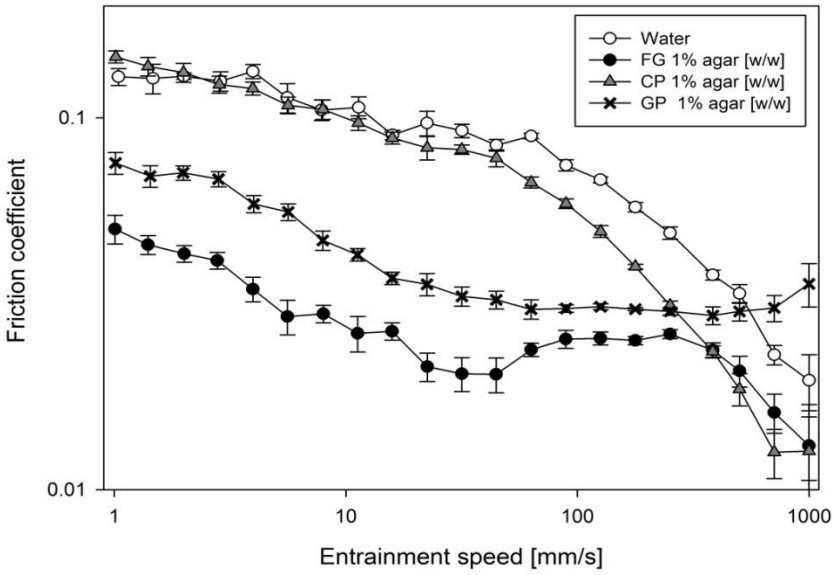

Figure 5.5: Comparison of Stribeck curve for water, fluid gel (FG), continuous phase (CP), particulate gelled phase (GP) produced from 1 % [w/w] agar.

In this study, it has been shown that the friction of water is significantly higher than that of the fluid gels at all speeds. This finding suggests that the particles, rather than being excluded at low speeds, are entrained thereby providing lubrication by preventing contact between the two rotating surfaces.

It is possible that the ordering transition did not occur to its full extent during fluid gel production and thus some disordered polymer chains would remain dissolved in the

continuous phase. The friction of the continuous phase containing the polymer would then be expected to be lower than that of water as it entrains into the contact zone to form mixed fluid-boundary lubricating films, as previously reported (de Vicente *et al.,* 2006).

Thus, the question arises as to whether the entrainment of the continuous phase containing the polymer is the only mechanism responsible for the observed decrease in friction or, rather, both the continuous phase and the particulate gel particles are entrained in boundary and mixed regimes. In order to address this question, it becomes necessary to decouple the relevant contributions of the continuous phase and the gelled phase to fluid gel lubrication. To this end, fluid gels were centrifuged using a Sigma 3K30 centrifuge (Laborzentrifugen GmbH, Germany) at 120,000 rpm for 30 minutes at 20 °C and the resulting supernatant and the sediment were used as samples of the continuous phase and the particulate gelled phase, respectively.

The continuous phase displays a behaviour similar to that of pure water at speeds up to 100 mm/s, above which the friction of is lower than water, suggesting that a certain amount of disordered polymer chains are present in the continuous phase. The Stribeck curve of the continuous phase displays a trend which is expected for a non-absorbing hydrocolloid solution. The non-charged agar molecules do not adsorb onto the hydrophobic disc surface, thus effective boundary lubrication does not occur and the friction is similar to that of water. The friction is reduced below the value of water upon increasing the speed in the mixed regime due to the formation of an elastohydrodynamic film (de Vicente *et al.*, 2006; Malone *et al.,* 2003). Two mechanisms have been suggested for this reduction in friction (Malone *et al*., 2003): One mechanism is that the formation of the polymer layer prevents

the two surfaces from contacting. The second mechanism is that the increased fluid viscosity supresses turbulent flow in the contact area thus limiting drag.

That the friction of the continuous phase is equivalent to that of water at low speeds and significantly higher than that of the fluid gel confirms the idea of particle entrainment occurring at all speeds, which contradicts the model of fluid gel lubrication proposed by Gabriele *et al.,* (2010). The suggestion of particles being present at the ball-in-disc gap at all speeds is also supported by previous data on fluid gels produced from agar (Gabriele *et al.*, 2010), alginates (Fernández Farrés *et al*., 2013; Chapter 3) and *k*-carrageenan (Garrec and Norton, 2013) which showed a reduction in friction on increasing the number and volume fraction of particles through raising polymer concentration.

At low rotational speeds in the mixed regime, the size of the film thickness is in the range of the size of the particles (microns). It is therefore likely that a film of micro-gel particles is confined within the gap at these speed conditions. This idea was first proposed by de Vicente *et al.* (2006) who showed that the friction of suspensions of neutralized carbopol micro-gelled particles (particle size of 2 µm- 4 µm) was lower than that of water. The Stribeck curve for these carbopol particles displayed a peak in the mixed regime but, unlike agar particles, friction did not decrease initially on increasing the speed from the stating conditions. Similar behaviour to that of these carbopol particles was reported for alginate fluids gels with particles having a size of 5 µm-10 µm (Fernández Farrés *et al.,* 2013; Chapter 3).

Thus, the difference in the lubricating behaviour at low speeds may relate to the physical properties of the confined particles. Agar particles, being reasonably large (100 µm), can deform into elongated shapes at low speeds in the tribometer where elongational flow is

expected to dominate over shear flow. This results in a reduction of the contact area between the surfaces hence decreasing the measured friction. In contrast, the smaller alginate particles (Fernández Farrés *et al*., 2013; Chapter 3), which are expected to be less deformable and harder than the agar particles, showed a peak in friction at the lowest speeds.

The mechanism responsible for this peak in the Stribeck curve is at present not fully understood. It could be consequence of the rolling and sliding motion of a particle monolayer, as previously suggested (Gabriele *et al*., 2010; de Wijk and Prinz, 2005). This is compatible with the idea of particle deformation occurring at the lowest speeds for the larger agar particle. As the speed is increased, the entrainment of the continuous phase would widen the gap until reaching the size of the individual particles. The rolling-sliding motion of these non-deformed particles as they enter the contact zone would increase friction. For the smaller particles, the rolling-sliding motion would occur at lower speeds, as the speed is increased from the static conditions.

Another possible explanation for the observed increase in friction is due to a build-up of particles around the ball-on-disc contact, thus momentarily preventing the entrainment of the continuous phase. Although adsorption of the non-charged agar particles to the hydrophobic surface is not expected, a stick-slip motion of the confined particles could occur. This would increase the residence time of the confined particles at the contact zone, leading to accumulation of particles outside the inlet of the contact zone, building up around the ball-on-disc contact.

The results of our study have shown that the friction in both boundary and mixed regimes relates to the confinement of particles in the thin film. The friction in these two regimes is a function of the structure of the particles (e.g. size, elasticity). A determination the disordered polymer present in the continuous phase could be achieved by spectroscopic techniques. This would further extend the developments presented in this work on the particulate phase and the continuous phase.

5.3.4. Lubrication of agar fluid gels with added co-solutes

The effects of glucose and glycerol on the lubrication properties of agar fluid gels have been investigated. As shown in Fig. 5.6.A, the lubrication by fluid gels is reduced at 10 % and 20 % glucose concentrations. Examining the lubrication provided by their corresponding continuous phase and gelled phase, it is seen that the decrease in lubrication of fluid gels with added glucose is caused by increased friction from the continuous phase (Fig. 5.6.B). The presence of glucose had no effect on the lubrication response of the gelled phase (Fig. 5.6.C) which is consistent with our previous suggestion that the structure of the particles remain unchanged for the range of glucose concentration studied.

(A)

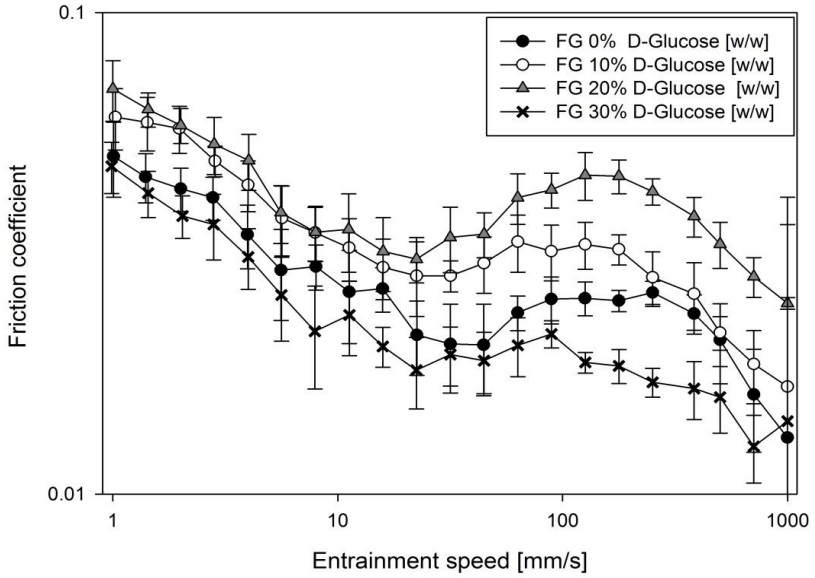
FG 0% D-Glucose [w/w]
FG 10% D-Glucose [w/w]
FG 20% D-Glucose [w/w]
FG 30% D-Glucose [w/w]
Friction coefficient
0.1
0.01
1
10
100
1000
Entrainment speed [mm/s]

(B)

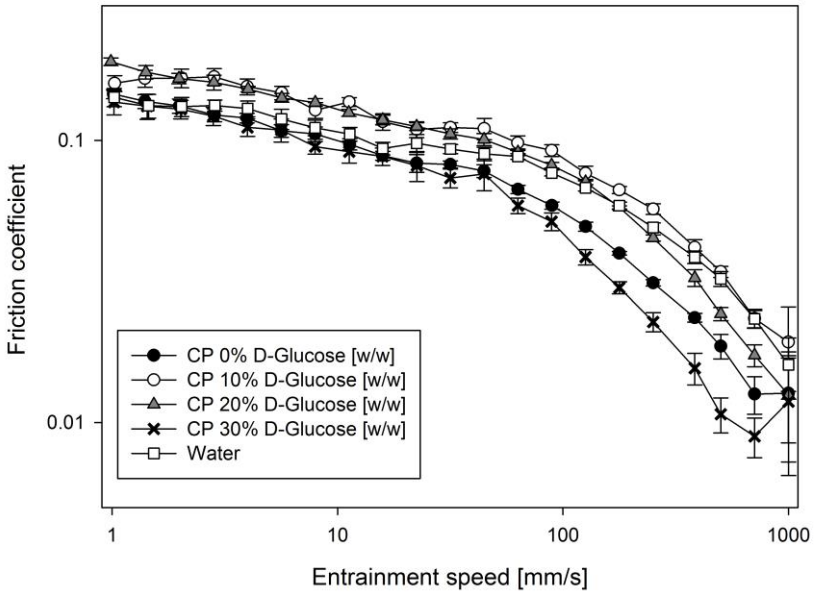
CP 0% D-Glucose [w/w]
CP 10% D-Glucose [w/w]
CP 20% D-Glucose [w/w]
CP 30% D-Glucose [w/w]
Water
Friction coefficient
0.1
0.01
1
10
100
1000
Entrainment speed [mm/s]

(C)

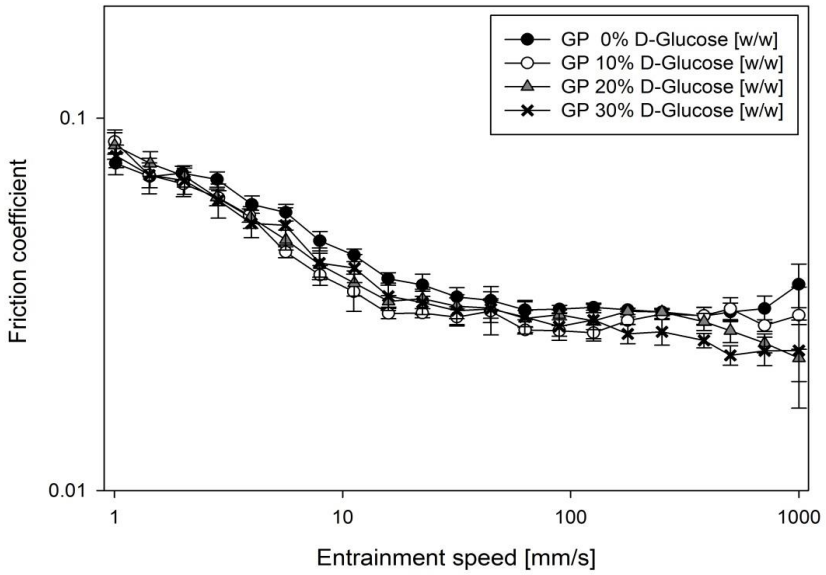

Figure 5.6: Stribeck curves for 1 % [w/w] agar fluid gels (A), aqueous continuous phase of 1 % [w/w] agar fluid gels (B) and the particulate gelled phase of 1 % [w/w] agar fluid gels (C) as function of glucose concentration.

The slight increase in the friction of the continuous phase is not attributed to changes in the water structure due to the presence of glucose since the differences between the friction of glucose solutions and that of water are negligible given the standard deviations (Table 5.1).

	μ at 1mm/s	μ at 125mm/s	μ at 500mm/s
water	0.14 (0.02)	0.07 (0.003)	0.03 (0.004)
10 % glucose	0.12 (0.01)	0.04 (0.002)	0.02 (0.004)
10 % glycerol	0.15 (0.04)	0.05 (0.003)	0.02 (0.005)
20 % glucose	0.16 (0.03)	0.04 (0.002)	0.009 (0.004)
20 % glycerol	0.13 (0.03)	0.04 (0.003)	0.008 (0.004)
30 % glucose	0.14 (0.01)	0.05 (0.003)	0.01 (0.002)
30% glycerol	0.13 (0.02)	0.05 (0.004)	0.009 (0.003)
50 % glycerol	0.13 (0.01)	0.04 (0.005)	0.01 (0.002)
70 % glycerol	0.12 (0.04)	0.02 (0.001)	0.005 (0.002)

Table 5.1: Friction coefficient for aqueous solutions of glycerol and glucose. Data are the means of 3 Stribeck curves with standard deviations in parentheses.

The reason for the increase in friction of the continuous phase could be due to an increase in the hydrodynamic volume of the disordered free polymer chains at the inlet zone, reducing the entrainment of fluid to the contact area hence diminishing lubrication. This is expected to have an effect in the lubrication of agar which, due to its random coil conformation (Norton *et al.*, 1986), is not expected to orient in the elongational and shear flow when compared to polysaccharides with rigid-rod or extended-coil conformations. As such, the ability of the disordered agar chains to provide lubrication by entering the contact zone in the presence of glucose may be diminished. More detail on the effect of hydrocolloid conformation on lubrication can be found in the work of Garrec and Norton (2012). The increase in the hydrodynamic volume of the disordered polymer chains could be the result of an increase in solvent quality at these low levels of glucose, as has been previously suggested (Normand *et al*. 2003; Sworn and Kasapis, 1998).

At 30 % concentration of glucose, the friction of fluid gels is similar to that of the fluid gels without added glucose due to the increased viscosity of the continuous phase overcoming the effect from the disordered polymer coils.

Examining the effects of glycerol, it is seen that the lubrication of fluid gels is reduced due to the increased friction of the particulate gel phase at low levels of glycerol (< 30 %)(Fig. 5.7.A-5.7.C) . As showed earlier in this paper, fluid gel particles become lager and their stiffness decreases with increasing addition of glycerol. This reduction in particle stiffness can account for the higher friction coefficients. The ability of particles to support the applied load decreases as they become increasingly softer, leading to an increased contact area between the two rotating surfaces such that the sliding friction coefficient is increased. These observations are consistent with previous research on *k*-carrageenan fluid gels which showed a reduction in boundary friction by increasing particle stiffness (Garrec and Norton, 2013). Furthermore, larger particles typically yield higher friction coefficients, as reported elsewhere (de Wijk and Prinz, 2005).

Our previous hypothesis of gel particles being present at the contact area at all speeds is supported by the results presented in Fig. 5.7.A which show that the increase in the friction of fluid gels due to the presence of softer particles occurs also at the lowest speeds.

Furthermore, the speed at which friction starts to increase is not affected by particle stiffness. This reinforces the view that particle entrainment takes place at all speeds as the speed required to induce particle entrainment is expected to depend on particle stiffness.

(A)

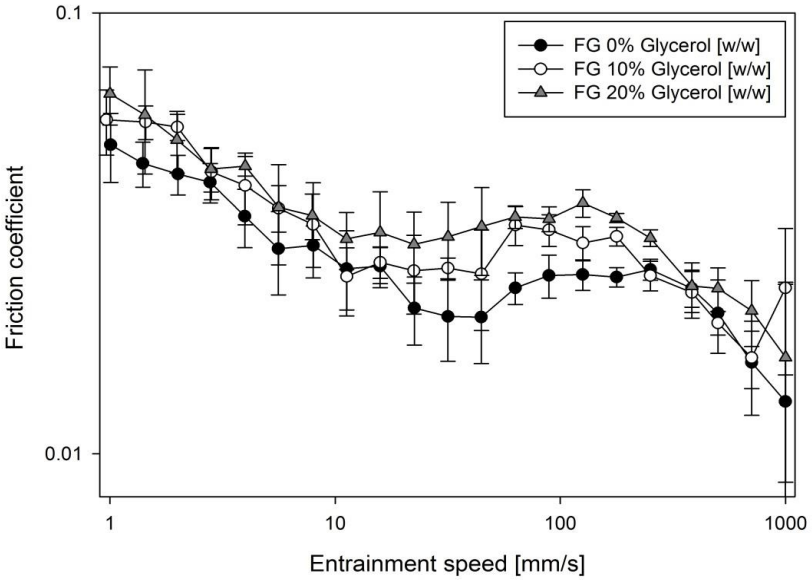
0.1
0.01
Friction coefficient
1
10
100
1000
Entrainment speed [mm/s]
FG 0% Glycerol [w/w]
FG 10% Glycerol [w/w]
FG 20% Glycerol [w/w]

(B)

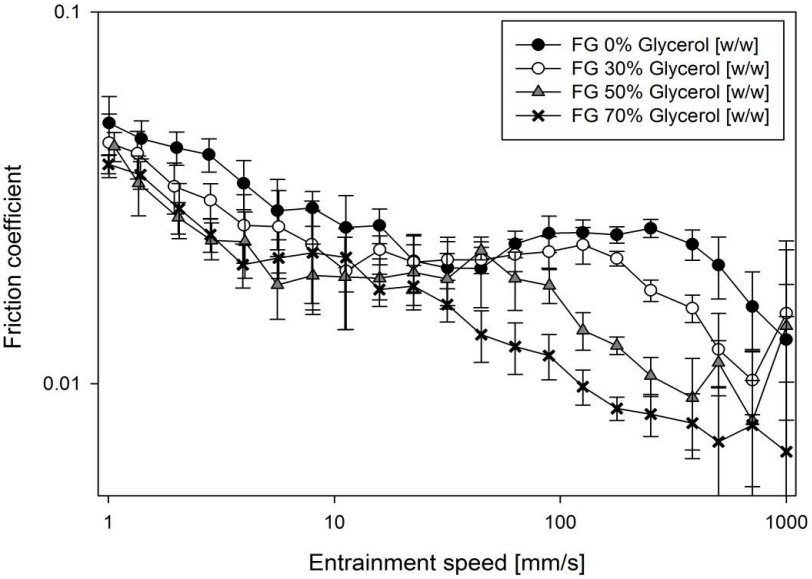
0.1
0.01
Friction coefficient
1
10
100
1000
Entrainment speed [mm/s]
FG 0% Glycerol [w/w]
FG 30% Glycerol [w/w]
FG 50% Glycerol [w/w]
FG 70% Glycerol [w/w]

(C)

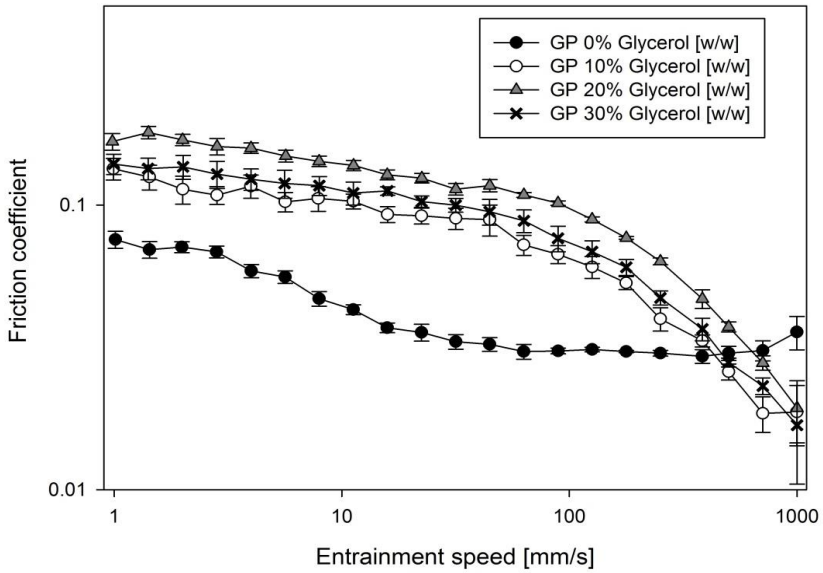

(D)

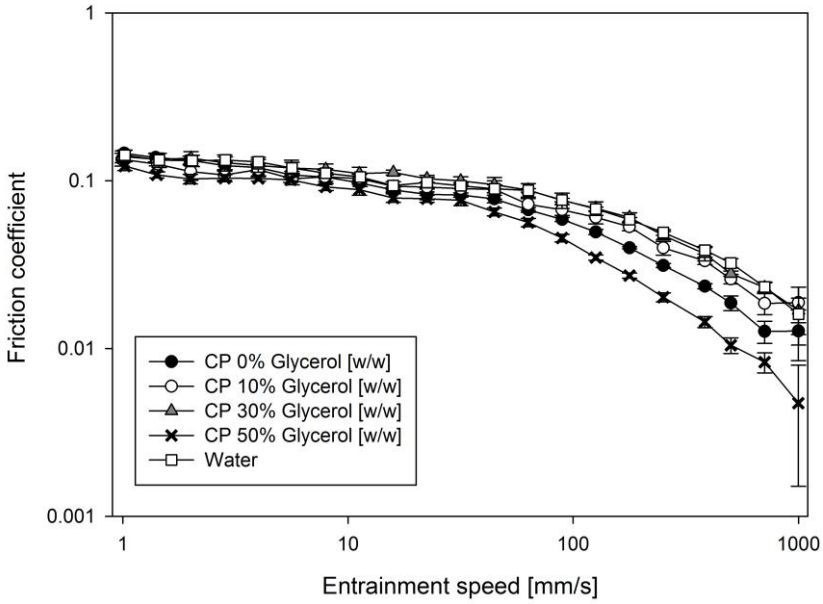

Figure 5.7: Stribeck curves for 1 % [w/w] agar fluid gels (A-B), the particulate gelled phase for 1 % [w/w] agar fluid gels (C) and the aqueous continuous phase of 1 % [w/w] agar fluid gels (D) as function of glycerol concentration.

At glycerol concentrations above 30 %, a shift in the lubrication mechanism is seen where friction progressively decreases with increasing glycerol concentration (Fig. 5.7.B). At these levels of glycerol, the effect of increased friction due to particle deformability is suppressed with increased lubrication from the highly viscous continuous phase. The fluid gel tribology is now controlled by the continuous phase which forms a lubricating layer with a film thickness exceeding the size of the particles. The effect of increasing the continuous phase viscosity through raising glycerol concentration is to increase the film thickness such that lubrication is further enhanced. These observations suggest that, at a sufficiently high solvent viscosity, a thin-film lubrication mechanism prevails where the deformation and motion of the confined particles no longer determines friction. Overall, the use of glucose and glycerol as co-solutes for agar fluid gels has been shown to modify their lubricating behaviour by affecting both the particle structure and the continuous phase properties. Tribological measurements of the continuous and the gelled particulate phase have been used to evaluate their relative contribution to fluid gel lubrication while providing a further insight into the underlying mechanism.

5.3.5. Effect of applied normal load

In order to gain further insight into the mechanism responsible for the increase in friction in the mixed regime, a range of Stribeck curves were generated with increasing normal loads. For agar without added sugars, both the friction coefficient and the velocity at which friction starts to increase are not influenced by the applied normal load (Fig. 5.8.A). For agar fluid gels with added glycerol, the velocity associated with the peak in friction deceases slightly (Fig. 5.8.B), which suggests a mechanism of particles building up around the ball-on-disc contact.

(A)

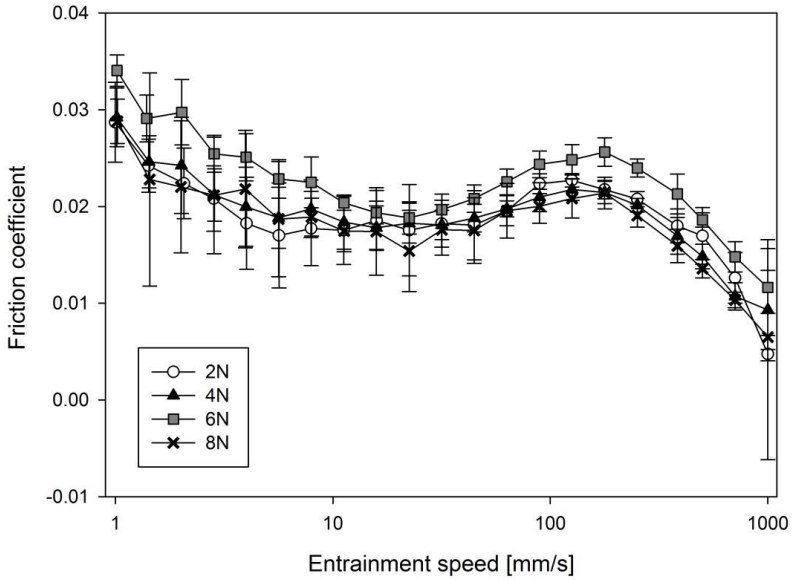

(B)

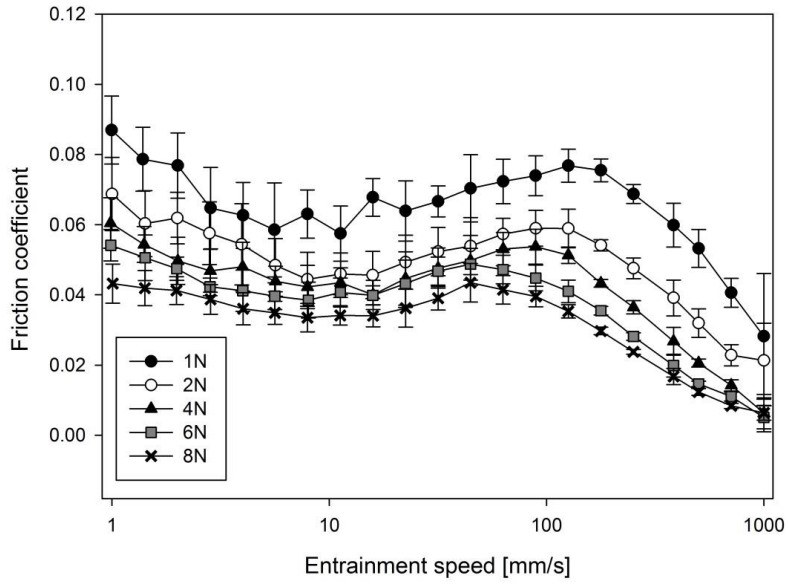

Figure 5.8: Stribeck curves as function of applied normal load (W) for agar fluid gels (A) and agar fluid gels with added glycerol (B).

On increasing the load, the width of the gap decreases leading to particles building up more rapidly around the contact for a given speed. The force exerted by the accumulated particles

in front of the contact may then be greater at lower speeds for higher normal loads. However, the idea of particle accumulation must be considered as a tentative suggestion since fluid gels without added glycerol did not show this load dependence on friction. The reason for these two different behaviours is not yet clear, but one possibility is that particle accumulation is promoted for the system with added glycerol due to the increased viscosity from the continuous phase. For these fluid gels with added glycerol, the friction coefficient decreases with increasing applied normal load which is expected for the compliant elastic surface used in this study, where the contact area is controlled by the elastic conformation over the plastic deformation at the contacting asperities.

According to the adhesion model (Bowden and Tabor, 1954), the contact between the surfaces takes place only between the asperity peaks and consequently, the real (interfacial) contact area A_r is lower than the apparent (geometrical) A_a contact area. During rolling-sliding, new contact points are constantly being created whist others disassociate. On the assumption that A_r remains constant on average and the interfacial shear strength τ is the same for all asperity contacts, the tangential frictional force F_t is given by $F_t = A_r\tau$ (Bowden and Tabor, 1954).

From Hertz theory for elastic contacts, the contact area between elastically deforming asperities increases proportionally to $W^{2/3}$ (Hertz, 1881). Thus, assuming that the real contact area is proportional to the Hertzian contact area then $F_t \propto W^{2/3}$ is expected. The friction coefficient $\mu = F_t / W$ then leads to $\mu = W^{2/3}/W \propto W^{-1/3}$.

Interestingly, whereas μ does not vary with W for fluid gels without glycerol, μ decreases with increasing W for fluid gels with glycerol. This behaviour is likely to be the consequence of the higher continuous phase viscosity of the system with added glycerol. In these systems, fluid film formation is enhanced due to the increased continuous phase viscosity which in turn increases the forces required to displace the continuous phase from the contact region. This enhanced lubrication from the continuous phase is expected to play a determining role on the effect of reduced μ with increasing W.

The deformability of the particles with glycerol could also be contributing to this observed behaviour, as more deformable particles would reduce the number of asperity contacts. Plots of the tangential frictional force against the applied normal load are presented in Fig. 5.9 where data are fitted to $F_t \propto W^{2/3}$.

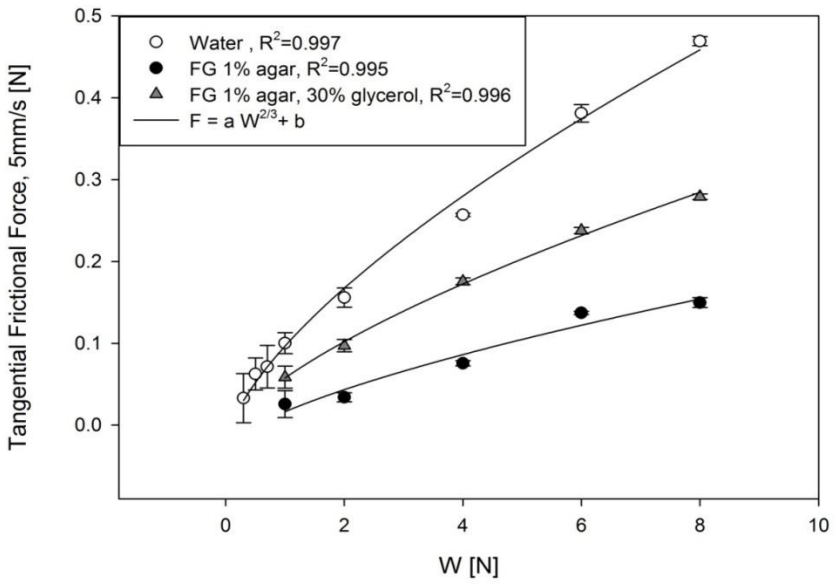

Figure 5.9: Tangential Frictional force at 5 mm/s as function of applied normal load (W) for water, agar fluid gels and agar fluid gels with added glycerol.

Normal forces below 2 N led to large variability in the F_t data for fluid gels and so data could not be fitted to the equation. Over the range of data obtained, fluid gels show good agreement with theoretical predictions. The deviation between ideal Hertzian behaviour and that measured from these fluid gel systems may be due to variation from perfect slip conditions which is an underlying assumption in Hertz theory.

5.4. Conclusions

In this work, a new approach to investigate the tribological behaviour of fluid gels using the continuous phase and the particulate gelled phase has been introduced. Results showed that the friction of the continuous phase is higher than that of the fluid gel in boundary, mixed and hydrodynamic regime, indicating that the entrainment of particles takes place at all speeds, in disagreement with previous suggestions.

The structure and lubrication properties of agar fluid gels were studied as function of solvent quality using a glucose and glycerol as co-solutes. The addition of glucose (up to 30 %) showed a minor effect on the structure of the particles and the particulate gelled phase displayed similar lubrication properties to the fluid gel with no added glucose. The friction of both the continuous phase and the fluid gels was higher for the systems containing glucose. This was attributed to a greater hydrodynamic volume of the disordered polymer coils existing in the continuous phase due to the increased solvent quality upon adding glucose. The increase in the hydrodynamic volume of the agar random coils at the inlet zone limits the entrainment of the fluid to the contact area such that lubrication decreases.

The effect of glycerol is to increase particle size and reduce particle stiffness such that the ability of particles to support the applied load diminishes. As a result, the contact area

between the surfaces increases thereby increasing friction. At high glycerol concentration, the lubrication of fluid gels is no longer driven by the presence of particles, but it is governed by the continuous phase which forms a lubricating layer with a thickness exceeding the dimensions of the particles. As such, the friction gradually decreases as the viscosity of the continuous phase is increased by raising glycerol concentration. Experiments using Surface Force Apparatus technique (Israelachvili and McGuiggan, 1990) where the interaction forces between the two contacting surfaces are measured would help to elucidate the exact processes involved during fluid gel lubrication.

Overall, results have shown that modifying both the kinetics of ordering transition and the degree of solvation of the hydrocolloid by changing solvent quality has a dramatic effect on the particle properties and thus the lubricating behaviour of fluid gels. The stiffness of the particles has a significant influence on lubrication as it determines the separation between the two tribological surfaces. Similarly, the continuous phase has an influence on fluid gel lubrication as it affects the film thickness as well as the structure of the disordered polymer coils.

As such, the lubrication properties of fluid gels cannot be predicted by rheology which is function of particle stiffness, particulate volume fraction as well as inter-particle interactions. This conclusion highlights the importance of studying the tribological properties together with rheology when designing food structures with desirable mouthfeel and textural attributes.

5.5. References

Araki, C. (1956). Structure of the Agarose Constituent of Agar-agar. *Bulletin of the Chemical Society of Japan 29*(4), 543 – 544.

Armisen, R., & Galatas, F. (2000). Agar. In G. O. Phillips, & P. A. Williams (Eds.), *Handbook of hydrocolloids* (pp. 21–40). Cambridge: Woodhead Publishing.

Arnott, S., Fulmer, A. S. W. E., Scott, W. E., Dea, I. C. M., Moorhouse, R., & Rees, D. A. (1974). The agarose double helix and its function in agarose gel structure. *Journal of Molecular Biology, 90*(2), 269-284.

Bowden, F. P., & Tabor, D. (1954). The friction and lubrification of solids, *Vol. I, Oxford Clarendon Press.*

De Vicente, J., Stokes, J. R., & Spikes, H. A. (2006). Soft lubrication of model hydrocolloids. *Food Hydrocolloids, 20*(4), 483-491.

de Wijk, R. A., & Prinz, J. F. (2005). The role of friction in perceived oral texture. *Food Quality and Preference, 16*(2), 121-129.

Fernández Farrés, I., Douaire, M., & Norton, I. T. (2013). Rheology and tribological properties of Ca-alginate fluid gels produced by diffusion-controlled method. *Food Hydrocolloids*, *32*(1), 115-122.

Foord, S. A., & Atkins, E. D. Y. (1989). New x-ray diffraction results from agarose: Extended single helix structures and implications for gelation mechanism. *Biopolymers, 28*(8), 1345-1365.

Frith, W. J., Garijo, X., Foster, T. J., & Norton, I. T. (2002). Microstructural origins of the rheology of fluid gels. *Special Publication-royal Society of Chemistry, 278*, 95-103.

Gabriele, A., Spyropoulos, F., & Norton, I. T. (2010). A conceptual model for fluid gel lubrication. *Soft Matter*, *6*(17), 4205-4213.

Garrec, D. A., & Norton, I. T. (2012). The influence of hydrocolloid hydrodynamics on lubrication. *Food Hydrocolloids, 26*(2), 389-397.

Garrec, D. A., & Norton, I. T. (2013). Kappa carrageenan fluid gel material properties. Part 2: Tribology. *Food Hydrocolloids, 33*(1), 160-167.

Hertz, H. (1881). On the contact of elastic solids. *Journal für die reine und angewandte Mathematik, 92,* 156-171.

Israelachvili, J. N., & McGuiggan, P. M. (1990). Adhesion and short-range forces between surfaces. Part I: New apparatus for surface force measurements. *Journal of Materials Research, 5*(10), 2223-2231.

Malone, M. E., Appelqvist, I. A. M., & Norton, I. T. (2003). Oral behaviour of food hydrocolloids and emulsions. Part 1. Lubrication and deposition considerations. *Food Hydrocolloids, 17*(6), 763-773.

Mills, T., Koay, A., & Norton, I. T. (2013). Fluid gel lubrication as a function of solvent quality. *Food Hydrocolloids, 32*(1), 172-177.

Moresi, M., & Bruno, M. (2007). Characterisation of alginate gels using quasi-static and dynamic methods. *Journal of Food Engineering, 82*(3), 298-309.

Morris, E. R. (1986). Molecular interactions in polysaccharide gelation. *British Polymer Journal, 18(*1), 14-21.

Nishinari, K., Koide, S., Williams, P. A., & Phillips, G. O. (1990). A zipper model approach to the thermoreversible gel-sol transition. *Journal de Physique, 51*(16), 1759-1768.

Nishinari, K., & Watase, M. (1987). Effects of Polyhydric Alcohols on Thermal and Rheological Properties of Polysaccharide Gels (Food & Nutrition). *Agricultural and biological chemistry, 51*(12), 3231-3238.

Nishinari, K., Watase, M., Kohyama, K., Nishinari, N., Oakenfull, D., Koide, S., Ogino, K., Williams, P. A., & Phillips, G. O. (1992). The effect of sucrose on the thermo-reversible gel–sol transition in agarose and gelatin. *Polymer Journal, 24*(9), 871–877.

Normand, V., Aymard, P., Lootens, D. L., Amici, E., Plucknett, K. P., & Frith, W. J. (2003). Effect of sucrose on agarose gels mechanical behaviour. *Carbohydrate polymers, 54*(1), 83-95.

Norton, A. B., Cox, P. W., & Spyropoulos, F. (2011). Acid gelation of low acyl gellan gum relevant to self-structuring in the human stomach. *Food Hydrocolloids, 25*(5), 1105-1111.

Norton, I. T., Frith, W. J., & Ablett, S. (2006). Fluid gels, mixed fluid gels and satiety. *Food Hydrocolloids, 20*(2), 229-239.

Norton, I. T., Goodall, D. M., Austen, K. R. J., Morris, E. R., & Rees, D. A. (1986). Dynamics of molecular organization in agarose sulphate. *Biopolymers, 25*(6), 1009-1029.

Norton, I. T., Jarvis, D. A., & Foster, T. J. (1999). A molecular model for the formation and properties of fluid gels. *International Journal of Biological Macromolecules, 26*(4), 255-261.

Oakenfull, D., & Scott, A. (1986). Stabilization of gelatin gels by sugars and polyols. *Food Hydrocolloids, 1*(2), 163-175.

Phillips, G. O., & Williams, P. A. (Eds.). (2009). *Handbook of Hydrocolloids*. Elsevier.

Schafer, S. E., & Stevens, E. S. (1995). A reexamination of the double-helix model for agarose gels using optical rotation. *Biopolymers, 36*(1), 103-108.

Sworn, G., & Kasapis, S. (1998). Effect of conformation and molecular weight of co-solute on the mechanical properties of gellan gum gels. *Food Hydrocolloids, 12*(3), 283-290.

Tako, M., & Nakamura, S. (1988). Gelation mechanism of agarose. *Carbohydrate Research, 180*(2), 277-284.

Watase, M., Kohyama, K., & Nishinari, K. (1992). Effects of sugars and polyols on the gel-sol transition of agarose by differential scanning calorimetry. *Thermochimica Acta, 206,* 163-173.

Watase, M., Nishinari, K., Williams, P. A., & Phillips, G. O. (1990). Agarose gels: effect of sucrose, glucose, urea, and guanidine hydrochloride on the rheological and thermal properties. *Journal of Agricultural and Food Chemistry, 38*(5), 1181-1187.

Chapter 6 : CONCLUSIONS AND FUTURE RECOMMENDATIONS

This thesis has enhanced the understanding of fluid gel formation by developing two new processing techniques for the production of alginate fluid gels.

The first technique uses a jacketed pin stirrer device with a Ca^{2+}-injection system in which the binding of Ca^{2+} to alginate occurs via diffusion-controlled method. By using this process, the microstructure, rheology and tribological properties of fluid gels have been studied as a function of alginate concentration. The obtained results, as presented in Chapter 3, have shown that alginate fluid gels have yield stresses and a shear thinning behavior similar to that of o/w emulsions, thereby offering promising opportunities for both fat replacement and texture enhancement in emulsion-based products.

The alginate fluid gel structure has been shown to be stable at high temperatures (110 °C). This thermal stability is a clear advantage compared to thermo-reversible fluid gels such as those produced from *k*-carrageenan, agar or gellan gum which melt when heated above their T_m (*e.g.* $T_m \approx$ 50-76 °C for *k*-carrageenan (Nishinari *et al.,* 1990), $T_m \approx$ 85 °C for agar (Phillips and Williams, 2009)).

Initial tribological measurements on alginate fluid gels produced by the diffusion-controlled method have shown that increasing alginate concentration increases lubrication due to an increase in both stiffness and volume fraction of particles present in the contact zone of the tribological surfaces.

The second processing technique employs a rheometer and an internal gelation method (*i.e.* in situ Calcium release) to produce alginate gels, allowing the rheological behavior to be measured during fluid gel formation. This technique has been used to investigate the

kinetics of fluid gel formation over a range of processing conditions (applied shear rate) and materials (Ca^{2+} concentration, alginate M_w). The obtained results, as presented in Chapter 4, have been used to develop empirical models for the structure-processing relationship, providing essential knowledge of the structuring process and potentially allowing structural design of alginate fluid gels.

The last experimental chapter of this thesis, Chapter 5, has investigated the lubrication properties of agar fluid gels as function of co-solute (D-glucose and glycerol) concentration. The reason for studying tribological changes with co-solutes arises from the correlations between tribology and perceived texture, as reported in Section 2.1 – General literature review. Results from this study have advanced the knowledge of fluid gel lubrication and thus may be relevant for the design of food products with desirable textural attributes.

The key conclusions from the experimental chapters of this thesis are provided below.

6.1. Alginate fluid gels produced within a Pin-stirrer: production and properties

- **Alginate fluid gels can be produced using a pin-stirrer device equipped with a Ca^{2+}-injection system:**

A new processing technique for the production of alginate fluid gels has been developed, where reactant solutions (alginate and $CaCl_2$) are separately injected into a pin stirrer device. The alginate solution is pumped using a peristaltic pump whilst a $CaCl_2$ solution is injected trough a syringe pump into the highest shear rate zone of the pin stirrer device, that is, between the tip of the pin and the outer wall.

- **Alginate fluid gels display a yield stress and shear thinning behavior:**

For suspensions of non-aggregated particles, the yield stress indicates the existence of inter-particle potential arising due to a net attractive force between particles. The presence of a yield stress is relevant in the formulation of emulsion-based products such as margarine which often contain proteins that confine oils droplets in a network structure and, as a result, exhibit yield stresses. From this perspective, alginate fluid gels could potentially be used as fat replacement in such foods.

- **Increasing alginate concentration leads to a reduction in particle size and an increase in both yield stresses and G':**

The reduction in particle size arises from greater shear stresses acting on the initial gel nuclei due to the increased viscosity. This relates to the concentration of disordered polymer chains which, as the particles are formed, increases with alginate concentration. In addition, the denser polymer chain matrix results in slower Ca^{2+} diffusion rates such that the mixing time of the two liquid phases at a molecular level decreases. These mechanisms therefore give advantage to the breaking process over gel formation.

The increase in both yield stress and G' with increasing alginate concentration is primarily attributed to an increase in both particulate volume and particle stiffness.

- **The lubrication of alginate fluid gels increases with increasing alginate concentration:**

The friction of alginate fluid gels decreases with increasing alginate concentrations due to an increase in both phase volume and particle stiffness. This relates to an increase in the ball-

on-disc separation due to an increased number of stiffer particles being present at the contact zone.

The Stribeck curves of alginate fluid gels show an increase in friction during the mixed regime similar to that of agar fluid gels. However, the evidence provided in this thesis is not sufficient as to describe the mechanism responsible for this behavior in alginate fluid gels.

6.2. Alginate fluid gels produced using in-situ calcium release: formation kinetics

- **Alginate fluid gels can be produced in a rheometer using the internal gelation method (*i.e.* in-situ Ca^{2+} release from $CaCO_3$):**

A new processing technique using a rheometer and the internal gelation method has been developed to produce alginate fluid gels. The slow and controlled Ca^{2+} release achieved by the internal gelation method allows the gelation kinetics to be controlled and more closely matched to the time scale of the applied shear rate. As such, the kinetics of fluid gel formation can be studied.

- **The onset time of gelation increases with increasing the applied shear rate:**

These results suggest lower rates of particle growth with higher applied shear rates. This was confirmed by measuring the increase in G' when stopping the shear before completion of the fluid gel production. The rate of G' increase under these conditions, attributed to the rate of particle growth, was lower for fluid gels produced at higher shear rates.

- **The re-ordering rate due to inter-particle interaction is not affected by the magnitude of the applied shear rate:**

The re-ordering rate was measured as the rate at which G' increased when stopping the shear after completion of the fluid gel structure. The increase in G' under these conditions does not change with applied shear rate.

- **Increasing alginate molecular weight (M_w) increases the gelation rate, viscosity and G' of fluid gels:**

Both the gelation rate and the viscosity increase during fluid gel formation are greater for high M_w alginates, arising from the greater length scale affected by the same interactions between calcium ions and alginate guluronic residues compared to low M_w alginates. This enhanced network formation along with an increased number of rheologically-effective crosslinks, leading to an increase in both viscosity and G'.

- **Increasing Ca^{2+} concentration increases gelation rate up to a critical calcium concentration**

The faster gelation kinetics measured as a result of increasing Ca^{2+} concentration relates to an increase in the rate of both the coil-dimer transition and the dimer-aggregated dimer transition. Thus, the structuring process occurs more rapidly and to a greater extent when more calcium ions are available. This progressive increase in ordering rate is an indication

that the release of calcium is rate limited by $CaCO_3$ dissolution rather than the glucono-δ-lactone (GDL) hydrolysis.

The same saturated calcium concentration, corresponding to a critical $CaCO_3$:alginate molar ratio, was identified for both quiescent and fluid gel systems. This suggested that fluid gels have similar network connectivity to quiescent gels with equivalent numbers of polysaccharides arranged in egg-box dimer. This is due to the rapid dimerization process of alginates which, when gelled under shear, leads to kinetically trapped fluid gel structures.

6.3. Tribology of agar fluid gels

- **The presence of particles in agar fluid gels reduces friction below that of their continuous phase for all lubrication regimes:**

This thesis has introduced a new approach to investigate the tribological behaviour of fluid gels using the continuous phase and the particulate gelled phase separately. Results on agar fluid gels showed that the friction of the continuous phase is higher than that of the complete fluid gel system in the boundary, mixed and hydrodynamic regimes, indicating that the entrainment of particles takes place at all speeds.

- **Both particle stiffness and the continuous phase influence the lubrication behavior of fluid gels:**

This conclusion was drawn from studying the lubrication of agar fluid gels with added glycerol. The effect of glycerol is to increase particle size and reduce particle stiffness such

that the ability of particles to support the applied load diminishes. This increases the contact area between the surfaces thereby increasing the friction of the particulate gel phase. As a result, the overall friction of fluid gels increases.

At glycerol concentrations above a critical value, the lubrication of fluid gels is no longer driven by the particulate gelled phase, but it is governed by the continuous phase which forms a lubricating layer with a thickness exceeding the dimensions of the particles. Under these conditions, the friction of fluid gels gradually decreases with increasing glycerol concentration due to the increase in the continuous phase viscosity.

- **The tangential friction (F_t) of fluid gels in a steel-on- silicone elastomer tribopair follows a $W^{2/3}$ dependency due to the elastic deformation of the asperity contacts:**

F_t of fluid gel lubricated steel-on-silicone elastomer contacts showed a $W^{2/3}$ dependency, as expected for the compliant elastomer surfaces. The contact area between elastically deforming asperities increases proportionally to $W^{2/3}$ according to Hertz theory. Since $F_t \propto A_r$ then $F_t \propto W^{2/3}$ is expected for the surfaces used in this thesis.

6.4. Future recommendations

- **Process optimization for alginate fluid gel production within the Pin-stirrer device:**

The shear rate created within the Pin-stirrer is not uniform. Fluid dynamic studies of fluid gel production based on Positron Emission Particle Tracking (PEPT) have indicated that low

shear rates zones (dead zones) are formed in the top corners of the pin stirrer whilst the highest shear rate zone is formed between the tip of the pin and the outer wall (Gabriele, 2011). In this thesis, the calcium injection point was located in the highest shear rate zone so as to achieve maximum dispersion. However, the exact distance between the injection point and the pin was unable to be determined.

In order to optimize this process, the effect of the injection point location on particle size should be studied. Results from this investigation may enable the design of a more robust method in which the location of the injection point is well defined so as to produce particles with controllable size. This will also lead to improved reproducibility in the production process.

- **Imaging fluid gel particles and measuring particle size:**

Precise particle size measurements in fluid gel systems present significant difficulties due to the similarity of the refractive index between particles and the continuous phase *i.e.* water. Measurements of particle size obtained in this thesis by optical microscopy should be validated using other techniques. One approach is comparing the optical microscopy results with those obtained using the Mastersizer with a given refractive index. Gabriele *et al.* (2010) used this method for agarose particles and reported that the optical microscopy results were in best agreement with Mastersizer data when the refractive index was set to 1.42. This investigation could also be carried out for alginate fluid gels. Measurements of particle size by means of light scattering will facilitate the process optimization of alginate fluid gel production as previously described. However, since fluid gels particles are generally

not spherical, results from light scattering techniques will need to be confirmed using other techniques. One possibility is imaging dried fluid gels by Scanning Electron Microscope (SEM) which has proven to be a valid technique to elucidate the structure of *k*-carrageenan fluid gel particles (Garrec *et al*., 2013).

An alternative simpler method could involve dying the particles. Work is currently being undertaken (Norton *et al*., in press) so as to develop a reliable method for staining and visualising quiescent gellan gum gels by using 5-(4,6-dichlorotriazinyl) aminofluorescein (DTAF) where the effect of the dye on the structure is considered.

- **Production of alginate particles layered with chitosan:**

An exciting microstructural approach which may allow encapsulation and controlled release of nutrients inside the gastrointestinal tract is building layered fluid gel structures arising from the association between alginate and chitosan. In acidic conditions, alginate gels contract due to reduced solubility of non-ionized carboxyl groups while, in alkaline conditions, the increased hydrophobicity of the ionized carboxyl groups leads to swelling and dissolution. On the contrary, chitosan dissolves in acidic medium due to the hydrophobicity the protonated amino groups and is insoluble in alkaline conditions. By mixing the two polymers, the electrostatic interaction between the carboxyl groups of alginate and the amino groups of chitosan form a polyelectrolyte complex which is insoluble at pH below 3.5 and dissolves at pH above 6 due to a reduction in charge density of the chitosan (George *et al*., 2006; Huguet *et al*., 1996; Tønnesen and Karlsen, 2002). Thus, chitosan coated alginate fluid gel particles should be stable during their passage through the

stomach (1.5 < pH < 3.5) and subsequently disintegrate in the intestine (pH ≈ 7) thereby releasing the encapsulated nutrient. In practical terms, the main challenge will be the formation of a defined chitosan layer which will reduce the porosity of the alginate network hence preventing leakage of encapsulated nutrients (Fernández Farrés *et al*. 2014).

- **Investigate in-mouth perception of fluid gels in relation to their tribological properties:**

This present work has investigated the effects of the hydrocolloid and co-solutes in relation to fluid gel microstructure and their lubrication properties. Results have shown that hydrocolloid and co-solute concentration determines fluid gel microstructure which in turn influences their tribological properties. Thus, considering the significant amount of studies that have correlated tribology to sensory data, the microstructure of fluid gels is expected to have an effect on perceived texture. However, the relevance of fluid gel tribology to sensory perception remains to be tested.

6.5. References

Fernández Farrés, I., Moakes, R. J. A., & Norton, I. T. (2014). Designing biopolymer fluid gels: A microstructural approach. *Food Hydrocolloids*, *42*, 362-372.

Gabriele, A. (2011). Fluid Gels: formation, production and lubrication. Doctoral dissertation, University of Birmingham.

Gabriele, A., Spyropoulos, F., & Norton, I. T. (2010). A conceptual model for fluid gel lubrication. *Soft Matter, 6*(17), 4205-4213.

Garrec, D. A., Guthrie, B., & Norton, I. T. (2013). Kappa carrageenan fluid gel material properties. Part 1: Rheology. *Food Hydrocolloids, 33*(1), 151-159.

George, M., & Abraham, T. E. (2006). Polyionic hydrocolloids for the intestinal delivery of protein drugs: alginate and chitosan—a review. *Journal of controlled release, 114*(1), 1-14.

Huguet, M. L., Neufeld, R. J., & Dellacherie, E. (1996). Calcium-alginate beads coated with polycationic polymers: comparison of chitosan and DEAE-dextran. *Process Biochemistry, 31*(4), 347-353.

Nishinari, K., Watase, M., Williams, P. A., & Phillips, G. O. (1990). kappa.-Carrageenan gels: effect of sucrose, glucose, urea, and guanidine hydrochloride on the rheological and thermal properties. *Journal of Agricultural and Food Chemistry, 38*(5), 1188-1193.

Norton, A.B., Hancocks R.D., Spyropoulos F., & Grover L.M. (in press). Development of 5-(4,6-dichlorotriazinyl)aminofluorescein (DTAF) staining for the characterization of low acyl gellan microstructures. Food Hydrocolloids.

Phillips, G. O., & Williams, P. A. (Eds.). (2009). *Handbook of hydrocolloids*. Elsevier.

Tønnesen, H. H., & Karlsen, J. (2002). Alginate in drug delivery systems. *Drug development and industrial pharmacy, 28*(6), 621-630.